University of Alberta

Characterizing the role of *CECR1* in cat eye syndrome by using mouse models

by

Fang Yang

A thesis submitted to the Faculty of Graduate Studies and Research
in partial fulfillment of the requirements for the degree of

Master of Science
in
Molecular Biology and Genetics

Department of Biological Sciences

Spring 2010
Edmonton, Alberta

Examining Committee

Heather McDermid, Biological Sciences

Andrew Waskiewicz, Biological Sciences

Roseline Godbout, Oncology

Abstract

CECR1 (cat eye syndrome chromosome region, candidate 1) is located on chromosome 22q11.2. Duplication of this region results in the human disorder cat eye syndrome (CES), which includes a variety of heart defects. *CECR1* is suggested to be dosage sensitive, based on a predicted role in controlling extracellular adenosine level during development, and thus may be responsible for some of the CES features, including heart abnormalities.

Animal models were established to study the effect of overexpressing *CECR1* in hearts. Abnormal phenotypes in hearts were not detected in zebrafish embryos overexpressing zebrafish *cecr1*. Thinner right ventricular walls and atrioventricular (AV) valve disorganization were observed in embryos of the transgenic mouse line FVB/N-Tg(MHC-hCECR1), which expressed human CECR1 specifically in cardiac muscle. The observed phenotypes were not typical of patients with CES; however, disrupted adenosine level resulting from increased adenosine deaminase activity might be responsible for the phenotypes.

Acknowledgement

I greatly thank my supervisor, Dr. Heather McDermid, for her constant guidance, support, criticism and helpfulness throughout my time of research and thesis writing. Sincere thanks to my committee members, Dr. Roseline Godbout and Dr. Andrew Waskiewicz, for their criticism, patience and ideas.

Thanks to all the past and current members of the lab who were great to work with and helped me from science to personal life. Special thanks to Dr. Stephanie Maier, who worked on the project before me, for her ceaseless help with techniques in general and valuable advice on the project. Thanks to Twila Yobb and Nic Fairbridge for their critical suggestions and their aid with the ADA activity experiments. Thanks to Grace Wong for helping me in sectioning mouse embryos. Thanks to Lisa Rae Chisholm-Dumesnil and Julie Man for assisting me with the mouse colony. Thanks to Christine Dawe and Megan Kooistra for their aid with experiments on mouse embryos. Thanks to Peter Thompson for his advice on protein work.

Sincere thanks to Randy Mandryk and Rakesh Bhatnagar for helping me with mouse tissue embedding and microscopy work. Special thanks to Dr. Ruth Stockey and Ashley Klymiuk for providing the AMIRA reconstruction software and helping me with it.

Finally, I thank my family for their encouragement and love. The completion of this thesis would not have been possible without their support.

Table of Contents

List of Tables

List of Figures

List of Abbreviations

aa	amino acids
ADA	adenosine deaminase
ADAL	adenosine deaminase-like
ADGF	adenosine deaminase-related growth factor
array CGH	array comparative genomic hybridization
APS	ammonium persulfate
ATP	adenosine triphosphate
AV	atrioventricular
BCIP	5-bromo-4-chloro-3-indolyl phosphate
BSA	bovine serum albumin
BLAST	basic local alignment search tool
bp	base pairs
cDNA	complementary DNA
CECR1	cat eye syndrome chromosome region, candidate 1
CES	cat eye syndrome
CMT1A	Charcot-Marie-Tooth disease type 1A
CNV	copy number variation
DCF	2'-deoxycoformycin
DEPC	diethyl pyrocarbonate
DGS	DiGeorge syndrome
DIG	digoxigenin
DNA	deoxyribonucleic acid
DNase	deoxyribonuclease
dNTPs	deoxynucleotide triphosphates
dpc	days post coitus
DTT	dithiothreitol
E	embryonic day
EDTA	ethylene diamine tetraacetic acid
EHNA	erythro-9-(2-Hydroxy-3-nonyl) adenine

EST(s)	expressed sequence tag(s)
FISH	fluorescence *in situ* hybridization
GST	glutathione-S-transferase
HNPP	hereditary neuropathy with liability to pressure palsies
hpf	hours post fertilization
IDGF	insect-derived growth factor
kb	kilobases (RNA) or kilobase pairs (DNA)
kDa	kilodaltons
LCR	low-copy repeat
LiCl	lithium chloride
LINE	long interspersed nuclear element
Mb	megabases (RNA) or megabase pairs (DNA)
MDGF	mollusk-derived growth factor
$MgCl_2$	magnesium chloride
MHC	myosin heavy chain
mRNA	messenger RNA
NaCl	sodium chloride
NaOAC	sodium acetate
NAHR	nonallelic homologous recombination
NBT	nitro blue tetrazolium chloride
OMIM	online mendelian inheritance in man
ORF	open reading frame
PAGE	polyacrylamide gel electrophoresis
PBS	phosphate buffered saline
PCR	polymerase chain reaction
PFGE	pulse-field gel electrophoresis
poly(A)	polyadenylated RNA
PTU	1-phenyl-2-thiourea
PVDF	polyvinylidene fluoride
RACE	rapid amplification of cDNA ends
RNA	ribonucleic acid

RNase	ribonuclease
rpm	revolutions per minute
rRNA	ribosomal RNA
RT-PCR	reverse transcriptase polymerase chain reaction
SDS	sodium dodecyl sulfate
SNP	single nucleotide polymorphism
ssDNA	single-stranded DNA
TAPVR	total anomalous pulmonary venous return
TEMED	tetramethyl ethylenediamine
Tm	melting temperature
TOF	Tetralogy of Fallot
TRE	Tet-responsive element
UTR	untranslated region
V	volts
VCFS	velocardiofacial syndrome

Chapter 1 . Introduction

Chromosomal structural rearrangements can cause genomic disorders in humans (Lupski, 2009). Dosage sensitive genes or essential regulatory elements present in the rearranged chromosomal regions are thought to be responsible for the abnormal phenotypes. Studying the dosage sensitive genes/elements has addressed the molecular basis of clinical phenotypes of numerous genomic disorders.

Cat eye syndrome (CES) is a genomic disorder associated with duplication in 22q11.2 region. *CECR1* is one of the 14 genes located in the smallest duplicated region of 22q11.2 (Footz et al., 2001). I hypothesized that overexpression of *CECR1* is responsible for at least some abnormalities in CES patients. CECR1 is thought to function as an adenosine deaminase to regulate extracellular adenosine in tissues expressing CECR1 (Charlab et al., 2001). Adenosine is a potent regulator of cell growth processes, such as cell proliferation and cell death (Borowiec et al., 2006). Overexpression of *CECR1* may lead to alteration in the levels of extracellular adenosine, thus affecting normal development of tissues expressing CECR1. This hypothesis is supported by the observations that *CECR1* is expressed in CES associated tissues in human embryos, such as heart and kidney (Footz et al., 2001). In this thesis, overexpression of *CECR1* in a mouse model of the heart is applied to address the hypothesis.

1.1 Genomic disorders on 22q11

1.1.1 Genomic disorders

Genomic disorders are conditions caused by DNA rearrangements that result in structural variations, such as deletion, duplication, triplication, insertion, or translocation (Lupski, 1998). Previously, a large rearrangement which is more than one chromosomal band and bigger than ~3-5 Mb could be observed with the conventional light microscope. Submicroscopic rearrangements shorter than ~3-5 Mb could be detected by techniques such as fluorescence *in situ* hybridization (FISH) and pulse-field gel electrophoresis (PFGE) (Gouas et al., 2008). Recently, the application of microarray techniques such as oligonucleotide array comparative genomic hybridization (array CGH) to analyze human genomes have led to the discovery of submicroscopic structural variations named copy number variations (CNVs) ranging in size from kilobases (kb) to megabases (Mb) in a resolution of 1 kilobases (Gouas et al., 2008; Sebat et al., 2004; Urban et al., 2006). It is anticipated that CNVs account for 13% of the normal human genome and occur more frequently than SNPs (Kidd et al., 2008). The structural variation of the human genome, through either genomic aneuploidy or CNVs, is responsible for human evolution, genetic diversity in individuals, and genomic disorders including Mendelian disease and complex traits such as behavior (Shaw & Lupski, 2004; Stankiewicz & Lupski, 2010).

Genomic aneuploidy in humans such as trisomy or monosomy normally results from meiotic non-disjunction. Most of the whole-chromosome aneuploidy of autosomes, except trisomy 13, 18 and 21, are incompatible with

life and will lead to spontaneous abortion (Azmanov et al., 2007). Trisomies account for ~0.3-0.5% of live births. The most frequent trisomy in live births is trisomy 21, which leads to Down syndrome (1 in ~750 live births)(Online Mendelian Inheritance in Man, OMIM 190685)(Lejeune, Turpin & Gautier, 1959). Partial trisomies or monosomies are much less frequent than whole-chromosome aneuploidy. Abnormal meiosis and segregation of balanced chromosomes (genomic inversions, reciprocal translocations) leads to partial trisomies or monosomies with either an unbalanced non-robertsonian rearrangement (1 in ~1,800 live births) or an unbalanced robertsonian translocation (1 in ~14,000 live births)(Antonarakis et al., 2004). Partial trisomies have also been observed in Down syndrome patients (Barlow et al., 2001), indicating that not all of the genes/regulatory elements on chromosome 21 are responsible for abnormal phenotypes of patients with Down syndrome.

Most CNVs are caused by non-allelic homologous recombination (NAHR) in meiosis mediated by low-copy repeats (LCRs). It is reported that up to 5% of the haploid human genome is present in two or more copies (Bailey et al., 2001). LCRs are those DNA fragments which have DNA sequence identity greater than ~90% and size larger than 1 kb (Stankiewicz & Lupski). When LCRs are located at a distance less than ~10 Mb from each other, they can cause misalignment of chromosomes or chromatids and result in NAHR. NAHRs mediated by directly oriented LCRs or inverted LCRs are the molecular mechanism for reciprocal deletions and duplications, or inversions. The first identified microduplication disorder Charcot-Marie-Tooth disease type 1A

(CMT1A, OMIM 118220), an inherited peripheral neuropathy, is caused by a ~1.4 Mb duplication within chromosome 17p12 mediated by two 24-kb low-copy repeats (CMT1A-REPs). The reciprocal deletion of the same fragment leads to hereditary neuropathy with liability to pressure palsies (HNPP)(Inoue et al., 2001; Pentao et al., 1992).

One of the most common mechanisms for producing abnormal phenotypes in genomic disorders is copy number imbalance of the genes or regulatory elements involved in the altered chromosome region. Potential dosage sensitive genes encode growth factors, subunits of multimeric proteins, transcription regulators, cell surface receptors and ligands, transporter molecules, cell adhesion molecules and morphogens (Antonarakis et al., 2004). Other molecular mechanisms, such as position effect, have been reported to cause phenotypic effects. A microduplication located downstream of proteolipid protein gene (*PLP1*) has been found to silence the *PLP1* gene and lead to the *PLP1*-related dysmyelinating disorder spastic paraplegia type 2 (Lee et al., 2006).

Usually there is more than one functional element present in a gene rich rearranged region. Not all of the functional elements in the region are involved in the pathology of a genomic disorder. For example, although other functional elements were located within the 1.4 Mb duplicated region in CMT1A, it was found that a point mutation in peripheral myelin protein-22 gene (*PMP22*) was sufficient to produce the CMT1A phenotype (Valentijn et al., 1992). Further examinations using a transgenic mouse model proved that only the duplication or

point mutation of *PMP22* gene accounted for the peripheral neuropathy in CMT1A patients (Huxley et al., 1996).

In genomic disorders associated with larger chromosomal regions, which involve multiple organ system and high degree of phenotypic variability, including Down syndrome and cat eye syndrome discussed in this thesis, it is likely that more than one gene acts interactively to produce the complete phenotypes, while a subset of gene/genes may account for only some of the phenotypes. As a consequence, it has been much harder to identify the genotype-phenotype correlations, when large chromosomal regions are involved. A combination of tools such as genome sequencing, comparative sequence analysis, and animal models have been used to identify candidate genes with specific phenotypes (Antonarakis et al., 2004).

The study of Down syndrome serves as a good example of well-examined genomic disorders. Most patients with Down syndrome carry an extra chromosome 21 (HSA21, the smallest chromosome in humans). Subsequent to the completion of sequencing the 33.6 Mb gene rich 21q-arm, 261 (data from ENSEMBL) to 334 (data from Denver analysis) protein-coding genes have been identified (Hattori et al., 2000; Nikolaienko et al., 2005; Pletcher et al., 2001), using computational prediction, comparative sequence analysis of human and mouse, EST sequencing and laboratory verification. Functional analysis of the HSA21 encoded proteins for protein families, domains and functional sites in the Gene Ontology Annotation database (http://www.ebi.ac.uk/GOA/newto.html)

suggests that the proteins are involved in 87 different biological processes and 81 different molecular functions (Antonarakis et al., 2004).

A transgenic mouse line, Tc1, which carries a stable almost complete human chromosome 21 (HSA21), has phenotypes that resemble human Down syndrome (O'Doherty et al., 2005). Transgenic mice with partial trisomies of mouse chromosome 16 (MMU16, homologous to HSA21), such as Ts65Dn, Ts1Cje, and Ms1Ts65, have also been produced (Davisson et al., 1993; Sago et al., 1998; Sago et al., 2000). Each of these transgenic lines overexpresses a subset of the HSA21 homologous genes and demonstrates several phenotypes associated with Down syndrome. It has been suggested that different duplicated regions could be responsible for specific phenotypes. For example, the Ts65Dn mouse overexpressing 132 genes located on the MMU16 region exhibited phenotypes that included learning and behavioural deficits, reduction of the cerebellar volume, reduced cell number and volume in the hippocampal dentate gyrus and other neurological phenotypes (Davisson et al., 1993). However, the Ts1Cje mouse and the Ms1Ts65 mouse, both overexpressing a subset of the 132 genes in the Ts65Dn mouse, showed only a subset of phenotypes observed in Ts65Dn mouse, such as less severe learning and behavioural deficits and cerebellar dysmorphology (Sago et al., 1998; Sago et al., 2000). In humans, susceptibility regions for 25 phenotypes of Down syndrome have been mapped in 19 partial trisomies for different segments of HSA21 using array CGH in patients with partial trisomy and unbalanced translocation with HSA21 (Lyle et al., 2009).

In order to pinpoint genes responsible for a specific feature of Down syndrome, mice engineered to have extra copies of a single gene from the Down syndrome region have also been produced. For example, transgenic mice carrying the human Cu/Zn-superoxide dismutase gene (*SOD*) showed learning defects similar to DS related features (Epstein et al., 1987). Another way to identify the role of a single gene in a genomic disorder with multiple phenotypes is to introduce the normal two copies of the gene in a trisomy mouse model; thus the role of the euploidy gene could be suggested from the deduced phenotypes of the partial euploidy model. For instance, a proto-oncogene *Est2* has a role in repressing the early stage of transformation. The Ts1Rhr mouse with partial trisomy of 33 genes on MMU16 engineered to have the normal two copies of the *Est2* gene but three copies of the other 32 genes showed an increased number of tumors (Sussan et al., 2008). Thus the extra copy of *Est2* is responsible for at least a portion of the tumor repression feature in the Ts1Rhr mouse.

1.1.2 Genomic disorders associated with 22q11

Chromosome 22 (HSA22) was the first human chromosome being fully sequenced. It is the second smallest human chromosome spanning approximately 49 Mb and comprising 1.6-1.8% of the genome DNA (Dunham et al., 1999). It is one of the five acrocentric chromosomes in humans. The short p-arm does not harbor any identified protein coding genes but contains tandemly repeated ribosomal RNA (rRNA) genes. The 34 Mb long q-arm is gene rich compared with other chromosomes. 946 genes were annotated in this region using differential hybridization mapping (DHM) microarray (Rinn et al., 2003).

Comparative mapping of human chromosome 22q with mouse genome showed that mouse chromosome 6, 16, 10, 5, 11, 8 and 15 contains regions of conserved synteny to HSA22q in order from centromere to telomere (Carver & Stubbs, 1997).

Eight low-copy repeats LCR22s are present in 22q11 (Edelmann et al., 1999) that might mediate non-allelic homologous recombination (NAHR) resulting in the chromosomal rearrangements seen in genomic disorders including cat eye syndrome, velocardiofacial/Digeorge syndrome, and der(22) syndrome (McDermid & Morrow, 2002). Cat eye syndrome is the subject of this thesis and will be discussed in detail in the next section.

The velocardiofacial/Digeorge syndrome (VCFS/DGS, OMIM 192430/188400) is also known as 22q11.2 deletion syndrome. VCFS/DGS has a prevalence estimated at 1:4000. It is typically associated with a 1.5 or 3 Mb microdeletion of 22q11.2 mediated by three LCR22s (Edelmann et al., 1999) (see Figure 1-1). Patients with 22q11.2 deletion syndrome show highly variable features including abnormal faces, cleft palate, cardiac defects such as ventricular septal defect and tetralogy of Fallot, hypoplasia of the thymus, obesity, learning disabilities and mental retardation (Bassett et al., 2005; Shprintzen et al., 1981). At least 30 genes have been identified in the deleted region. However, haploinsufficiency for *TBX1* (T-box 1), a gene encoding a transcription factor, is probably responsible for some of the major features of the patients (Yagi et al., 2003). *Tbx1*-/- mice have phenotypes encompassing almost all the feature of 22q11.2 deletion syndrome (Jerome & Papaioannou, 2001).

Microduplication of the exact same region has also been reported. The phenotypes of microduplication of 22q11.2 are variable, ranging from common features observed in 22q11.2 deletion syndrome (such as heart defects, urogenital abnormalities, velopharyngeal insufficiency) to normal (Ensenauer et al., 2003; Yobb et al., 2005). *TBX1* overexpression may also be responsible for the 22q11.2 duplication disorder (Portnoi, 2009).

Der(22) syndrome is trisomic for 22pter-q11.2 and 11q23.3-qter resulting from a meiotic nondisjunction event in a normal carrier with balanced t(11; 22) (Fraccaro et al., 1980; Zackai & Emanuel, 1980). Features of Der(22) syndrome include preauricular skin tag and/or sinus, ear anomaly, cleft palate, hypotonia, micrognathia, congenital heart diseases, genital anomalies in males and mental retardation (Funke et al., 1999). Many of the clinical features for der(22) syndrome are the same as those for CES. This may be due to overlap of part of the region that is trisomic in der(22) syndrome with the region that is duplicated in most CES patients (see Figure 1-1). However, some common features in CES, such as colobomata, microphthalmia, and TAPVR, are not seen in der(22) patients; while features like cleft palate, hypotonia and mental retardation are much more frequent in der(22) (Berends et al., 2001; Fraccaro et al., 1980). The extra copy of 11q23.3-qter in der(22) syndrome may account for the more frequent features in der(22) and reduce some of the effect of the 22q11.2 duplication.

1.2 Cat eye syndrome

1.2.1 Molecular pathology of cat eye syndrome

Cat eye syndrome (OMIM 115470) is a rare congenital disorder (Schachenmann et al., 1965). Typical CES patients carry a CES marker chromosome in the form of a supernumerary bisatellited dicentric chromosome (inv dup (22) (pter; q11.2)), which results in four copies of the entire p-arm and the most proximal part of the q-arm (22pter-22q11.2 region)(McDermid et al., 1986). The marker chromosome is variable in size and can be symmetric when one breakpoint is used or asymmetric when two breakpoints are used to generate it (Mears et al., 1994). The type I CES chromosome is symmetric and is the outcome of breakpoints at the proximal LCR22-2 in both segments. In the larger type IIb symmetric CES chromosome, both of the breakpoints occur at the distal LCR22-4. The asymmetric type IIa chromosome results from the breakpoints at LCR22-2 in one segment and LCR22-4 in the other segment (see Figure 1-1). The same two breakpoints are also responsible for the generation of the 3 Mb deletion in VCFS/DGS (McTaggart et al., 1998).

Interestingly, there is no obvious correlation between the severity of the phenotypes and the size or copy number of the duplication, which suggests that genes responsible for the CES features may not be located in the extra type II CES region. For example, in one family, the CES marker chromosome is a minute supernumerary double ring with one or two extra copies of the 22pter-22q11.2 region, which results in CES with most of the typical features (Mears et al., 1995). A few patients do not have a CES chromosome but harbor an

interstitial duplication that results in trisomy of the CES region (Knoll et al., 1995; Lindsay et al., 1995; Meins et al., 2003; Reiss et al., 1985), suggesting triplication of genes in the interstitial duplication is sufficient to cause common CES features.

1.2.2 Phenotypes of patients with cat eye syndrome

Patients with CES show high variability in phenotypes and penetrance, ranging from apparently normal to multiple severe congenital malformations (Berends et al., 2001; Denavit et al., 2004; Rosias et al., 2001; Schinzel et al., 1981). Major features of cat eye syndrome in an order of decreasing frequency include anal atresia, coloboma of the iris (a gap or split in the iris, thus the name "cat eye"), ear tags or pits, microphthalmia (almost always unilateral), cleft palate, congenital heart defects, mostly totally anomalous pulmonary venous return (TAPVR) and tetralogy of Fallot (TOF, ventricular septal defect, pulmonic stenosis, overriding aorta, right ventricular hypertrophy), renal malformations (such as absence of one kidney, hydronephrosis, supernumerary kidneys or renal hypoplasia), hernias, reduction of the ear pinnae to several tags and mild to moderate mental retardation. Minor anomalies include hypertelorism, strabismus, inner epicanthic folds, flat nasal bridge and small mandible.

1.2.3 Genes in the CES critical region

The cat eye "critical region" has been narrowed down by mapping small duplications in patients with CES using microsatellite probes. The distal

boundary of the critical region of CES was first delineated to probe D22S36 with a ~3.6 Mb distance to centromere (McDermid et al., 1996; Mears et al., 1994). The individual who harboured a minute supernumerary double ring chromosome and had all major features of the CES contained only the first 2 Mb of 22q, thus further narrowing down the distal region of the CES critical region (Mears et al., 1995).

The first 1-1.5 Mb proximal to the centromere are pericentromeric repeats that are not likely to contain functional genes (Footz et al., 2001). In the distal approximately 700 kb region, 14 putative or known genes were identified by various techniques including exon trapping, sequence annotation, EST analysis, comparative genomics and RT-PCR (see Figure 1-2) (Footz et al., 2001; Johnson et al., 1999; McDermid et al., 1996). Of the 14 human genes, 10 of them were found in the syntenic region on mouse chromosome 6.

Two of the 14 genes, *CECR7* and *CECR8*, map to the pericentromeric region and seem to be non functional. *CECR3*, *CECR4* and *CECR9* may be pseudogenes, since they have either incomplete gene structure or are not predicted to encode a protein. The *IL-17R* gene encodes the receptor of interleukin IL-17 cytokine (Yao et al., 1997). Its ligand IL-17 is only expressed in CD4+ T-cells (Yao et al., 1995), which suggests that dosage changes of IL-17R cannot lead to features in various systems other than the immune system, which is not affected in CES. *CECR5* shows similarity to a hydrolase which is not expected to be dosage sensitive. Genes similar to *SLC25A18* and *ATP6E* lead to autosomal recessive disorders when mutated and therefore are unlikely to be

responsible for CES features. *MIL-1* and *BID* are probably located outside of the CES critical region (Mears et al., 1995). Finally, *CECR1*, *CECR2* and *CECR6* were chosen for further study in the lab because of their expression patterns and the fact that they may be dosage sensitive based on their predicted functions. *CECR6* is expressed in some tissues affected in patients with CES, such as fetal brain and kidney, and adult heart. *CECR6* encodes a protein that contains multiple transmembrane domains, but its function is unknown (Mousseau, 2005). *CECR2* encodes a component of the chromatin remodeling complex CERF (Banting et al., 2005). The function of *CECR2* is being examined using knockout mouse by other students in the lab and thus is not discussed here. *CECR1* is the focus of my thesis and will be discussed in detail in the following section.

1.3 *CECR1* as a candidate gene for CES

1.3.1 Expression pattern of *CECR1*

CECR1 (cat eye syndrome chromosome region, candidate gene 1), is a secreted member of the adenyl-deaminase growth factor family (Maier, Galellis & McDermid, 2005; Riazi et al., 2000). It spans approximately 30.5 kb in the genome. The *CECR1* transcript is 3941 bp in length based on sequencing of the IMAGE clone 54445 (Genbank AA348024) combined with 5' RACE. The open reading frame of *CECR1* is 1536 bp in length. The gene consists of 9 exons encoding a 511 amino acid protein of approximately molecular weight of 59 kDa. A signal peptide involving the first 29 amino acids was predicted using the

SignalP program. The remaining 2.2 kb 3' UTR of the transcript is mainly *Alu* and LINE repeat sequences (Riazi et al., 2000) (see Figure 1-3).

Based on Northern blot analysis, human *CECR1* mRNA is alternatively spliced to generate a 4.4 kb *CECR1 variant 1* (*CECR1v1*) and a 3.5 kb *CECR1 variant 2* (*CECR1v2*)(Riazi et al., 2000). The 4.4 kb *CECR1v1* was suggested to be the full length 3941 bp transcript with an unknown 5' UTR. The 511 amino acid protein was designated as CECR1 isoform a (CECR1a). The shorter *CECR1v2* begins in intron 3 of the *CECR1* gene and splices to exon 4 of the *CECR1v1*, resulting a truncated 270 amino acid protein CECR1 isoform b (CECR1b), with 10 unique amino acids followed by a region identical to the sequence encoded by *CECR1v1* exon 4 to 9 (Maier, 2005)(see Figure1-3).

The expression patterns of the two variants are different in humans. *CECR1v1* is expressed in adult thymus, spleen, kidney, lung, placenta, and lymphoblast cells. *CECR1v2* is expressed in adult heart, pancreas, kidney, and lymphoblast cells. Of the five fetal tissues (late in gestation) tested, *CECR1v1* was expressed in lung and liver; *CECR1v2* was expressed in lung, kidney and heart with faint expression in brain and liver (Footz et al., 2001; Maier, 2005)(see Figure1-4).

RNA *in situ* hybridization in early human and pig embryos revealed the expression profile of the two *CECR1* variants. In pigs, *CECR1* expression was observed in early embryos. A RNA probe that hybridizes to both *CECR1* variants revealed *CECR1* expression of in kidney tubules, liver, gut epithelia and faint expression in kidney glomeruli, heart atrium and ventricle at embryonic (E)

day 20, 28 and 31. In humans, *CECR1v1* RNA was detected in embryonic heart, kidney, pancreas and gonad. At E34 in humans (equivalent to E20 in pigs), *CECR1v1* RNA was detected throughout the liver, in the excretory tubules of the developing mesonephric kidney, in the outer edge of the truncus arteriosis and atrium, and throughout the ventricle of the heart. However, expression of *CECR1v1* was not detected in heart at E47 or in 8.5 week embryos (Maier, 2005). Based on these data, it is likely that *CECR1v1* has a role at early stage of heart development.

1.3.2 Predicted function of CECR1

Based on sequence data, CECR1a belongs to the adenosine deaminase-related growth factor (ADGF) subfamily of the adenyl-deaminase family (Maier et al., 2005). This family includes proteins similar to adenosine deaminase (ADA, EC 3.5.4.4) with conserved ADA active sites. Unlike the classical cytoplasmic ADA, ADGFs contain a signal peptide and are predicted to be secreted. Adenosine deaminase breaks down adenosine to inosine in purine metabolism (see Figure 1-5). Adenosine plays an important role in normal development as an effective modulator of cell proliferation and migration (Borowiec et al., 2006; Jacobson et al., 1999; Thiel et al., 2005). It also mediates various physiological effects such as vasodilation (Dubey et al., 1996; Mosqueda-Garcia, 1992). Some members of the ADGFs, such as IDGF in flesh fly (Homma, Matsushita & Natori, 1996; Homma et al., 2001; Tanaka et al., 2006), ADGF-A and ADGF-D in fruit fly (Maier et al., 2001; Zurovec et al., 2002), MDGF in sea slug (Akalal et al., 2003; Akalal, Schein & Nagle, 2004),

and Ll_ADA in sand fly (Charlab et al., 2001) have been shown to be growth factors whose function requires their adenosine deaminase activity. In vertebrates, *Xenopus* CECR1 has recently been shown to have growth factor activity dependent on its ADA activity (Iijima et al., 2008). Thus, ADGFs may act as secreted growth factors by reducing extracellular adenosine.

1.3.3 ADA1 and ADA2

Human ADA activity consists of two kinetically distinct isoenzymes, ADA1 and ADA2, which are encoded by separate genes (Hirschhorn & Ratech, 1980). Both ADA1 and ADA2 catalyze the hydrolytic deamination of adenosine or 2'-deoxyadenosine to inosine or 2'-deoxyinosine, which are further broken down and excreted as uric acid by purine nucleoside phosphorylase (PNP) and xanthine oxidase (XO) (see Figure 1-5). The activity of both ADA1 and ADA2 is inhibited by 2'-deoxycoformycin (DCF). However, erythro-9-(2-hydroxy-3-nonyl) adenine (EHNA) is an ADA1 specific inhibitor, and thus can distinguish the two activities (Niedzwicki et al., 1995).

The *ADA1* gene is located on chromosome 20q13.11. It encodes a 363 amino acid protein of approximate molecular mass of 41 kDa (Van der Weyden, Bailey & Garson, 1978). ADA1 is expressed ubiquitously in the human body, particularly in lymphocytes and macrophages. In these cells, ADA1 is present both inside the cells in cytosol and nucleus and outside of the cells on the cell membrane attached to CD26 (Franco et al., 1997; Van der Weyden & Kelley, 1976). Null mutations in ADA1 result in one type of severe combined immunodeficiency (SCID, OMIM 102700).

The *ADA2* gene is suggested to be *CECR1* (Iwaki-Egawa, Namiki & Watanabe, 2004). ADA2 is mostly found in human blood plasma, lymphocytes and macrophages (Ungerer et al., 1992). In chickens and humans, purified ADA2 has similar molecular weight to the predicted weight of chicken and human CECR1 (Iwaki-Egawa et al., 2004; Iwaki-Egawa, Yamamoto & Watanabe, 2006). Additionally, the N-terminal amino acid sequence of the chicken ADA2 is similar to the chicken CECR1. However, ADA activity of purified ADA2 in human serum can only be detected using substrate adenosine with a concentration of at least 34 mM, which is much higher than the physiological adenosine concentration ranging from 0.1-1 μM in the human blood plasma, 25-300 nM in the interstitial fluid, or around 10 μM under hypoxia or inflammatory injury (Lonnroth et al., 1989; Moser, Schrader & Deussen, 1989; Zavialov & Engstrom, 2005). The much higher concentration required for the *in vitro* detection of ADA2 activity indicates that there may be certain essential elements missing in the *in vitro* enzymatic assay.

Surprisingly, CECR1 homologs have not been found in mice and rats. However, adenosine deaminase-like (ADAL), a little-known member of the adenyl deaminase family, has a mouse homolog (Maier et al., 2005). It is possible that ADAL in mice together with ADA takes over the role of CECR1a in rodents.

While the function of CECR1a has been predicted to be that of ADA2, little is known about the function of the truncated CECR1b. CECR1b may not be secreted since no signal peptide is predicted (Maier, 2005). It may not have the

ADA enzymatic activity because two of the conserved residues in the catalytic domain of ADA are missing in this truncated protein or it may have an altered activity. One possibility is that CECR1b regulates CECR1a, by interacting with CECR1a in a dominant negative manner. It is also possible that CECR1b is not functional at all. The specific expression of *CECR1v2* in the CES-affected tissues such as heart and kidney suggests that a high ADA activity of CECR1a is not required in normal heart or kidney embryonic development. Duplication of the CES region may lead to overexpression of *CECR1*a in heart or kidney, thus produce the abnormal phenotypes in the patients with CES.

1.4 Adenosine regulation and heart development

Adenosine is a potent modulator of physiological effects such as heart rhythm and vasodilation (Dubey et al., 1996; Mosqueda-Garcia, 1992). Adenosine also modulates cell proliferation, cell death and migration of many cell types such as epithelial, endothelial, smooth muscle cells, and immune and neural lineage cells (Borowiec et al., 2006; Jacobson et al., 1999; Thiel et al., 2005). When there is cellular stress or damage caused by hypoxia, ischemia or inflammation, the level of extracellular adenosine increases more than 100-fold in order to protect the cells (Ijzerman A, July 1997).

The cellular signaling of adenosine is transduced through four types of G protein-coupled adenosine receptors, which are A_1 adenosine receptor (A_1AR), A_{2a}AR, A_{2b}AR and A_3AR (Fredholm et al., 2000). Based on which receptors are present on the cell surface, combined with the activation level of adenosine receptors and the concentration of extracellular adenosine, the effect produced

by adenosine may be different. For example, A_2AR may play a role in immune cell death and immunosuppression caused by the accumulation of adenosine (Lukashev et al., 2004). A_3AR may attenuate vascular dysfunction and improve long-term outcome from myocardial insult (modulating hypertrophy and angiogenesis) (Headrick & Peart, 2005). However, the signaling pathway that leads to cell proliferation or cell death is not clear. Adenosine and A_1AR have been shown to be involved in embryonic heart development (Rivkees, 1995).

Adenosine levels are elevated under hypoxic conditions. Severe fetal hypoxia resulting from pregnant women living at high altitude or smoking may cause fetal growth inhibition and cardiovascular disease (Giussani, 2006). Chicken and mouse embryos exposed to hypoxia also show growth retardation, reduction in heart size and thinner ventricular walls (Ghatpande et al., 2008; Wendler et al., 2007). A_1AR is the only adenosine receptor expressed in embryonic heart when the myocardium becomes visible, therefore, the effects of altered adenosine level may be mediated through A_1AR. A_1AR is activated by a modest increase in adenosine level (Fredholm et al., 1994). *In vitro* experiments showed that A_1AR activation significantly decreased heart rates in cultured mouse embryos (Porter & Rivkees, 2001). Experiments also showed that reduced A_1AR affected cardiac structural development in mouse by decreasing ventricular size in fetuses as a result of reduced cardiac cell proliferation (Zhao & Rivkees, 2001). However, partial hypoxia (which results in a moderately high level of adenosine) is required in normal heart development in order to drive the shortening and rotation of the outflow tract (Sugishita, Watanabe & Fisher,

2004). These data suggest that adenosine is a potential regulator of cardiac cell division during early development, and therefore changes in extracellular adenosine levels through deamination may lead to the aberrant development of heart.

1.5 Research objectives

The goal of my project was to characterize the *CECR1v1* gene and its possible roles in producing the CES phenotypes in the heart. I posed the following questions:

1. What is the expression profile of *cecr1* in zebrafish? Can a subset of the phenotypes of CES be reproduced in zebrafish overexpressing Cecr1?
2. What is the expression ratio of *CECR1v1* and *CECR1v2* in pigs? Could the answer shed light on the mechanism of the features observed in patients with CES?
3. Can at least a subset of the CES heart phenotypes be reproduced in transgenic mice by overexpressing human *CECR1v1* in the heart?
4. If there are phenotypes in the mice expressing *CECR1v1*, what is the mechanism?

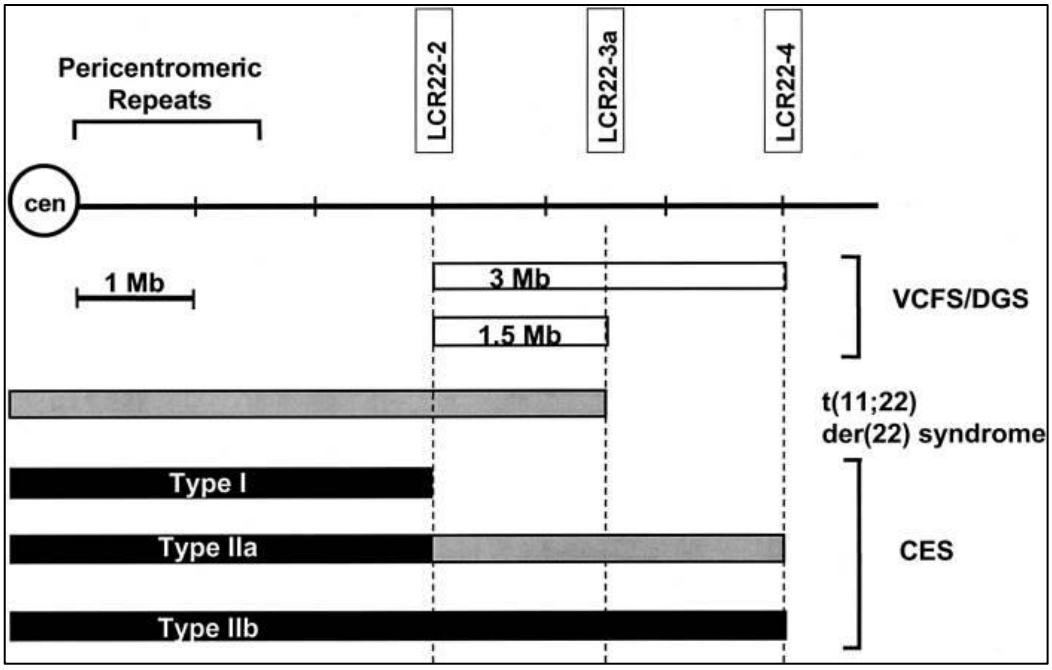

Figure 1-1. Schematic representation of the rearrangement regions in genomic disorders involving chromosome 22q11.

The three LCR22s that mediate the chromosomal rearrangements in VCFS/DGS, der(22) syndrome and CES are shown. White boxes indicate deletions; gray boxes represent three copies; black boxes demonstrate four copies. This diagram was obtained from McDermid & Morrow, 2002.

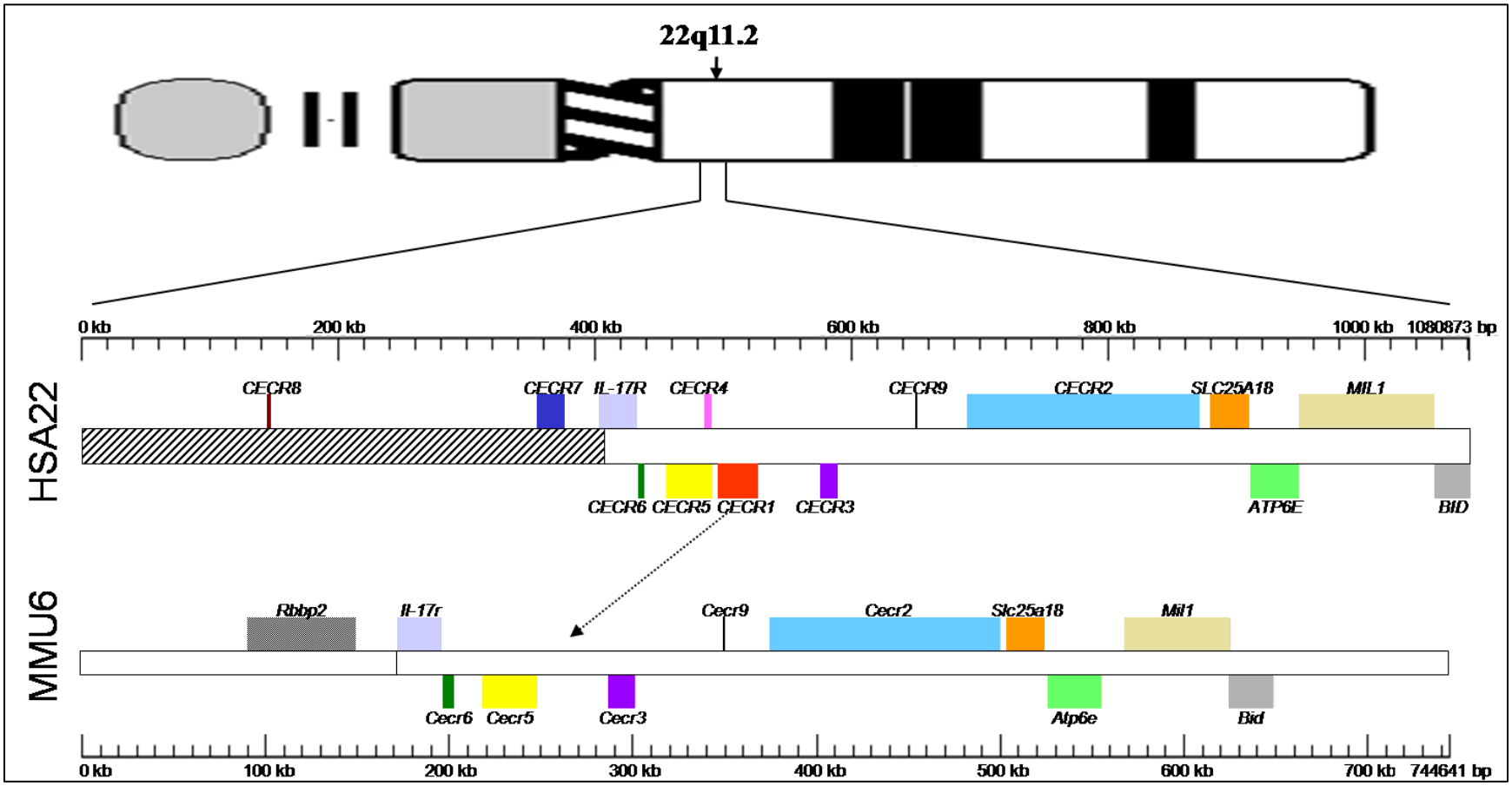

Figure 1-2. Schematic representation of the putative genes identified in the CES critical region and syntenic region in mouse.

The approximate location of the CES critical region within 22q11.2 is shown. Colored boxes indicate genes; hatched boxes represent the pericentromeric region. The arrow highlights the missing *CECR1* homolog in mouse. Adapted from Footz *et al*., 2001.

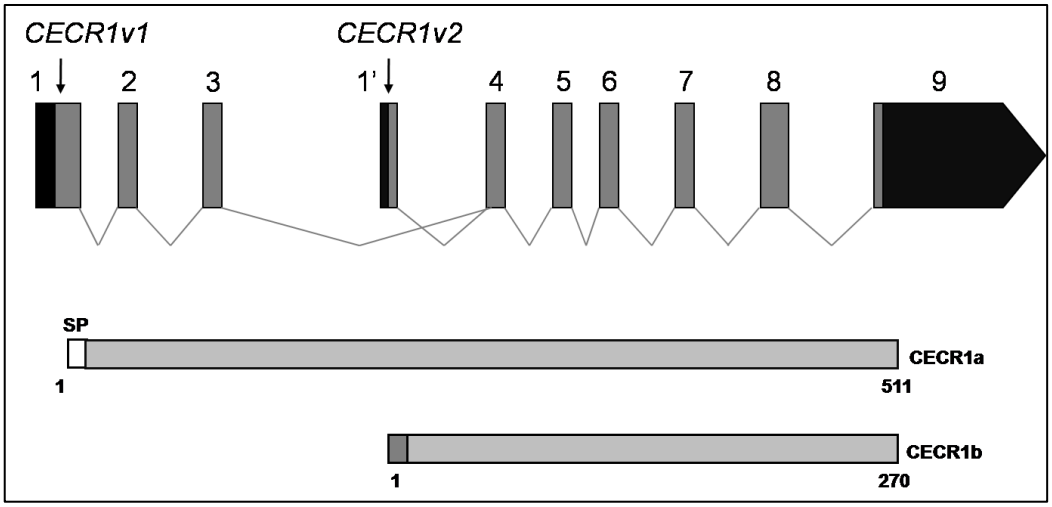

Figure 1-3. Genomic structure and predicted protein sequence of human *CECR1*.

Human *CECR1* mRNA is alternatively spliced to *CECR1v1* and *CECR1v2*. *CECR1v1* encodes a 511 amino acid protein CECR1a. The shorter *CECR1v2* begins in intron 3 of the *CECR1v1* and splices to exon 4 of the *CECR1v1*, resulting a truncated 270 amino acid protein CECR1b. In the gene structure diagram, black boxes represent 5' or 3' UTRs; grey boxes indicate exons. In the protein structure diagram, open box represents signal peptide (SP); light grey boxes indicates protein regions; dark grey box shows the location of CECR1b unique sequence. The diagram were drawn based on information from Footz *et al*., 2001, S. Maier, 2005 and my 5' RACE data.

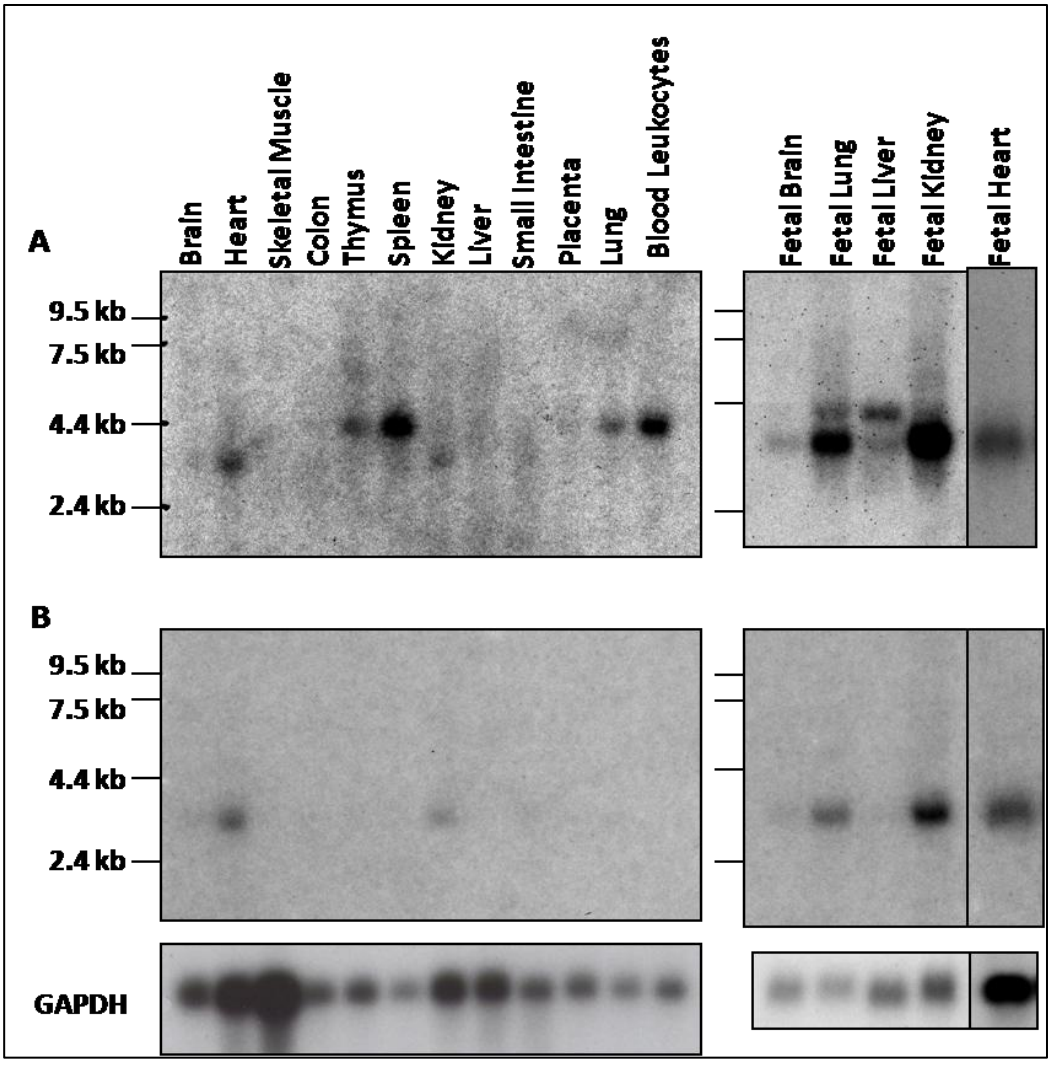

Figure 1-4. Northern blot analysis of human *CECR1v1* and *CECR1v2*.

Human adult and fetal RNAs were hybridized with A) a probe detecting both *CECR1v1* and *CECR1v2* or B) a probe detecting only *CECR1v2*. The 4.4 kb *CECR1v1* transcript was expressed in thymus, speen, liver, lung, blood leukocytes, and fetal lung and liver. The 3.5 kb *CECR1v2* transcript was expressed in adult heart, kidney, and fetal brain, lung, kidney, and heart. Lower panel represents GAPDH loading controls. The figure was obtained from Maier, 2005.

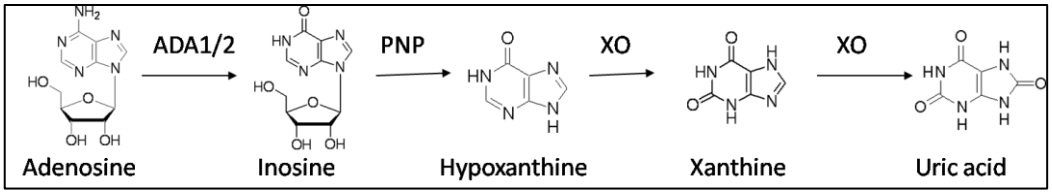

Figure 1-5. Breakdown of adenosine to uric acid in purine metabolism.

ADA1 and ADA2 catalyze the hydrolytic deamination of adenosine to inosine. Inosine is further broken down and excreted as uric acid by purine nucleoside phosphorylase (PNP) and xanthine oxidase (XO).

Chapter 2 . Materials and Methods

2.1 Isolation of nucleic acids

2.1.1 Plasmid DNA

E. *coli* bacteria containing the required plasmid were normally streaked on a LB (Luria-Bertani) plate (1% Tryptone, 0.5% Yeast extract, 1% NaCl, 1.5% Agar, pH 7.0) supplemented with appropriate selective antibiotics. A single colony from the above plate was grown overnight in a 5 ml LB medium (1% Bacto-Tryptone, 0.5% Bacto-Yeast extract, 1% NaCl, pH 7.0) with antibiotics at 37℃ in a shaker.

The bacterial cells were harvested by centrifugation at 13,000 rpm for 30 seconds. Plasmid DNA was then isolated using a QIAprep Spin Miniprep kit (Qiagen) following the manufacturer's instructions. Briefly, cell pellets were resuspended completely in 250 μl Qiagen Buffer P1 with 100 μg/ml RNase A. After adding 250 μl Buffer P2, 350 μl of Buffer N3 was added and mixed gently and immediately by inverting the tube 4-6 times. The above solution was centrifuged at 13,000 rpm for 10 minutes. The supernatant was added to a QIAprep spin column and centrifuged for 15 seconds. The flow-through was discarded and the column was then washed with 500 μl Buffer PB and centrifuged for 1 minute. The column was washed again with 750 μl Buffer PE and centrifuged twice for 1 minute each time. Finally, 50 μl ddH_2O (double distilled H_2O) was added to the column. DNA was then collected into a clean

microcentrifuge tube by centrifuging for 1 minute. The DNA was digested with appropriate restriction enzymes or stored at -20 ℃ until further use.

2.1.2 Purification of DNA from agarose gel

Digested plasmid DNA or PCR products were electrophoresed on a 0.8%-1.5% agarose gel together with a 1 Kb Plus DNA ladder (Invitrogen) with 1× loading dye (10× loading dye: 50% glycerol, 10 mM Tris pH 7.5, 100 mM EDTA, 0.1% bromophenol blue, 0.1% xylene cyanol, and 0.1% orange G) in 1× TAE (40 mM Tris-acetate, 1 mM EDTA, pH 8.4) buffer. The gel slice containing the DNA was cut out with a clean scalpel and extracted from the agarose gel using a QIAquick Gel Extraction kit (Qiagen) according to the manufacturer's instructions. The gel slice was incubated in 3 gel volumes of Qiagen Buffer QG at 50 ℃ for 10 minutes until completely dissolved. Then a mixture of the above solution and 1 gel volume of isopropanol was added to a QIAquick column and centrifuged for 1 minute at 14,000 rpm. Another 500 µl Buffer QG was added to the column and centrifuged for 1 minute to get rid of all traces of agarose. The column was then washed by adding 750 µl Buffer PE and centrifuged for 1 minute. The flow-through was discarded and the column was centrifuged for another 1 minute to remove the trace buffer PE. Finally, 30 µl of ddH_2O was added to the column and centrifuged for 1 minute to collect the DNA in a microcentrifuge tube. 2 µl of the samples was electrophoresed on a 0.8% agarose gel and compared with the DNA ladder with knowing amount to determine the concentration of the purified DNA samples. Alternatively, PCR

products were isolated directly from the PCR reaction using a MinElute PCR Purification kit (Qiagen).

2.1.3 Mouse genomic DNA

Mouse genomic DNA was isolated either from mouse tails, mouse ear notches, mouse livers, or extraembryonic membranes for genotyping or Southern blot analysis. Different methods were used depending on the source of the tissue.

For mouse tails or ears, each biopsy was digested in 350 µl of proteinase K digestion buffer (50 mM Tris pH 8.0, 100 mM EDTA pH 8.0, 0.2% SDS) with 300 µg proteinase K (Invitrogen) at 60 ℃ overnight in a water bath (Banting, 2003). The sample was cooled down on ice for 5 minutes, followed by addition of 125 µl of 5 M NaCl on ice for another 5 minutes to precipitate proteins. The sample was then centrifuged for 15 minutes at 14,000 rpm. The supernatant was transferred to a new microcentrifuge tube and mixed with 500 µl of isopropanol and 0.75 µl of 2% dextran blue. The mixture was kept at -20 ℃ for at least 20 minutes and then centrifuged for 15 minutes at 14,000 rpm. The DNA pellet was washed with 500 µl 70% ethanol and centrifuged for another 15 minutes at 14,000 rpm. The DNA pellet was then dried in air before the DNA was dissolved in 10 µl or 20 µl of distilled H_2O.

DNA from mouse extraembryonic membranes was extracted using the following method. The extraembryonic membranes were digested in Lysis buffer (50 mM Tris pH 8.0, 0.5 mM EDTA, 0.5% SDS, and 0.1 M NaCl) with 150 µg proteinase K at 60 ℃ overnight. The samples were digested for another hour at 60°C with 75 µg proteinase K the next day. After adding 75 µl of 8 M potassium

acetate and 500 µl of chloroform, the mixture was kept at -20℃ for at least 30 minutes. The solution was centrifuged for 5 minutes at 14,000 rpm and the aqueous layer was transferred to a new microcentrifuge tube. After adding 2 volumes of 100% ethanol to the tube to precipitate the DNA, the DNA was pelleted by centrifuge at 14,000 rpm for 15 minutes. The DNA pellet was washed with 500 µl 70% ethanol and then centrifuged for 3 minutes. Finally, the DNA pellet was dry and dissolved in 75 µl of TE buffer (100 mM Tris, 10 mM EDTA, pH8.0).

DNA from mouse livers was isolated based on a modification of a procedure published in the book "Molecular Cloning: A laboratory Manual" (Third edition)(Sambrook, 2001). About 0.2 g of liver tissue was digested in 6 ml of SNET buffer (20 mM Tris pH 8.0, 5 mM EDTA, 0.4 M NaCl, and 1% SDS) with 2.4 mg proteinase K at 55℃ overnight in a shaker incubator. An equal volume of phenol:chloroform:isoamylalcohol (25:24:1, v/v) was added and the samples were rocked at room temperature for 30 minutes. The samples were then centrifuged at 2000 rpm for 5 minutes in a Sorvall GSA rotor. The supernatants were to new microcentrifuge tubes. The samples were centrifuged at 14,000 rpm for 15 minutes after equal volume of isopropanol was added. The precipitated DNA pellets were then washed with 1 ml 70% ethanol and centrifuged at 14,000 rpm for 5 minutes. The ethanol was removed and the DNA pellets were left to dry and then dissolved in 100 µl TE buffer. The concentration of DNA was determined by a NanoDrop ND-1000 spectrophotometer (NanoDrop Technologies, Inc.).

2.1.4 RNA

Total RNA was isolated from mouse, pig, and zebrafish tissues using Trizol reagent (Invitrogen) according to the manufacturer's instructions. Briefly, 0.1-0.2 g of tissue was homogenized in 1 ml Trizol using an Ultra-Turrax homogenizer. The homogenate was incubated at room temperature for at least 5 minutes. 200 µl of chloroform was added to the homogenate and mixed vigorously for 30 seconds before incubation at room temperature for another 2 minutes. The upper aqueous phase was collected and mixed with 1 volume (600 µl) of ice-cold isopropanol and kept at room temperature for 10 minutes before centrifuging at 4℃ for 15 minutes at 14,000 rpm. The supernatant was removed and the RNA pellet was washed with 1 ml ice-cold 75% ethanol in 0.1% DEPC-treated H_2O and centrifuged for 10 minutes at 4℃. The ethanol was then removed. The pellet was dried for about 5 minutes in air and dissolved in 50 µl DEPC-treated H_2O. Concentration and purity of RNA was tested by using a NanoDrop ND-1000 spectrophotometer at 260 nm and 280 nm.

2.2 Southern analysis

2.2.1 DNA probe preparation

The DNA template used for hybridization was amplified by PCR using HID-F5 and HID-R8 primers (Table 2-1) and then purified using a MinElute PCR Purification kit (Qiagen). DNA concentration was determined using a NanoDrop spectrophotometer. The DNA was then labeled using a DECAprimer II random priming DNA labeling kit (Ambion) according to the manufacturer's

instructions. Briefly, the DNA template was diluted with TE buffer to 2.5 ng/μl. Ten μl of the dilution was mixed with 2.5 μl of 10× Decamer solution and denatured by boiling for 5 minutes. The solution was then snap-frozen in dry ice/ethanol to prevent self-annealing of the template DNA. After adding 5 μl of 5× Reaction buffer (concluding dGTP, dATP and dTTP), 5 μl of (α-P^{32})-dCTP (PerkinElmer), 1 μl of Exo-klenow polymerase, and 1.5 μl of ddH_2O to the above thawed solution; the mixture was incubated at 37℃ for 30 minutes. The reaction was stopped by adding 1 μl of 0.5 M EDTA and the unincorporated nucleotides were removed by passing through a Sephadex G-50 column. The flow-through probe was collected and added to 50 ml of hybridization buffer with 100 μl of 20 mg/ml herring sperm DNA.

2.2.2 Southern blot analysis

Approximately 10 μg of each genomic DNA samples or 1 μl of pBiG-CECR1 plasmid DNA was digested with appropriate restriction enzymes overnight. The concentration of the digested DNA samples was determined by using a NanoDrop spectrophotometer. Ten μg of each genomic DNA sample were electrophoresed on a 0.8% agarose (Invitrogen) gel in 1× TAE at 30 V overnight. The gel was agitated in 0.25 N HCl for approximately 10 minutes and then was denatured by soaking in 0.4 N NaOH for 30 minutes. At the same time, Gene Screen Plus nylon membrane (NEN Life Sciences Products) was cut to exactly the same size of the gel and equilibrated in 0.4 N NaOH for 10 minutes after pre-wetting in ddH_2O. The DNA in the gel was capillary transferred to the

nylon membrane in 0.4 N NaOH overnight according the manufacturer's instructions.

The membrane was removed from the gel and rinsed in 2× SSC for 1 minute and dried on Whatman paper. The blot was prehybridized in "Church's buffer" (1% BSA [added fresh], 1 mM EDTA, 0.5 M Na_2HPO_4, 0.4% H_3PO_4, and 7% SDS) for at least 1 hour at 65℃ in a roller-bottle hybridization oven (Tyler Research). The P^{32} labeled probe was then added to fresh hybridization buffer and incubated overnight at 65℃. Two low stringency washes (1.5× SSC, 0.2% SDS) for 10 minutes each were carried out at room temperature following by one or two high stringency washes (0.2× SSC, 0.2% SDS) at 65℃ depending on the radioactive signal. In some cases, a highly stringent wash (0.1× SSC, 0.2% SDS) at 65℃ was required to get rid of high background. Finally, the membrane was exposed to Biomax XAR film (Kodak) at -70℃ for an appropriate length of time (one hour to a week).

2.3 PCR

2.3.1 PCR reactions

A standard PCR reaction used in this study contained 1× PCR buffer (25 mM Tris pH 9.0, 50 mM KCl, 1.5 mM $MgCl_2$, and 0.02 mg/ml bovine serum albumin [BSA]), 0.2 mM dNTPs (Invitrogen), 0.4 μM of each primer (IDT), 1 μl of DNA (around 0.5 μg), and 1 U of *Taq* polymerase (Department of Microbiology, University of Alberta) in a 25 μl volume. PCR reactions were performed in a PTC-200 programmable thermal cycler (MJ research) using

either 200 µl clear tubes or a PCR plate sealed by mineral oil to prevent evaporation of the solutions. A typical PCR program procedure was: a 90 seconds "hot start" at 94 ℃; followed by 25-30 cycles at 94 ℃ for 30 seconds, annealing for 30 seconds at an appropriate temperature based on the primers used, 72 ℃ for 60 seconds per kb of amplification; and one final extension step at 72 ℃ for 5 minutes. The annealing temperature of a primer pair was determined by the calculated melting temperature minus 5-10 ℃. The formula used to calculate the melting temperature was: Tm = 67.5+34(%G+C)-395/# of bases (Stephanie Maier, personal communication). The size and concentration of the PCR products was checked by running 2 µl of the samples on an agarose gel. The PCR products were sequenced either after purification using a MinElute PCR Purification kit (Qiagen) or after cloning into pGEM-T Easy vector (Promega, Figure A1).

2.3.2 RT-PCR

Total RNA was extracted from tissues using the Trizol reagent (Invitrogen). RT-PCR was performed using ThermoScript RT-PCR system with modifications. Approximately 1 µg of RNA was treated with 1 U DNase I (Invitrogen) and 1 µl (40 U) RNaseOUT (Invitrogen) in 1× DNase I buffer in a 10 µl reaction at room temperature for at least 15 minutes. The reaction was stopped by incubating at 65 ℃ for 10 minutes with 1 µl of 25 mM EDTA. The first-strand cDNA synthesis was carried out in a 20 µl volume reaction with the above treated RNA mixed with 2.5 µM Oligo$(dT)_{20}$ primer, 1 mM dNTPs, 1× cDNA synthesis buffer, 5 mM dithiothreitol (DTT), and 15 U ThermoScript

reverse transcriptase. The reaction was performed in a PTC-100 programmable thermal cycler (MJ Research) using the following conditions: 42 ℃ incubation for 30 minutes, followed by 10 minutes in each of 50 ℃, 53 ℃, 55 ℃, 57 ℃ and 60 ℃, and 5 minutes incubation at 85 ℃. Finally, the reaction was incubated for 20 minutes at 37 ℃ with 2 U of RNase H to remove traces of RNA. The first-strand cDNA could be stored at -20 ℃ for up to a month. Around 2 μl of a 1:4 dilution of cDNA was used in a standard PCR reaction. As a negative control, each RNA sample underwent the above procedure without reverse transcriptase present in the first-strand cDNA synthesis reaction.

2.3.3 RACE

5’ and 3’-rapid amplification of cDNA ends (RACE) was performed to identify human and pig *CECR1v1* and *CECR1v2*’s 5’ ends, and in order to obtain the full length human *CECR1* antisense transcripts. BD SMART RACE cDNA Amplification kit (BD Biosciences Clontech) was used according to the manufacturer’s instructions. 5’-RACE ready cDNA was synthesized in a 10 μl volume reaction containing 1 μg of RNA sample, 1 μl of 5’-CDS primer (which is a modified oligo (dT) primer), 1 μl of BD SMART II A oligo (which anneals to the cDNA tail and serves as an extended template for RT), 1× First-Strand buffer, 2 mM DTT, 1 mM dNTPs, and 1 μl BD PowerScript Reverse Transcriptase. 3’-RACE ready cDNA was also synthesized in 10 μl volume reaction containing 1 μg of RNA sample, 1 μl of 3’-CDS primer (which was a modified oligo (dT) primer and also had a portion of BD SMART oligo at its 5’ end), 1× First-Strand buffer, 2 mM DTT, 1 mM dNTPs, and 1 μl BD

PowerScript Reverse Transcriptase. The reactions were incubated at 42 ℃ for 1.5 hours in a PTC-100 programmable thermal cycler. The products were then diluted with 100 μl Tricine-EDTA buffer and heated at 72 ℃ for 7 minutes before storage at -20 ℃.

The subsequent PCR reaction was performed in a 50 μl reaction containing 2.5 μl cDNA, 1× BD Advantage 2 PCR buffer, 1 mM dNTPs, 1 μl of BD advantage 2 Polymerase mix, 1× Universal Primer A mix (UPM, which recognized the BD SMART oligo), and 0.2 μM 5'-gene-specific primer (5'-GSP) or 3'-gene-specific primer (3'-GSP). The conditions for the reaction were as follows: 5 cycles at 94 ℃ for 30 seconds and 72 ℃ for 3 minutes; another 5 cycles at 94 ℃ for 30 seconds, 70 ℃ for 30 seconds, 72 ℃ for 3 minutes; and finally 25 cycles at 94 ℃ for 30 seconds, 68 ℃ for 30 seconds, and 72 ℃ for 3 minutes.

In some cases, a secondary PCR was conducted with the above PCR product to decrease nonspecific background. The "nested" PCR reaction was performed in a 50 μl reaction containing 5 μl of the above PCR product diluted to 1:50 with Tricine-EDTA buffer, 1× BD Advantage 2 PCR buffer, 1 mM dNTPs, 1 μl of BD advantage 2 Polymerase mix, 0.2 μM of Nested Universal Primer A (NUP) and 0.2 μM of customer designed nested GSP (NGSP). The conditions for the reaction were as follows: 25 cycles at 94 ℃ for 30 seconds, 68 ℃ for 30 seconds, and 72 ℃ for 3 minutes. Five μl of the reaction were analyzed on an agarose gel to determine the size of the PCR-amplified product. The remaining 45 μl of the reaction was then separated and isolated from an

agarose gel and cloned into pGEM-T Easy vector (Promega, Figure A1) for sequencing.

2.3.4 Sequencing

Sequencing of PCR products and clones was performed with the fluorescently labeled DYEnamic ET terminator cycle sequencing kit (Amersham Biosciences) using an ABI 377 automated sequencer (Applied Biosystems). The reactions were conducted according to the manufacturer's instructions with some modifications. A 10 μl reaction contained up to 4.5 μl of DNA (or 400 ng of DNA), 2 pmol of the appropriate primer, and 4 μl of the sequencing premix. The reaction was performed as follows: of 95 ℃ incubation for 1 minute following by 30 cycles of 95 ℃ for 40 seconds, 60 ℃ for 40 seconds, and 50 ℃ for 1.5 minutes, with 5 minutes of extension at 72 ℃. The reaction product was precipitated by adding 1 μl of 1.5 M NaOAc/250 mM EDTA and 40 μl of 95% ethanol at -20 ℃. Samples were kept at -20 ℃ for at least 30 minutes and then centrifuged for 15 minutes at 14,000 rpm. The ethanol was aspirated and the pellet was washed with 200 μl of 70% ethanol followed by centrifuging for 5 minutes at 14,000 rpm. The pellet was dried for 5 to 10 minutes and sent to the Molecular Biology Service Unit (MBSU) for the remainder of the sequencing. Chromatographs obtained from the automated sequencer were analyzed by GeneTool v2.0 (Biotools)

2.4 *In situ* hybridization in zebrafish

2.4.1 Embryo collection and storage

Zebrafish AB or *nacre* from the Aquatics facility (Department of Biological Sciences, University of Alberta) was naturally spawned to obtain embryos. Embryos were maintained at 28.5 ℃ in embryo medium according to standard procedures (Westerfield, 1995). 0.003% 1-phenyl-2-thiourea (PTU) was added to embryo medium to reduce pigmentation of embryos at 24 hours post fertilization (hpf). Embryos ranging from 8 to 72 hpf were collected and fixed in 4% paraformaldehyde (PFA) in 1× PBS (137 mM NaCl, 2.7 mM KCl, 10 mM Na_2HPO_4, 2 mM KH_2PO_4, pH 7.4) overnight at 4 ℃. The chorions of older embryos (24-72 hpf) were removed with forceps under a dissecting microscope to straighten embryo tails. The chorions of younger embryos (less than 24 hpf) were removed after fixation. After fixation, embryos were washed in 1× PBS twice for 2 minutes each, dehydrated in a methanol gradient (2 minutes each in 25%, 50%, 75% and twice in 100% methanol), and then stored in 100% methanol at -20 ℃ until required.

2.4.2 Preparation and testing of digoxigenin-labeled RNA probes

Linearized plasmid DNAs used as templates for making digoxigenin (DIG)-labeled RNA probes using the T7 promoter obtained in two ways. First, the zebrafish *cecr1a* containing plasmid (pBluescript SK (-)-*zfcecr1a*) was linearized with *Hap* I which cuts in the middle of the gene, thus producing an antisense probe covering a region from the *Hind* III in the multiple cloning

region at the 3' end of the gene. Second, the probe regions for *cecr1b* were amplified by RT-PCR using zebrafish total RNA and specific primers (Table 2-1) and then cloned into the EcoRV site of pBluescript Sk- vector (Stratagene, Figure A2) in both directions, such that both sense and antisense probes could be made separately using the T7 promoter. Plasmids were linearized with *Hind* III which cuts outside the 5' end of the probe region. The linearized plasmids were electrophoresed on a 0.8% agarose gel and isolated using a QIAquick Gel Extraction kit (Qiagen).

Single-stranded RNA probes for *in situ* hybridization were generated in a 20 µl reaction containing 2 µl of the linearized DNA template, 4 µl of DIG RNA labeling mix (Roche), 20 mM DTT, 2 µl (80 U) RNaseOUT (Invitrogen), and 40 U of T7 RNA polymerase (Invitrogen). The reaction was incubated at 37 ℃ for 2 hours in a PTC-100 programmable thermal cycler (MJ Research). The RNA probe was then precipitated with ethanol and dissolved in 0.1% DEPC-treated water.

The probe was tested for incorporation efficiency of the DIG-labeled UTP by carrying out a dot detection reaction. 0.5 µl of a serial dilution of the probe from 10^{0} to 10^{-3} was dotted on a piece of GeneScreen Plus (NEN Life Sciences Products) membrane. After fixing the probe to the membrane by UV crosslinking, the membrane was washed in Buffer 1 (10 mM Tris pH 7.5, 150 mM NaCl) for 5 minutes and blocked in fresh 1% blocking reagent in Buffer 1 (10% stock blocking reagent: 10% Blocking reagent [Boehringer-Mannhein] in maleic acid buffer [100 mM maleic acid, 150 mM NaCl, pH 7.5]) for 30 minutes

at room temperature. The membrane was then incubated with the antibody solution (1:2000 anti-DIG antibody conjugated to alkaline phosphatase [Roche] in 1% blocking reagent in Buffer 1) for 30 minutes at room temperature. After washing twice with Buffer 1 for 15 minutes each, the membrane was washed twice with Buffer 2 (100 mM Tris pH 9.5, 100 mM NaCl, 50 mM $MgCl_2$) for 5 minutes each. The antibody was detected using staining solution (0.45% NBT, [nitro-blue-tetrazolium chloride, Boehringer-Mannhein] and 0.35% BCIP [5-bromo-4-chloro-3-indolyl phosphate, Invitrogen]) in Buffer 2 in the dark until a purple colored stain was visible (usually about 10 minutes). The relative success of DIG labeling of the probe was indicated by the color density of the dots.

2.4.3 Whole mount *in situ* hybridization

The protocol used was based on a protocol obtained from Dr. Bryan Crawford. All embryos were washed at room temperature on a rotating shaker. All solutions were prepared using 0.1% DEPC-treated water. Fixed embryos were rinsed and dechorionated in 1× PBS. After washing four times in PBS/Tw (1× PBS with 0.1% Tween-20) for 5 minutes each, the embryos were permeabilized with 10 μg/ml proteinase K in PBS/Tw for 30 seconds for early embryos (less than 14 somites), or 1 to 2 minutes for embryos with 18 somites to 24 hpf, 5 minutes for 24 hpf to 60 hpf embryos, and 10 minutes for post-hatching larvae (after 72 hpf). The embryos were post-fixed for 20 minutes in 4% paraformaldehyde in 1× PBS. After washing five times in PBS/Tw for 5 minutes each, the embryos were incubated in pre-hybridization solution (50% formamide, 5× SSC, 0.1% Tween-20, 40 μg/ml heparin [Fisher], 500 μg/ml tRNA [Roche],

pH to 6.0 with citric acid) for two to five hours in microcentrifuge tubes at 70 ℃ in a water bath. The pre-hybridization solution was then removed and the hybridization solution (DIG-labeled probe diluted 1:10 in pre-hybridization solution) was added. Embryos were incubated in hybridization solution at 70 ℃ overnight.

The used probe was collected and stored at -20 ℃ for reuse. The embryos underwent a series of washes at 70 ℃ or as indicated. The embryos were first washed once in pre-hybridization solution and in a pre-hybridization gradient in 2× SSC (3:1 pre-hybridization solution: 2× SSC; 1:1 pre-hybridization solution: 2× SSC; 1:3 pre-hybridization solution: 2× SSC) for 15 minutes each. The embryos were then washed twice in 0.2× SSC for 30 minutes each and in an SSC gradient in PBS/Tw (3:1 0.2× SSC:PBS/Tw; 1:1 0.2× SSC:PBS/Tw; 1:3 0.2× SSC:PBS/Tw; and PBS/Tw) for 10 minutes each at room temperature. Then the embryos were blocked with 5% BSA in PBS/Tx (1×PBS with 0.1% Triton X-100) for 2 hours or overnight at 4 ℃.

After blocking, the embryos were incubated with 1:7000 anti-DIG antibody in blocking solution on a shaker at 4 ℃ overnight. Unbounded antibody was washed away using PBS/Tx by rinsing once followed by five washes of 15 minutes. In order to detect the signal, embryos were washed three times (5 minutes per wash) in AP (alkaline phosphatase) developing solution (100 mM Tris pH 9.5, 50 mM $MgCl_2$, 100 mM NaCl, 0.1% Tween-20), followed by incubation with staining solution (0.45% NBT and 0.35% BCIP in AP developing solution) in the dark until a purple colored stain was observed. To

stop the reaction, the embryos were rinsed once in stopping buffer (1 mM EDTA pH 5.5 in 1× PBS), then dehydrated and stored in methanol at 4 ℃. The embryos were mounted in 3% methylcellulose for photorgraphing. Digital images of the embryos were captured on a Qimaging MicroPublisher 3.3 RTV digital camera attached to an Olympus SZ X12 dissecting microscope.

2.5 Preparation of mRNA for overexpression in zebrafish

Zebrafish *cecr1a* containing plasmid pBluescript-*zfcecr1a* or *cecr1a-myc* containing plasmid pGEM-T-*zfcecr1a-myc* was linearized with *Xho* I or *Sst* I (located at the 3' end of the insert), then separated and purified from a 0.8% agarose gel. In order to add the Myc tag to the 3' end of the *cecr1a* cDNA, *cecr1a* full length cDNA was amplified with a forward primer (ZFmyctagF1) located 5' of the translation start site and a reverse primer (ZFmyctagR1) which spans the stop site of the cDNA but includs a mutated translation stop site of translation and linked with an in frame Myc tag sequence followed by a stop site (see Table 2-1). The modified cDNA fragment was then cloned into the pGEM-T Easy vector.

7-methyl guanosine capped RNAs (which mimic eukaryotic mRNAs) were synthesized *in vitro* using a T3 or T7 mMessage mMachine kit (Ambion Inc.). The mRNA was synthesized by incubation of a 20 μl reaction containing 1μg of the linearized plasmid DNA, 10 μl of 2× NTP/CAP, 1× reaction buffer, 2 μl of T3 Enzyme mix at 37 ℃ for 2 hours. The template DNA was removed by incubation with 1 μl of DNase 1 (Invitrogen) at 37 ℃ for 15 minutes. The mRNA was then precipitated by LiCl and washed by 70% ethanol. The precipitated

mRNA was dissolved in 10 µl of nuclease-free water and stored at -20 ℃ before zebrafish embryo injection.

RNA concentration was determined using a spectrophotometer at 260 nm and 280 nm. RNA integrity was tested by electrophoresis on an agarose-formaldehyde gel (1.2% agarose, 0.615 M formaldehyde, 1× MOPS [20 mM MOPS, 2 mM NaOAc, 1 mM EDTA, pH 7.5]) in 1× MOPS buffer at 80 V until the bromophenol blue dye was near the bottom of the gel. The RNA samples were heated at 60 ℃ for 15 minutes in sample buffer (50% formamide, 2.2 M formaldehyde, 1× MOPS) before loading on the gel with 1/5 volume of RNA loading dye (50% glycerol, 1 mM EDTA pH 8.0, 0.25% bromophenol blue, 0.25% xylene cyanol). The gel was stained in an ethidium bromide solution for 15 minutes following by destaining in ddH_2O for 1 hour before photographing.

0.8 to 4 ng of RNA was injected into the yolks of fertilized embryos between the 1 and 4-cell stage.

2.6 Morpholino design for knockdown in zebrafish

Zebrafish antisense morpholino oligonucleotides *cecr1a* MO (5′ TGCATGTCTGTAAGGTAATTCAACC 3′) (-20 to +5 with respect to the translation initiation site) was designed by Nyssa Ritzel and provided by Gene Tools, LLC (Philomath, OR, USA). The *cecr1a* morpholino covered the translational start site of the *cecr1a* transcript. The morpholino was diluted in Danieau buffer (58 mM NaCl, 0.7 mM KCl, 0.4 mM $MgSO_4$, 0.6 mM $Ca(NO_3)_2$, 5 mM HEPES, pH 7.6) (Nasevicius & Ekker, 2000) to 2.5 ng/µl working

concentration. 2.5-12.5 ng of morpholino was injected into the yolks of fertilized embryos between the 1 and 4-cell stage.

2.7 Immunostaining of zebrafish embryos

The overexpression of zebrafish *cecr1a-myc* in embryos was tested by examine the expression of the myc tag using immunostaining. Zebrafish embryos injected with *cecr1a-myc* mRNA at 1 to 4-cell stages were collected at 3 hpf and fixed in 4% paraformaldehyde overnight at 4℃. After removal of the chorions, the embryos were washed 5 times in PBS/Tx for 5 minutes each and blocked with blocking solution (5% BSA in PBS/Tx with 0.1% sodium azide) for 2 hours. Then the embryos were incubated in mouse anti-c-Myc monoclonal antibody (Molecular Probes) at a dilution of 1:500 in blocking solution at 4℃ overnight. After washing 3 times in PBS/Tx for 15 minutes each, the binding of the primary antibody was detected by incubation with the secondary antibody goat anti-mouse Alexa-488 (Molecular Probes) at a dilution of 1:1000 in the dark for 2 hours. The immunostained embryos were washed 5 times in PBS/Tx for 10 minutes each, mounted in 3% methylcellulose, viewed on a Zeiss Axioskop 2 mot *plus* compound microscope and photographed using a Retiga EXi camera.

2.8 Western analysis

2.8.1 Protein sample preparation

Western blot analysis was performed to confirm that an increased amount of Cecr1a protein was present in the *cecr1a-myc* injected embryos. Embryos

injected with *cecr1a-myc* were collected, frozen in liquid nitrogen and stored at -70℃ until required. Embryo lysates were prepared by homogenization in an equal volume of 2× SDS loading buffer (1× SDS loading buffer: 58 mM Tris pH 6.8, 1.7% SDS, 5% glycerol, 100 mM DTT, and 0.01% bromophenol blue) using a microfuge pestle. After centrifuging at 14,000 rpm for 10 minutes, the supernatant was transferred to a new microcentrifuge tube for immediate electrophoresis or placed at -70℃ for long-term storage until required.

2.8.2 Western gel electrophoresis and transfer

The equivalent of 1 to 5 embryos per lane was loaded along with BenchMark protein ladder (Invirogen) into the stacking layer (5% acrylamide, 62.5 mM Tris pH 6.8, 0.1% SDS, 1.2% APS, and 10 μl of TEMED) and separated on a 7.5% acrylamide-SDS gel (7.5% acrylamide, 420 mM Tris pH 8.8, 0.1% SDS, 0.07% APS, and 8 μl TEMED). The SDS-PAGE gel was electrophoresed in running buffer (25 mM Tris, 190 mM glycine, and 0.1% SDS; pH 8.3) at 200V using a mini-PROTEAN 3 cell gel electrophoresis apparatus (BioRad) until the bromophenol blue dye reached the bottom of the gel (Ames, 2006). The proteins were then electroblotted onto Immobilon-P PVDF membrane (Millipore) at 100 V for 1.5 hours at room temperature or 30 V overnight at 4℃ in transfer buffer (25 mM Tris, 190 mM glycine, and 20% methanol) using a mini-PROTEAN 3 cell gel transfer apparatus (BioRad). The proteins were then visualized by incubating the membrane in 1× Ponceau S solution (0.1% Ponceau S in 1.5% trichloroacetic acid and 1.5% sulfosalicylic

acid, Sigma) for 30 minutes, followed by destaing in 5% acetic acid. The protein markers were traced with a pencil.

2.8.3 Detection of proteins

All the steps of the following detection procedures were carried out at room temperature on a rocker. The membrane was rinsed twice in PBS/Tw before being blocked in 5% skim milk powder (Carnation) in PBS/Tw for 1 hour and then washed 3 times in PBS/Tw for 5 minutes each. The membrane was then incubated with mouse anti-c-myc monoclonal antibody (Molecular Probes) diluted 1:10,000 in 2.5% BSA (Sigma) in PBS/Tw for 1 hour. After washing away the excess primary antibody with 2 rinses and two washes for 10 minutes and 5 minutes respectively in high salt PBS/Tw (HS-PBS/Tw, 0.1% Tween-20 and 500 mM NaCl in 1 × PBS), the membrane was incubated in goat anti-mouse HRP antibody diluted1:10,000 in 2.5% BSA in HS-PBS/Tw for 1 hour. After being rinsed twice and washed twice for 5 minutes in PBS/Tw, the HRP signal was detected using an ECL western blotting analysis system (Amersham Biosciences). The blot was exposed to Biomax XAR film for 5 minutes to 1 hour.

2.9 Preparation of DNA fragments to create *CECR1* transgenic mice

2.9.1 FVB/N-Tg(MHC-hCECR1) line

DNA fragments for pronuclear injection to create the FVB/N-Tg(MHC-hCECR1) transgenic mice were generated by linearizing the pMHC-hCECR1 plasmid obtained from Dr. Ali Riazi (Riazi, Van Arsdell & Buchwald, 2005). This pMHC-hCECR1 plasmid contained the 1603 bp human *CECR1* (*hCECR1*)

opening reading frame (ORF) (GenBank NM_017424) cloned into the α-MyHC clone 26 (GenBank U71441) (Gulick et al., 1991) at the *Sal* I cloning site. The α-MyHC clone 26 contained the promoter region of the murine alpha cardiac myosin heavy chain (α-MHC) in a pBluescript SK II (+) vector.

XL-1 Blue bacteria were transformed with the pMHC-hCECR1 plasmid and streaked on a LB plate supplemented with 100 μg/ml Ampicillin (Amp). A single colony from the above plate was inoculated into LB medium with 50 μg/ml Amp and grown overnight at 37 ℃. The plasmid DNA was isolated using a QIAprep Spin Miniprep kit (Qiagen). The *CECR1* ORF was then sequenced to confirm the correct sequence of the gene.

The plasmid was then digested with *Not* I (Invitrogen), which released the approximately 7 kb fragment of the human *CECR1* ORF linked to the α-MHC promoter. In general, restriction enzyme digestions were performed in a 20 μl reaction volume containing 1 μl of plasmid DNA, 0.1 μg/μl BSA, 2 μl of appropriate 10 × React buffer (Invitrogen), and 1 U enzyme for 2 hours at 37 ℃. Multiple digestions were performed to generate sufficient DNA. Ten μl of the digested plasmid was separated on a 0.8% agarose gel along with 0.5 μg of 1 kb Plus ladder (Invitrogen) to check the sizes and the concentration of the fragments. The concentration of the DNA fragments were determined by comparison with the intensity of the 1650 bp band which constitutes 8% of the ladder or 40 ng DNA.

The digested fragments were sent to Dr. Peter Dickie at Health Sciences Laboratory Animal Services (HSLAS) in University of Alberta for pronuclear

injection (Andras Nagy, 2003). Briefly, the DNA was injected into male pronuclei of fertilized eggs generated from fertilized FVB/N females. A number of injected eggs were then implanted into several pseudopregnant FVB/N females. Tail biopsies from the resultant pups were tested for the presence of the human *CECR1* gene by genotyping PCR using HID-F5 and HID-R8 primers (Table 2-1).

2.9.2 FVB/N-Tg(tTA-hCECR1/βgal) line

DNA fragments for pronuclear injection to create the FVB/N-Tg(tTA-hCECR1/βgal) transgenic mice were generated by linearizing the pBIG-hCECR1 plasmid. The pBIG-hCECR1 plasmid was made by cloning the human *CECR1* ORF to the pBI-G vector (Figure A3). Human *CECR1* ORF was amplified from human *CECR1* EST54445 (GenBank AA348024) with CECR1F_PstI and CECR1R_SalI primers (Table 2-1) containing the indicated restriction enzyme sites using Platinum Taq DNA Polymerase High Fidelity (Invitrogen). The *CECR1* ORF with *Pst* I and *Sal* I linkers was then cloned into the pBI-G vector. The pBIG-hCECR1 plasmid was transformed into XL-1 Blue bacteria and isolated by a QIAprep Spin Miniprep kit. The correct sequence of the inserted *CECR1* was confirmed by sequencing.

The pBIG-hCECR1 plasmid was then digested with *Ase* I to cut out the vector sequence and release the 8040 bp DNA fragment containing the β-galactosidase reporter gene and the *CECR1* gene controlled by the bidirectional tet-responsive promoter P_{bi-1}. The digested fragments were sent to Dr. Peter Dickie for pronuclear injection. Tail biopsies from the resultant pups were tested

for the presence of the *CECR1* gene by genotyping PCR using HID-F5 and HID-R8 primers (Table 2-1).

2.10 Maintaining the mouse colony

2.10.1 Mouse husbandry

Mice were housed at the Biological Sciences Animal Services (BSAS) at the University of Alberta. The mice were maintained on a 14 hours light/10 hours dark cycle at 22±2℃. At most five mice per cage were kept in microisolators in ventilated cabinet (Techiplast, Italy). Normally, mice were fed with Laboratory Rodent Diet 5001 (LabDiet) containing 4% fat. Breeding females were fed with Mouse Diet 9F 5020 (LabDiet) with 9% fat from the beginning of breeding until the pups were weaned.

2.10.2 Breeding and identification

Normally, male mice were mated with individual females without separation, which increased the frequency of litters born by post partum mating. In some cases, harem mating was used to increase the number of litters in a short time. Up to three females were put in one cage with a single male. The females were separated from the male when pregnancy was visible. Once a litter was born, the pups were ear notched at around two weeks. The ear biopsies were stored at -20℃ until DNA extraction and genotyping. The pups were weaned at 20 days.

When embryos at a specific embryonic age were needed, one male with up to four females were put together in one cage in the afternoon of a Monday.

From Tuesday to Friday mornings, the females were checked by the BSAS staff for the presence of a vaginal plug left by the male during copulation. The female was separated to another cage if a plug was found. The noon of the plugged day was considered as 0.5 day post coitus (dpc). Unplugged females were removed from the male on Friday and kept for 20 days to check for pregnancy due to missed plugs.

2.10.3 Euthanasia

Mice were euthanized in a microfilter cage with dry ice underneath a rack. Mice were monitored for at least 5 minutes until breathing stopped. Toe pinching for pain response was performed to confirm death. Mice euthanized for heart harvest were dissected immediately. Mice euthanized to keep the colony small were stored at -20 ℃ freezer until incineration.

2.11 Manipulating mouse embryos and hearts

2.11.1 Dissection of mouse embryos and adult hearts

Embryos were removed from the uterus and dissection carried out in 1× PBS under a dissecting microscope. A small piece of extraembryonic membranes or the tip of the tail was removed and used for DNA extraction and genotyping. The embryos were fixed immediately in 4% PFA in 1× PBS at 4 ℃ for 3-6 hours depending on the age of the embryos. Embryos aged between 10.5 dpc and 13.5 dpc were fixed for 3 hours. Embryos older than 14.5 dpc were fixed for 6 hours; embryos older than 16.5 dpc were cut in half at diaphragm position in order to allow the fixative to penetrate into the hearts.

Adult hearts were collected by opening the mouse chest. Before the hearts were dissected, the bodies were weighted. Mouse hearts were weighted after washing in 1× PBS once and dabbed on paper towel to remove all remaining liquid in the heart. The hearts were fixed in 4% PFA at 4℃ overnight.

Fixed hearts and embryos were washed three times in 1× PBS for 5 minutes each. The tissues were then dehydrated in a methanol gradient in 1× PBS (5 minutes each of 25%, 50%, twice of 75%), and stored in 75% methanol at 4℃ until embedding in paraffin.

2.11.2 X-gal staining

X-gal staining was performed to detect the expression of the β-galactosidase reporter gene in the BIG/tTA mice. Fixed mouse hearts and embryos were washed three times in 1× PBS for 5 minutes each followed by three washes in *LacZ* washing solution (2 mM $MgCl_2$, 0.01% deoxycholic acid, 0.02% IGEPAL in 1× PBS) for 15 minutes each. The tissues were then stained in the dark at 37℃ in an incubator with freshly prepared *LacZ* staining solution (2 mM $MgCl_2$, 0.01% deoxycholic acid, 0.02% IGEPAL, 5 mM potassium ferricyanide, 5 mM potassium ferrocyanide, 1 mg/ml X-gal in 1× PBS) overnight or until desired staining intensity was observed. After staining, the tissues were washed three times in 1× PBS for 5 minutes each, followed by dehydrating in a methanol gradient (5 minutes each of 25%, 50%, twice of 75%), and then stored in 75% methanol at 4℃ until embedding.

2.11.3 Tissue sectioning and H&E staining

Embryos older than dpc 14.5 were decalcified in RDO rapid decalcifier (Apex Engineering Products) for 2 hours prior to embedding. The embryos and adult hearts stored in 75% methanol were brought to the Advanced Microscopy Facility at University of Alberta for embedding. The tissues were put in little screen cassettes along with labels written in pencil and processed in a Histomatic tissue processor (Fisher, model 166). Briefly, the samples were dehydrated in 100% ethanol twice for 1 hour each. Then ethanol was cleared by washing in 50% ethanol/50% Toluene for 1 hour and 100% Toluene twice for 0.5 hour each. After infiltration with paraffin twice for 2 hours each under vacuum, each tissue was transferred into an embedding mould with molten paraffin in desired position in relation to the cutting axis. An embedding ring (Simport) was then added on top of the mold and paraffin was filled to the upper lip of the ring. The moulds and cassettes were cooled on a cooling plate until the paraffin was set. The paraffin block was the stored at room temperature until sectioning.

The tissues embedded in paraffin were sectioned at 7 microns using an Autocut 2040 microtome (Reichert-Jung). Serial sections were then mounted on Superfrost Plus slides (Fisher) in a 42 ℃ water bath and dried overnight at room temperature.

Sections were stained with Harris's hematoxylin-eosin following standard procedures used by the Advanced Microscopy Facility. The sections were washed in Toluene twice for 5 minutes to get the paraffin out of the tissue, followed by rehydration in an ethanol gradient, consisting of two washes of 2

minutes in 100% ethanol and 2 minutes washes in each of 90%, 70%, and 50% ethanol in 1 × PBS. The sections were then rinsed in distilled H_2O and stained in Harris's hematoxylin for 5 minutes, followed by another distilled H_2O rinse. Before staining in eosin for 30 seconds, the sections were washed under running tap water for 15 minutes and dehydrated in 70% ethanol for 2 minutes. After eosin staining, the sections were dehydrated in 100% ethanol twice for 2 minutes each and washed in Toluene twice for 2 minutes each. Finally, the sections were covered with coverslips using a few drops of DPX mounting medium (VWR). The slides were dried in a fume hood overnight before photographing. Images were taken using a Leica DM RXA microscope with Optronics digital camera and Picture Frame software.

2.12 ADA assay

2.12.1 ADA activity test in serum

Total ADA activity in mouse or human serum was tested using an Adenosine Deaminase Assay kit (Diazyme). The ADA assay was based on the enzymatic deamination of adenosine to inosine which was converted to uric acid and hydrogen peroxide (H_2O_2) by purine nucleoside phosphorylase (PNP) and xanthine oxidase (XOD). H_2O_2 was further reacted with N-Ethyl-N-(2-hydroxy-3-sulfopropyl)-3-methylaniline (EHSPT) and 4-aminoantipyine (4-AA) in the presence of peroxidase (POD) to generate quinine dye which was then detected by a spectrophotometer (Thermo Scientific) at 550 nm.

Mouse blood was collected by cardiac puncture after deep anesthesia. After leaving the blood to clot at room temperature for 20 minutes, serum was separated by centrifuging at 2500 rpm for 15 minutes. Serum was then kept at 4℃ until the ADA activity assay was performed. Briefly, 10 μl of serum was incubated with 180 μl of Reagent 1 at 37℃ for 5 minutes and then for 3 more minutes after adding 90 μl of Reagent 2. The increase in the A_{550nm} was monitored in a spectrophotometer for 3 minutes with readings recorded at 1 minute interval.

Total activity of ADA was calculated according to the formula: ADA (U/L) $=(\frac{\Delta A}{min} \times Tv)/(\varepsilon \times Sv \times L)$ (Tv= total volume (in milliliters) of the assay; ε= millimolar extinction coefficient of quinine at 550 nm; Sv= volume of sample (in milliliters) used; L= length of the curvet (in milliliters); ε= 32.2×10^{-3}/μM·cm for quinine at 550 nm). The above formula was simplified to ADA (U/L) = 869.6×ΔA/min.

The total ADA activity consisted of ADA1 and ADA2 activity. ADA1 activity could be inhibited completely by EHNA. Thus ADA2 activity was tested using the above reaction with 0.1 mM EHNA added together with Reagent 1.

2.12.2 ADA activity assay in mouse heart protein extracts

Mouse heart cytoplasmic protein was extracted as followed. Mouse hearts were washed 3 times in ice-cold 1× PBS and minced into small pieces with a clean scalpel. Each heart was homogenized using an Ultra-Turrax homogenizer with 500 μl of 250-STM buffer (250 mM sucrose, 50 mM Tris pH

7.4, 5 mM $MgCl_2$) supplemented with 10 µl of protease inhibitor cocktail (Sigma) and 1 mM PMSF. The homogenate was centrifuged at 20,000 g for 10 minutes at 4℃ to remove debris. The protein supernatant was collected, aliquoted and stored at -70℃ until used.

A DC assay Kit (BioRad) was used to quantify protein concentration following the manufacturer's instructions. Known concentrations of BSA were used as protein standards. Twenty five µl of protein sample was combined with 125 µl of reagent A and 1 ml of reagent B and incubated for 15 minutes before the absorbance at 750 nm was recorded using a spectrophotometer (Thermo). Protein concentration was determined by comparing the A_{750} reading of the sample with the standard curve produced using the BSA standards.

The naturally produced O_2^- during oxygen metabolism in mouse heart protein extracts will interfere with the detection of ADA activity using the Adenosine Deaminase Assay kit. Thus a modified procedure for adenosine deaminase enzymatic assay publishing by Sigma was used. The assay was based on the decrease of adenosine by deamination of adenosine to inosine. Ten µl of protein sample was mixed with 50 mM potassium phosphate buffer pH 7.5, 0.045 mM adenosine, and 0.003% (w/v) BSA in a 300 µl reaction. The decrease in the A_{265nm} was recorded in a spectrophotometer for 5 minutes at 0.5 minute interval. Total activity of ADA was calculated using the formula: ADA (U/L) $=(\frac{\Delta A}{min} \times Tv)/(\varepsilon \times Sv \times L)$ ($\varepsilon = 8.1\times10^{-3}$/µM·cm for adenosine at 265 nm). The above formula was simplified to ADA (U/L) = 3704×ΔA/min. ADA2 activity was tested using the above reaction with 10 µM EHNA added.

2.13 Three-dimension reconstruction of mouse hearts

In order to visualize the structural anomalies in mouse embryonic hearts, three-dimension (3-D) images of mouse hearts were generated using Amira software (version 5.2, Visage Imaging). Using serial sections, images of mouse hearts were taken using a Leica DN RXA microscope and a 1.6× objective with a 1.6 auxiliary lens at every three sections. The images from one heart were loaded into the Amira software where the images were aligned. Then structures of the heart were labeled manually on each of the heart images. After completing the tracing of the structures in the heart, a 3-D object was generated.

Table 2-1. Primer sequences used in this study.

Species_Gene	Primer name	5'-3' sequence
Danio rerio_cecr1a	ZFmyctagF1	TGAATTACCTTACAGAC
	ZFmyctagR1	TCAGAGGTCCTCCTCGGAGATGAGCTTCT GCTCAAGTAAACTTTCCCAAA
Danio rerio_cecr1b	ZID2-F1	CGTCAGAGAGAGCAGATGCT
	ZID2-F2	GCCCGATATTCAAACTGCTG
	ZID2-F8	ATTCCTCTAAAAACTAACAC
	ZID2-R1	CAGCCCAGACAGAGCAATG
	ZID2-R2	CTGTGGTCCCGAATAAACTG
	ZID2-R3	CTGTGGTCCCGAATAAACTG
Homo sapiens_CECR1	HID-F5[LP]	GCTGCTGCCGGTGTATGA
	HID-R8[LP]	GCACCTGGTTAGAGATGG
	CECR1F_PstI	GGGCTGCAGCCCGATGTTGGTGGATGG
	CECR1R_SalI	GGCGTCGACCTGGCTAGCTTCTCCTCA
	HID-R1[SM]	CTCCATACAGAGGCCATTGA
	HID-R2[SM]	TGTGAGCTCTCCAAGTGCAT
	HID-I8-A[SM]	TGGGCTCCTCCTCTTCCTG
	ASGSP5-2	ATGAAATCAATGGCCTCTGTATGGA
	V2GSP5	CATTTGAGGTGGGCGTGGCTATTAGGAC
	HID-V2F1	GGGCTCCTAAGTTCGTCG
	HID-V2F2	GTGGCTGGACCCAGACCA
Sus scrofa_CECR1	PID-GSP5	CCCCGGCGTGGAAGAAGTAAGGCAG
	PID-GSP5-2	TGCGGAAGTGCCCTGCCAGTCTGTCTC
	PID-GSP5-3	GCAGGGTGGTTTCTCAGGTCCGACA
	PID-V2F2	CTGCGAGGCTAAGGCTGATC
	PID-R4	GGCGTGGAAGAAGTAAGGCA
Gallus gallus_Cecr1	CHID-GSP5	GGGTATCTGGGAAGTGGGCTCTGAG
Mus musculus	MMU SRY FOR	GAGAGCATGGAGGGCCAT
	MMU SRY REV	CCACTCCTCTGTGACACT
tTA mouse	Tcrd-F	CAAATGTTGCTTGTCTGGTG
	Tcrd-R	GTCAGTCAGTGCACAGTTT
	CamK2tTA-F	CGCTGTGGGGCATTTTACTTTAG
	CamK2tTA-R	CATGTCCAGATCGAAATCGTC
Various vectors	T7	GTAATACGACTCACTATAGGGC
	T3	AATTAACCCTCACTACCGGG
	SP6	ATTTAGGTGACACTATAGAATACT
	M13 forward	GTAAAACGACGGCCAGT

Primers were designed by Fang Yang unless otherwise indicated by the designer: LP, Lynn Podemski; SM, Stephanie Maier. Sequences highlighted in grey depict restriction enzyme sites.

Chapter 3 . Results

3.1 Expression analysis of *cecr1* in zebrafish

Zebrafish (*Danio rerio*) was initially chosen as a model organism to study the effect of *CECR1* dosage alteration, because zebrafish has a nearly transparent body during embryonic development, which provides unique visual access to the animal's internal anatomy. Preliminary experiments also showed that *cecr1* was expressed in zebrafish using northern blot analysis (Maier, 2005). In order to interpret the results caused by overexpression or knockdown of zebrafish *cecr1*, an expression profile of the gene during development was obtained by *in situ* hybridization.

3.1.1 Identification of zebrafish *cecr1b* gene

Two *CECR1* homologues were identified in zebrafish: *cecr1a* and *cecr1b*. The *cecr1a* cDNA was obtained by screening a 19-25 hpf zebrafish lambda-ZAP library and cloned into pBluescript SK- vector by Dr. Stephanie Maier (GenBank AF384217). The presence of *cecr1b* was predicted by GENSCAN (http://genes.mit.edu/GENSCAN.html) analysis of genomic sequences carried out by Dr. Stephanie Maier (Maier, 2005). The presence of *cecr1b* was confirmed by RT-PCR of the *cecr1b* fragments at various stages (Figure 3-1). An initial attempt to generate *cecr1b* full length cDNA by RT-PCR failed. However, the 1535 bp *cecr1b* full length cDNA was obtained by PCR with primers ZID2-F8 and ZID2-R3 using three DNA fragment templates generated by RT-PCR from adult zebrafish total RNA using Platinum Taq DNA

Polymerase High Fidelity which would be less likely to introduce mistakes during the PCR reaction. Location of the fragments A, B and C and primers is indicated in Figure 3-2. Eight single nucleotide mismatches were found in the synthesized *cecr1b*, which led to 6 mismatched amino acids in the protein sequence compared to the predicted protein sequence translated from the genomic DNA (Maier et al., 2005). However, protein sequence alignment showed that the amino acids important for ADA activity were conserved in both zebrafish Cecr1a and Cecr1b (Figure 3-3).

3.1.2 Expression of *cecr1a* and *cecr1b* in zebrafish

Antisense (AS) probes detect the presence of sense transcripts, while sense (S) probes detect antisense transcripts, thus serving as negative controls. Location of the *cecr1a* and *cecr1b* probes used for *in situ* hybridization is shown in Figure 3-4. Two AS probes were made against different regions of zebrafish *cecr1a* gene. The 616 bp probe *ZID1-1* (*ZID1* refers to zebrafish *cecr1a* for historical reasons; *ZID2* refers to *cecr1b*) was located at the 3' UTR of the gene; the 411 bp probe *ZID1-2* spanned exons 9 and 10 of the gene. Two AS and two S probes were prepared for *cecr1b*. Probe *ZID2-1* was generated by RT-PCR using primers ZID2-F1 and ZID2-R1 (Table 2-1). Probe *ZID2-2* was made using ZID2-F2 and ZID2-R3 (Table 2-1). The above fragments were cloned into pGEM-T Easy vector in both directions, thus both antisense and sense probes were made against the above regions.

An *unc-45* probe (obtained from Serene Wohlgemuth) which gave a staining pattern in the striated muscle tissue, including the somites (Wohlgemuth,

Crawford & Pilgrim, 2007) was used as a positive control. The *unc45* probe gave the expected staining pattern in the somites. Both *ZID1* and ZID2 probes gave widespread staining over the embryo body at 9-14 hpf stages tested (Figure 3-5). In 24 hpf embryos, *cecr1a* and *cecr1b* transcripts were found concentrated in the head region; while weak and broad expression was identified in the truck. Trapping of the probe in the head often occurs. The staining in the forebrain region of the head may be artifactual, since staining was observed in this region using the negative control *ZID2-1* S probe. However, *cecr1a* and *cecr1b* transcripts were observed in the midbrain and cerebellum regions. Also a higher level of *cecr1b* transcript was observed in the ventral neural tube using *ZID2-1* probe (see the arrow in Figure 3-6). The staining was focused in the head in 48 hpf embryos, with possible increased staining in the roof plate midbrain region using *ZID2-1* AS probe (see the arrow in Figure 3-7). Faint staining was observed in the head in 72 hpf embryos (Figure 3-8). However, the stain in the head may be artifactual, since the probe is trapped in the head and the trunk is impenetrable and cannot be stained at this older stage. The observed expression pattern of *cecr1a* was consistent with the published data that *cecr1a* is generally expressed in 1-cell to Pec-fin (60 hpf) embryos using *in situ* hybridization (ZFIN database) (Thisse, 2004) and in adult brain, gills, liver and heart tissues using semi-quantitative PCR published after this work was done (Rosemberg et al., 2007).

3.1.3 Overexpression and knockdown of *cecr1a* in zebrafish

In order to study the effect of overexpression of *CECR1* in a model organism, synthetically capped RNAs were produced from linearized pBluescript SK(-)-*zfcecr1a* or pBluescript SK(-)-*zfcecr1a-myc*. Concentration of the mRNA was 0.8 ng/nl and 0.5 ng/nl for *cecr1a* and *cecr1a-myc*, respectively. Embryos were injected with 0.8 to 5 ng of RNA. The embryos were maintained in the embryo media and observed until 72 hpf. At the first day and the third day, the survival rate of the Danieau buffer injected and the mRNA injected embryos was recorded. The gross morphology of the embryos, the size of the eyes, the shape of the hearts, and the heart beat rate were examined 24 hours after injection. However, no obvious abnormalities were observed in *cecr1a* overexpressed embryos, compared to the uninjected control embryos or embryos injected with Danieau buffer. Myc protein levels were assessed at approximately 3 hpf by immunostaining using a myc antibody (Figure 3-9). The protein levels of cecr1a-myc were also confirmed by detecting the myc epitope expression in 9 hpf embryos using western blot analysis (Figure 3-10). Expression of the myc tag was detected using both immunostaining and western blot analysis, which indirectly confirmed successful overexpression of *cecr1a* in the injected embryos.

Zebrafish *cecr1a* antisense morpholino oligonucleotides *cecr1a* MO (5′ TGCATGTCTGTAAGGTAATTCAACC 3′) was designed to cover the translational start site of *cecr1a* transcript. 2.5-12.5 ng of *cecr1a* MO was injected into the yolks of fertilized eggs at the 1 to 4-cell stages. The embryos

were raised in the embryo media and observed until 72 hpf. Embryos were examined in the same way as the *cecr1a* overexpression embryos. The survival rate of the Danieau buffer injected and MO injected embryos was recorded at day 1 and day 3. The gross morphology of the embryos, the size of the eyes, the shape of the hearts and the heart beat rate were observed 24 hours after injection. No obvious phenotype was observed in the zebrafish *cecr1a* knockdown embryos. The overexpression and knockdown of zebrafish *cecr1a* did not produce any conclusive results. The overexpression and knockdown of zebrafish *cecr1b* were not conducted due to time constraints.

3.2 Structure of *CECR1* antisense transcripts in humans

The presence of *CECR1* antisense transcripts mapping to the 3' end of the *CECR1* gene was detected and confirmed both in humans and pigs using *in situ* hybridization, RT-PCR and northern blot by Dr. Stephanie Maier (Maier, 2005). A 3.4 kb antisense transcript was present in human fetal kidney (23-36 weeks). RT-PCR was carried out by Dr. Maier to detect full-length antisense transcript in human fetal kidney. The longest RT-PCR product was generated using HID-I8-A in intron 8 as the reverse primer and HID-R1 in exon 9 of human *CECR1* as the forward primer (Figure 3-11). The product was 229 bp, which is much shorter than the expected 3.4 kb transcript. Thus, both 5' and 3' RACE were carried out to detect the full-length antisense transcript using human fetal kidney RNA (23-36 weeks). First strand cDNA for 5' RACE was synthesized as instructed. Three ASGSP5 primers were designed to amplify the antisense cDNA. Only one RACE product was generated using ASGSP5-2 primer. This

product of ~ 1 kb was ligated to pGEM-T Easy vector and sequenced from both ends of the insertion using SP6 and M13 primers, and in the middle of the sequence using HID-R2 primer. The existence of this transcript was confirmed by RT-PCR using HID-R2 as forward primer and HID-I8-A or ASGSP5-3 as reverse primer. However, the attempt to obtain the 3' end of the antisense transcript using 3' RACE was not successful. Thus the longest antisense fragment obtained so far is an 1174 bp fragment which starts from HID-I8-A to the middle of exon 9 (Figure 3-11).

3.3 Characterizing *CECR1* variants in humans, pigs and chickens

The *CECR1* gene was initially discovered by Dr. Ali Riazi and further characterized by Dr. Stephanie Maier (Maier, 2005; Riazi et al., 2000). Northern blot analysis of *CECR1* in humans suggested there were two variants, one of 4.4 kb and the other of 3.5 kb. The 4.4 kb band was suggested to represent the 3941 bp full length *CECR1v1* transcript obtained by Dr. Ali Riazi using 5' RACE. The shorter 3.5 kb band was suggested to be *CECR1v2*, which has an alternative 107 bp exon 1' beginning in intron 3 and splicing to exon 4 of *CECR1v1*. This novel transcript was found after analysis of an EST (IMAGE clone 2190534, GenBank AI613429) by Dr. Stephanie Maier. Sequencing of a "full-insert sequence" EST (GenBank AK074702) gave rise to a 3071 bp "full length" *CECR1v2*, suggesting that *CECR1v2* may be the 3.5 kb band observed in the northern blot. Northern blot analysis using a probe spanning the exon 1' region indicated that *CECR1v2* was expressed in adult heart and kidney, and fetal lung and kidney in humans. The *CECR1v1* transcript encodes a 511 aa CECR1a. The *CECR1v2* transcript

encodes a predicted protein CECR1b with 10 unique amino acids encoded by exon 1' following by an in frame portion of the CECR1a sequence encoded by exons 4 to 9.

However, there was a question whether the methionine codon of the predicted CECR1b was the actual start site, since there was no upstream stop codon in the *CECR1v2* sequence. Thus, 5' RACE using human fetal kidney total RNA was conducted to identify the start site of the *CECR1v2* transcript. V2-GSP5 primer was used to generate a RACE product. The product was ligated into the pGEM-T Easy vector for sequencing using SP6 primer. A 154 bp exon 1' with an upstream stop codon was found, thus confirming that the predicted start codon was the actual translation start site. A RT-PCR product generated using forward primers HID-V2F1 and HID-V2F2 at the exon 1' region with reverse primer HID-R8 confirmed the presence of the new exon 1' sequence detected by RACE.

The existence of *CECR1v2* in other organisms was examined by 5' RACE. Chicken *Cecr1v1* full-length sequence (GeneBank AY902779, 1962 bp) was obtained by sequencing an EST (GenBank CD738959). Searching for chicken *Cecr1v2* in NCBI nucleotide database was not successful. 5' RACE was then conducted using chicken E12 kidney total RNA with CHID-GSP5 primer which was located in exon 6 of chicken *Cecr1v1*, which should detect both transcripts if *Cecr1v2* existed. However, only one 1.2 kb RACE product was obtained and it was *Cecr1v1*, confirmed by sequencing. Thus it is possible that only *Cecr1v1* was expressed in chickens, at least in the kidney.

The genomic region containing pig *CECR1* had not been sequenced when these experiments were carried out. Exon junctions in pig *CECR1v1* (GenBank AF384216) was predicted by comparing with the exon junctions in human *CECR1v1* (Maier, 2005). 5' RACE was carried out with pig adult heart and kidney total RNA using the PID-GSP5-2 primer, which is located in the predicted exon 6 of pig *CECR1v1* (Figure 3-12). Two RACE products were obtained. Other than the expected pig *CECR1v1*, *CECR1v2* with a unique 212 bp exon 1' with an upstream stop codon was found. This pig *CECR1v2* transcript encoded a predicted pig CECR1b protein with 25 unique amino acids encoded by exon 1' following by an in frame portion of the pig CECR1a protein encoded by the predicted exon 4 to exon 8 sequence.

To confirm the expression of *CECR1v2* in pigs, RT-PCR was conducted in various pig E28-31 embryonic tissues with PID-V2F2 and PID-R4 primers (Figure 3-12). Besides the expected pig *CECR1v2*, a pig *CECR1v2*', whose exon 1' was spliced to exon 5 of the pig *CECR1v1*, was also found (Figure 3-12). It is possible that the existence of pig *CECR1v2*' is not real, since it was only present in some of the embryonic tissues, and the translation of the pig *CECR1v2'* was not in frame with the pig CECR1a protein. The expression of the variants in different pig tissues are shown in Table 3-1. All embryonic and adult tissues tested expressed pig *CECR1v1* and *CECR1v2*, which suggests that *CECR1v1* and *CECR1v2* are both expressed in most of the tissues during the development in both pigs and humans. The comparative levels of expression of *CECR1v1 vs CECR1v2* in some of the human or pig tissues could not be

determined due to the insensitive techniques used to detect the variants, such as northern blot and nonquantitative RT-PCR.

3.4 Overexpression of human *CECR1* in a mouse model

Since overexpression of *cecr1a* in zebrafish did not generate obvious abnormal phenotypes, transgenic mice expressing human *CECR1v1* were constructed to study the effect of overexpression of *CECR1v1* in a model system more similar to humans. CECR1 homolog is not found in mice. However, the other two members of the adenyl-deaminase family, mouse ADA and ADAL, may have similar functions and compensate for the absence of mouse CECR1.

3.4.1 MHC-hCECR1 mouse lines

Transgenic mouse line FVB/N-Tg(MHC-hCECR1) (designated as MHC line) overexpressing human *CECR1v1* was generated by pronuclear injection of the human *CECR1v1* ORF controlled by the heart specific α-MHC promoter through collaboration with Dr. Peter Dickie (HSLAS, University of Alberta).

3.4.1.1 Presence and expression of human CECR1 in the MHC lines

In the FVB/N-Tg(MHC-hCECR1) line, five founders were identified through PCR out of 35 pups produced by pronuclear injection. The presence of the human *CECR1* was detected by PCR of genomic DNA extracted from mouse biopsies using HID-F5 and HID-R8 primers, which produced a 500 bp band in an agarose gel. The founders were mated with normal FVB/N mice (Jackson Laboratories) to establish lines. The MHC transgenic lines were established from

3 founders, designated as MHC42, MHC47 and MHC69 (Figure 3-13). The other 2 founders did not produce transgenic offspring.

Southern blot analysis was used to confirm the presence and detect the copy number of the insertions (Table 3-2). MHC42 line contained approximately 5 copies of inserted human *CECR1*, while MHC47 line and MHC69 line only had 2 copies and 1 copy of *CECR1*, respectively. RT-PCR using various mouse adult tissues confirmed that *CECR1* was only transcribed in hearts, not in other tissues, such as lung, spleen, and kidney, in all the MHC lines (Figure 3-15).

Previous attempts to generate CECR1a antibodies by Dr. Stephanie Maier and me were not successful. Commercial CECR1a antibody purchased from ATLAS Antibodies failed to recognize purified GST-CECR1a recombinant protein in western analysis. Thus expression of human CECR1a was examined through its ADA2 activity. ADA2 activity was tested in human, mouse and rat serum (Figure 3-17) by detecting the H_2O_2 produced in a series of enzymatic reactions using ADA assay kit (Diazyme). As expected, ADA2 activity contributed to the majority (80%) of the total ADA activity in human serum. Mouse and rat serum only exhibited ADA1 activity, which was consistent with the evidence that rodents do not have the *Cecr1* gene. ADA2 activity was tested in transgenic and normal FVB/N mice heart cytoplasmic protein by detecting the consumption of adenosine by ADA. ADA2 activity was detected in normal mouse heart cytoplasmic protein extracts, which was inconsistent with the fact that rodents do not express CECR1. The observed "ADA2 activity" in normal mice may due to the existence of H_2O_2 in the heart cytoplasmic protein extracts.

A higher level of ADA2 activity was observed in MHC47 transgenic mouse heart cytoplasmic protein extracts comparing to normal littermates, indicated by a p-value = 0.02, using single factor Anova test (Figure 3-18). However, MHC42 and MHC69 lines did not exhibit a higher ADA2 activity, indicated by p-value = 0.1, using Anova test.

3.4.1.2 Phenotypic observations of the MHC lines

The MHC mice were examined for phenotypes similar to CES that might be due to overexpression of human *CECR1v1*. However, each founder produced phenotypically normal and healthy pups in most of the cases. Lethality at embryonic stages was not observed in all three of the MHC lines. The ratio of the transgenic pups in the weaned animals was consistent with a Mendelian ratio in both MHC42 and MHC47 lines (Table 3-3), although there were always less than 50% transgenic pups. The above observations suggests that overexpression of *CECR1* in mouse heart may not produce severe phenotypes. More wild type pups were found in the MHC69 line, which possibly was not due to the loss of the transgenic embryos during early embryonic development. However, the surviving transgenic pups were as healthy as the wild type mice.

Since smaller hearts were observed in MHC transgenic mouse lines in Dr. Ali Riazi's study (Riazi et al., 2005), MHC47 mouse hearts were weighted at about 9-week old. No significant difference was observed in the weight of transgenic and normal mouse hearts, based on single factor Anova test (p = 0.775). (Figure 3-19). This difference from the Riazi study may be due to the

different genetic backgrounds of the transgenic mouse lines used in my study (FVB/N) and Dr. Riazi's study (C57B1/6).

By E14.5, all components of the heart are formed. Both the heart and the vascular system have achieved their definitive prenatal configuration. Morphology of E14.5-16.5 embryonic hearts was accessed by histological sections visualized by H&E staining. MHC42 and MHC47 embryos manifested thinner right ventricular walls, as well as left and right atrioventricular valve disorganization (Figure 3-20 & 3-21). None of the examined 9 normal embryos showed these phenotypes.

In order to visualize the observed phenotype, a 3D model of one mutant embryonic heart MHC47e15 at E15.5 (showed in Figure 3-21) was constructed using Amira software. A 3D model of a normal heart MHC47e18 at the same age was also generated as a control. Thinner ventricular wall and ventricular septum were observed in the transgenic embryo comparing to the normal littermate. The video files were attached this thesis. No obvious differences in the position or structure of vessels were observed.

3.4.2 tTA-hCECR1/βgal mouse lines

A "tet off" binary transgenic mouse model, which consisted of an FVB/N-Tg(tTA-hCECR1/βgal) line (carrying an tet-responsive Bidirectional promoter which controls expression of Galactosidase and the inserted *CECR1* gene, thus named the BIG line), and an FVB/N-Tg(MHCAtTA) line (tTA line, purchased from Jackson Laboratories). The BIG lines were produced by pronuclear

injection of the DNA fragment containing the *CECR1v1* ORF downstream of the tet-responsive promoter pBi-1.

When originally planning these experiments, there was a concern that viable progeny with no or minor abnormalities would be selected in the FVB/N-Tg(MHC-hCECR1) lines if severe phenotypes led to embryonic lethality. Moreover, founders or progeny with severe abnormalities could make the lines difficult to maintain, thus preventing further characterization (although this turned out not the case). To circumvent this situation, the "tet-off" system was established. In this system, the tTA line expresses the tetracycline-controlled transactivator (tTA). The FVB/N-Tg(tTA-hCECR1/βgal) should express neither CECR1a nor β-gal without the presence of tetracycline-controlled transactivator, thus to be phenotypically normal. It is only when the BIG line and the tTA line are mated, that the CECR1a is expressed under the control of tTA in the double transgenic pups. Additionally, the bi-directional promoter pBi-1 also drives the transcription of the *β-gal* gene, which serves as a marker indicating coexpression of CECR1 and β-gal (Figure 3-14).

Two founders out of 35 pups produced by pronuclear injection (designated BIG1 and BIG19) were identified by PCR using HID-F5 and HID-R8 primers. They were mated to normal FVB/N to produce stable FVB/N-Tg(tTA-hCECR1/βgal) lines.

Southern blot analysis was used to confirm the presence and detect the copy number of the insertions (Table 3-2). Only one or two copies of the insertion were detected in these two lines. RT-PCR using various mouse adult

tissues confirmed that *CECR1* was only transcribed in hearts in the double transgenic pups (Figure 3-16).

The BIG/tTA double transgenic mouse pups were phenotypically normal and healthy in most of the cases. Lethality at embryonic stages was not observed in either of the BIG lines or the double transgenic pups, as shown by the Mendelian ratio of the transgenic pups in weaned animals (Table 3-4). BIG19/tTA mouse hearts were weighted at about 6-week old. No significant difference was observed in the weight of transgenic and normal mouse hearts by Anova test (Figure 3-22).

Morphology of E14.5-18.5 embryonic hearts was accessed based on histological section visualized by H&E staining. One of the eight BIG19/tTA embryos manifested right atrioventricular valve disorganization (Figure 3-23).

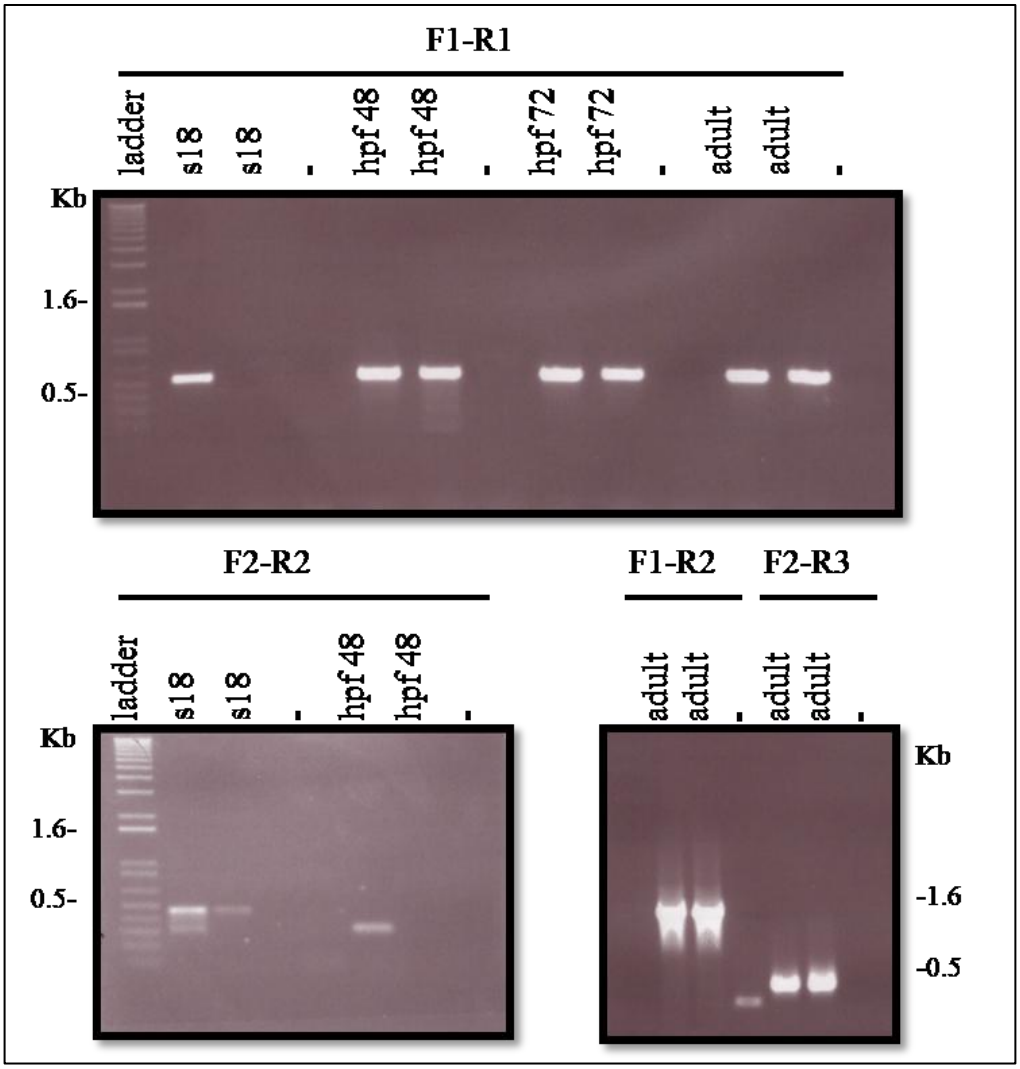

Figure 3-1. Confirmation of expression of zebrafish *cecr1b* by RT-PCR.

One μg total RNA from embryos or adults was used for cDNA synthesis. Primers used for PCR are indicated in the figure. RT-PCR reactions were done in duplicate to ensure detection success. Positions of the primers in *cecr1b* cDNA are illustrated in Figure 3-2. All PCR products have been sequence-confirmed. Sequencing of the two ZID2-F2/ZID2-R2 PCR product indicated alternative intron splicing at an early stage (s18) of development. "-", thermoscript-negative controls; s, somite; hpf, hours post fertilization.

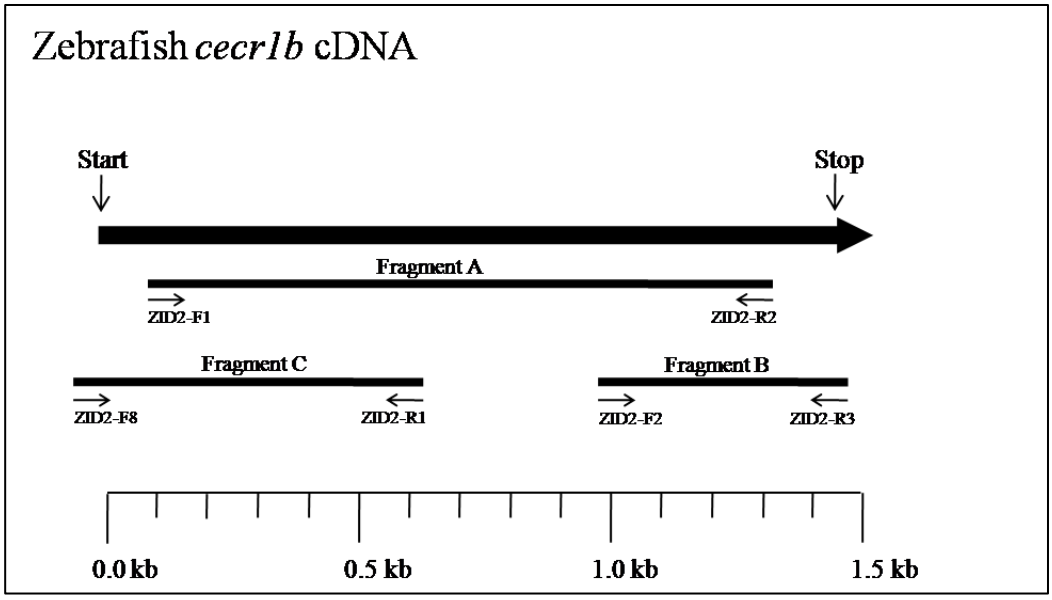

Figure 3-2. Schematic representation of PCR fragments used to generate zebrafish *cecr1b* cDNA .

The 1535 bp zebrafish *cecr1b* full length cDNA was generated by PCR using ZID2-F8 and ZID2-R3 primer pairs and combining the overlapping DNA fragments A, B and C as templates. Fragments A, B and C were obtained by RT-PCR using adult zebrafish RNA with primers illustrated in the figure. The cDNA is represented as an arrow from 5' to 3', with fragments produced by RT-PCR indicated underneath.

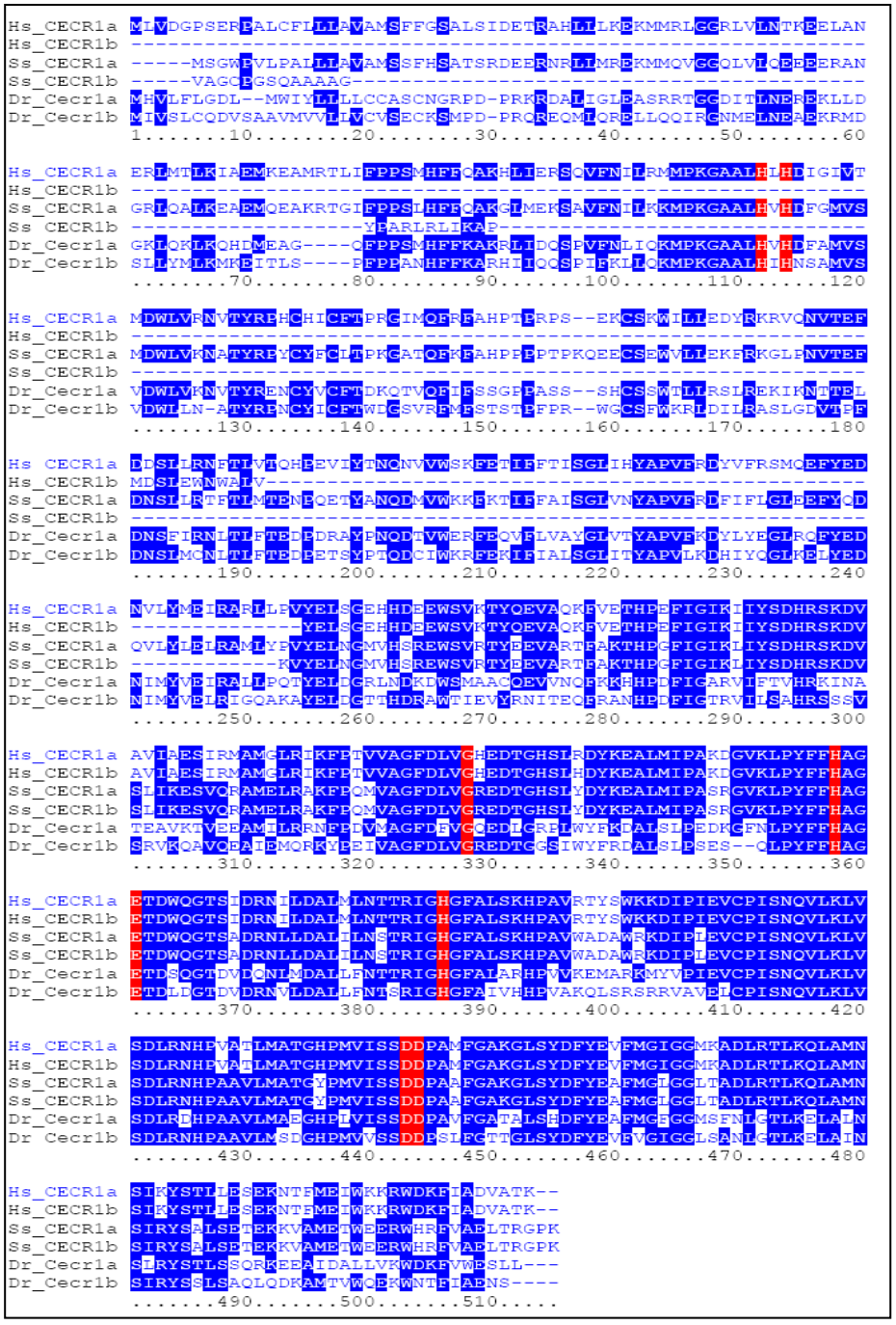

Figure 3-3. Alignment and conserved domains in CECR1 proteins.

Blue ackground indicates identity. The amino acids important for ADA activity are highlighted as red. Hs: *Homo Sapiens*; Ss: *Sus scrofa*; Dr: *Danio rerio*.

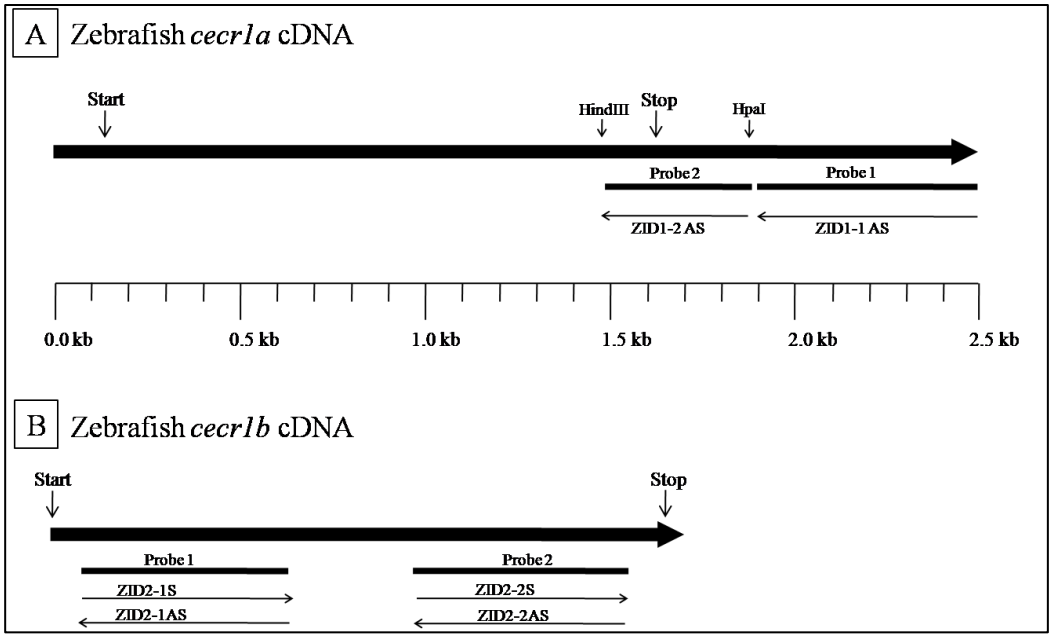

Figure 3-4. Location of the zebrafish *cecr1a and cecr1b* probes used for *in situ* hybridization.

Zebrafish *cecr1a* (A) and zebrafish *cecr1b* (B) cDNAs are represented as arrows from 5' to 3', with the probes indicated underneath. Restriction sites used to linearize the cDNA containing plasmid are illustrated. Start and Stop refer to translation start and stop sites.

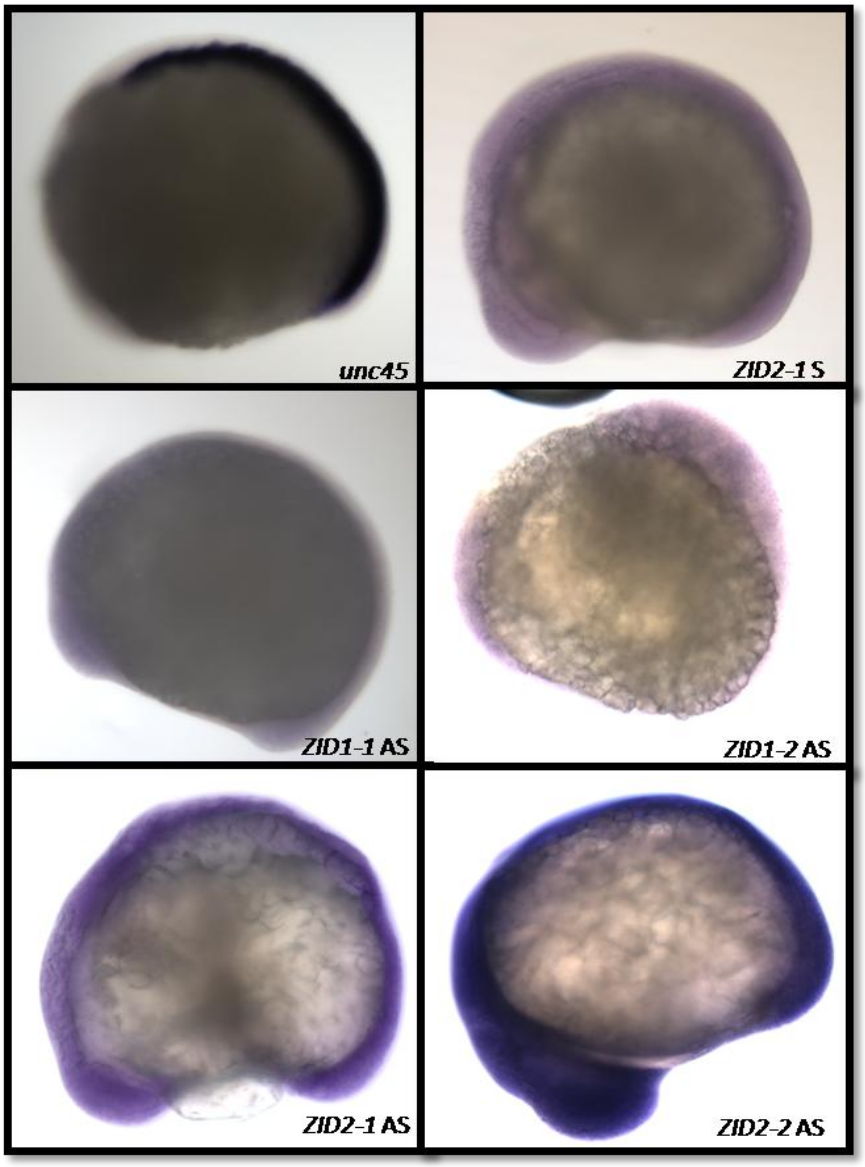

Figure 3-5. Whole-mount *in situ* hybridization of zebrafish 9-14 hpf embryos using various probes.

Embryos are shown in lateral view with anterior region to the left. Probes include *unc45* as a positive control; *ZID2-1* sense (S) as a negative control; and *ZID1-1* antisense (AS), *ZID1-2* AS, *ZID2*-1 AS, *ZID2-2* AS. *ZID1* refers to *cecr1a* gene and *ZID2* refers to *cecr1b* gene. Widespread expression of zebrafish *cecr1a* and *cecr1b* was observed.

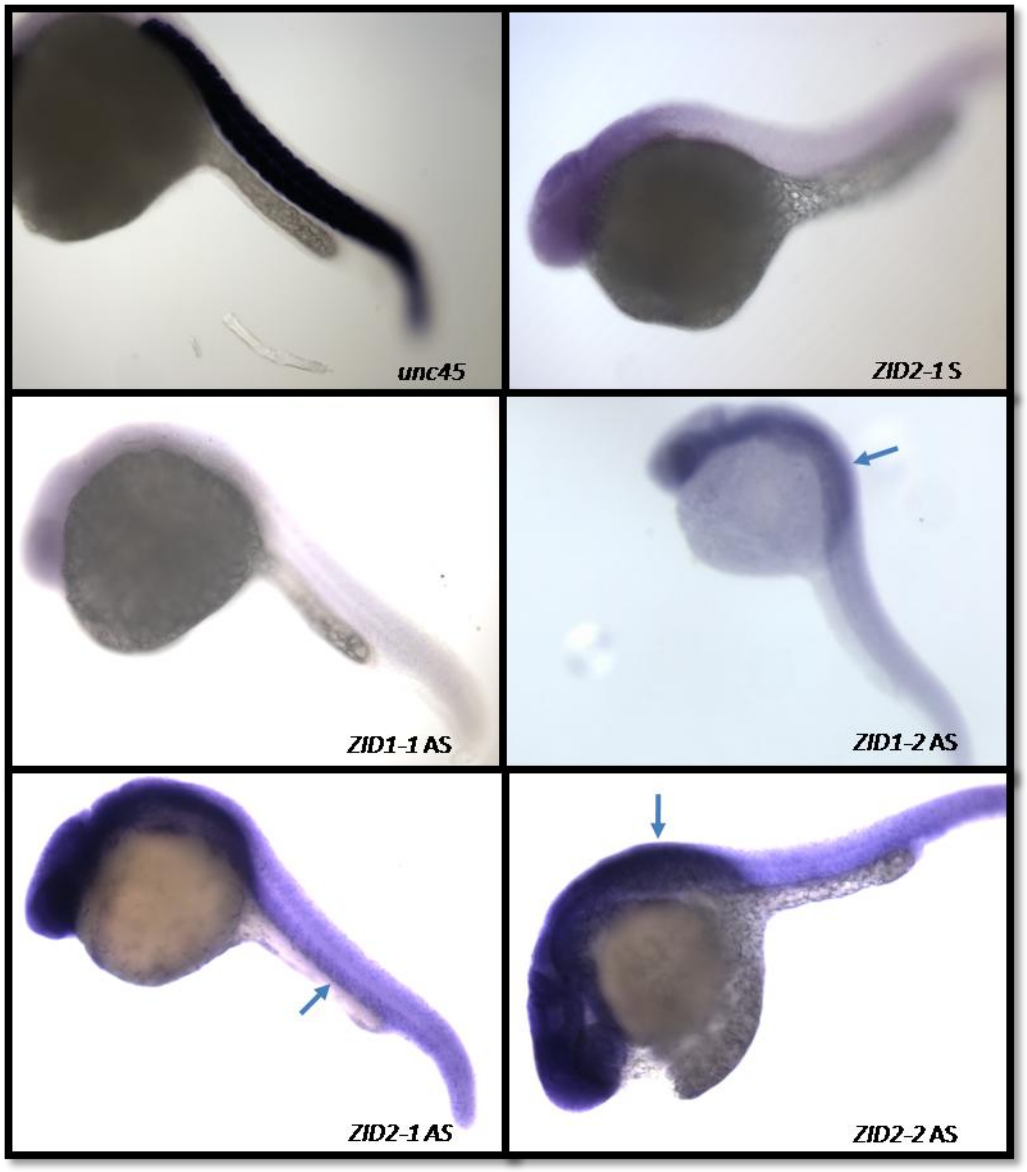

Figure 3-6. Whole-mount *in situ* hybridization of zebrafish 24 hpf embryos using various probes.

Embryos are shown in lateral view with anterior to the left. Probes used were the same as in Figure 3-5. High level of *cecr1a* and *cecr1b* expression was observed in the midbrain and cerebellum regions as the arrows indicated. Weak and broad expression was identified in the truck. A higher level of *cecr1b* transcript was observed in the ventral neural tube using *ZID2-1* AS probe as the arrow indicated.

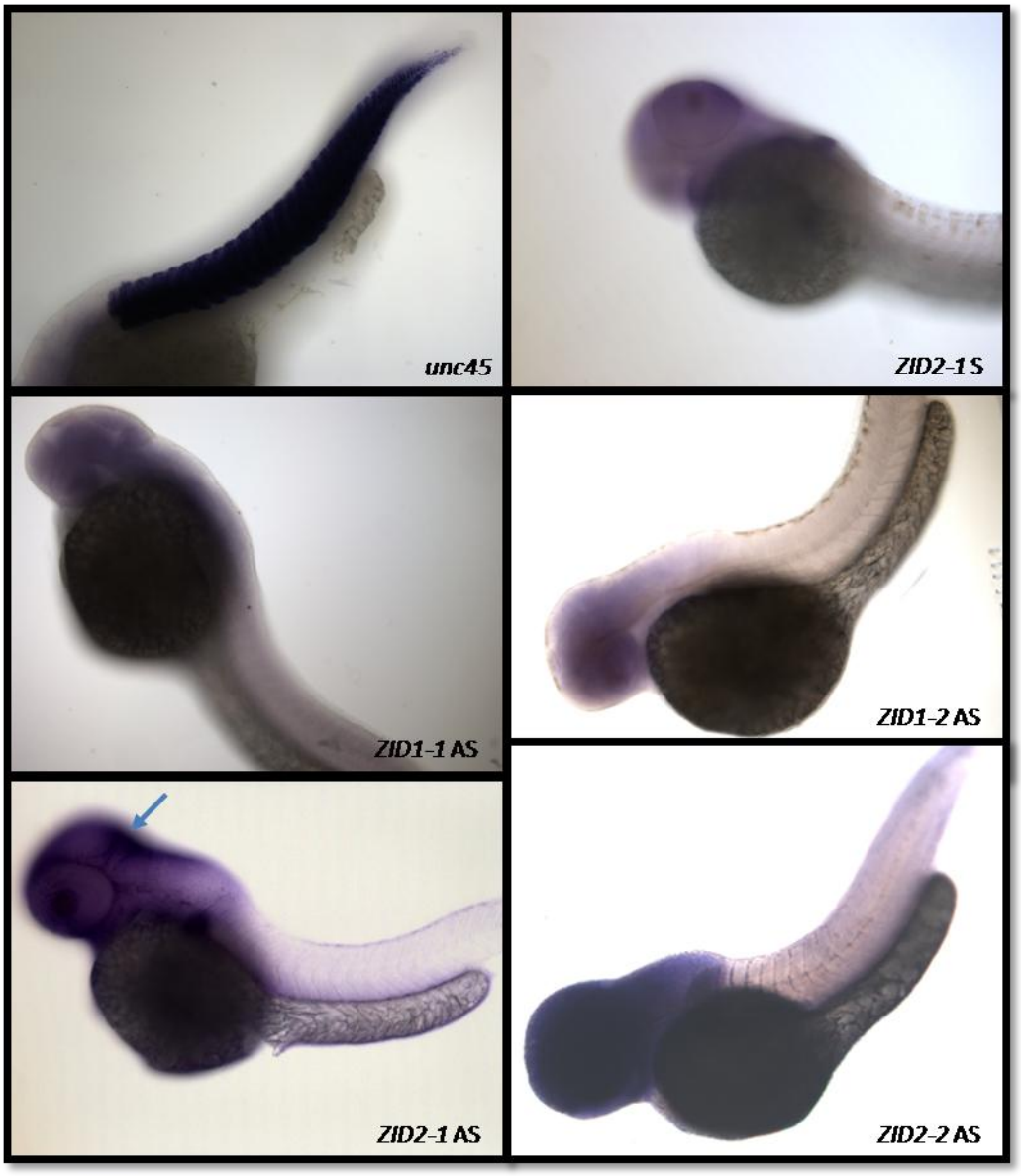

Figure 3-7. Whole-mount *in situ* hybridization of zebrafish 48 hpf embryos using various probes.

Embryos are shown in lateral view with anterior to the left. Probes used were the same as in Figure 3-5. The staining was focused in the head in 48 hpf embryos, with possible increased staining in the roof plate midbrain region using *ZID2-1* AS probe as the arrow indicated.

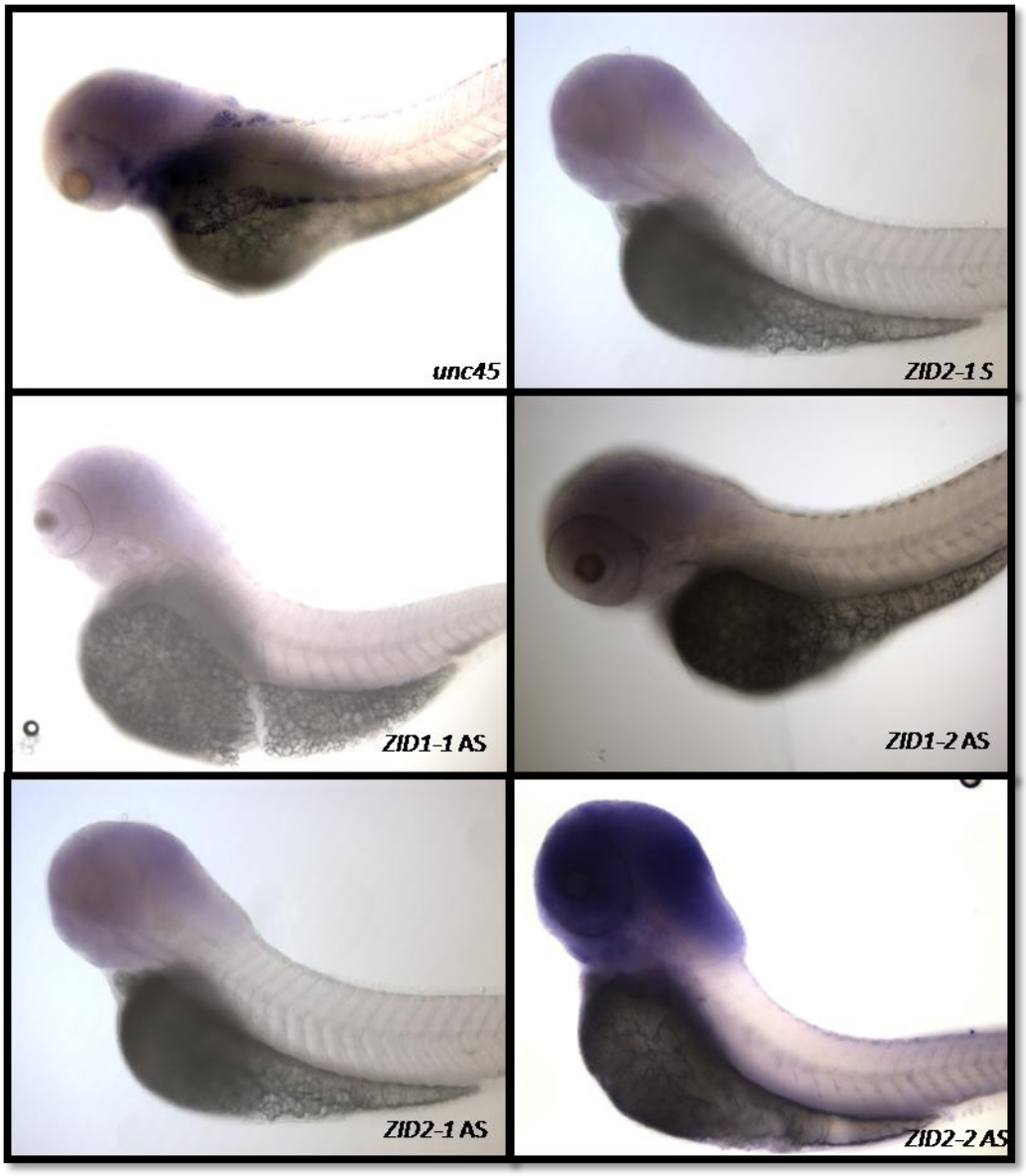

Figure 3-8. Whole-mount *in situ* hybridization of zebrafish 72 hpf embryos using various probes.

Embryos are shown in lateral view with anterior to the left. Probes used were the same as in Figure 3-5. Faint staining was observed in the head. However, the stain in the head may be artifactual.

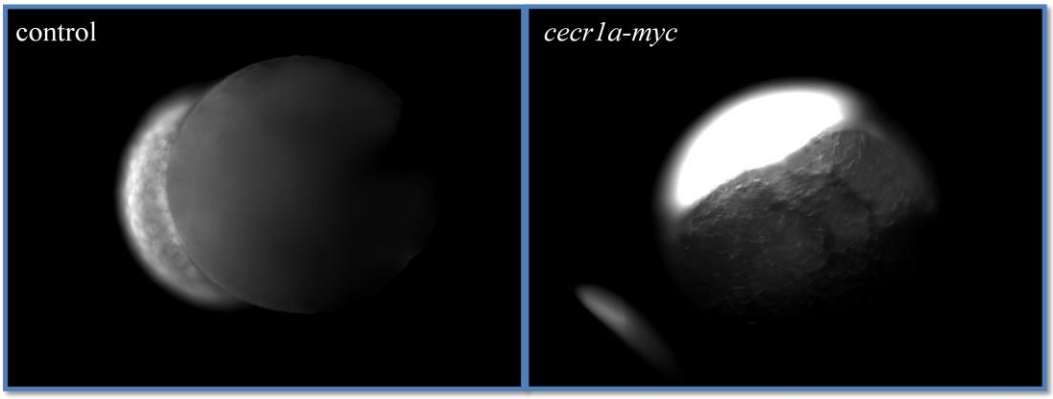

Figure 3-9. Immunostaining of overexpressed *cecr1a-myc* in 3 hpf zebrafish embryos.

2.5 ng of *in vitro* synthesized *cecr1a-myc* mRNA or control Danieau buffer was injected into zebrafish fertilized eggs at the 1 to 4-cell stages. The expression of *cecr1a* at 3 hpf was detected indirectly by immunostaining of myc using mouse anti-c-myc monoclonal antibody and visualized using goat anti-mouse Alexa-488. Strong expression of myc tag in the cells was detected only in the *cecr1a-myc* injected embryos. Embryos were viewed with a Zeiss Axioskop 2 mot plus compound microscope and photographed using a Retiga EXi camera.

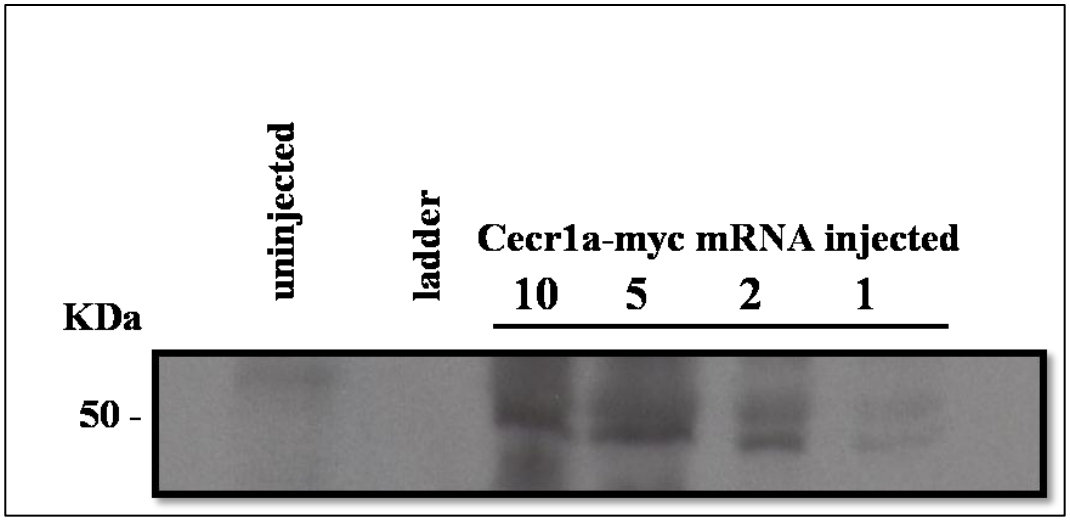

Figure 3-10. Detection of c-terminus myc-tagged zebrafish Cecr1a expression using western blot analysis.

Embryo lysates were prepared at 9 hpf after 5 ng of *cecr1a-myc* mRNA was injected into fertilized eggs at the 1 to 4-cell stages. Numbers above the lane indicate the number of embryos loaded in each well. Lysates from 5 uninjected embryos was loaded in one well as negative control. A band of approximately 50 kDa was found only in *cecr1a-myc* injected embryos, which was close to the predicted 58 kDa molecular mass of the myc-tagged Cecr1a protein.

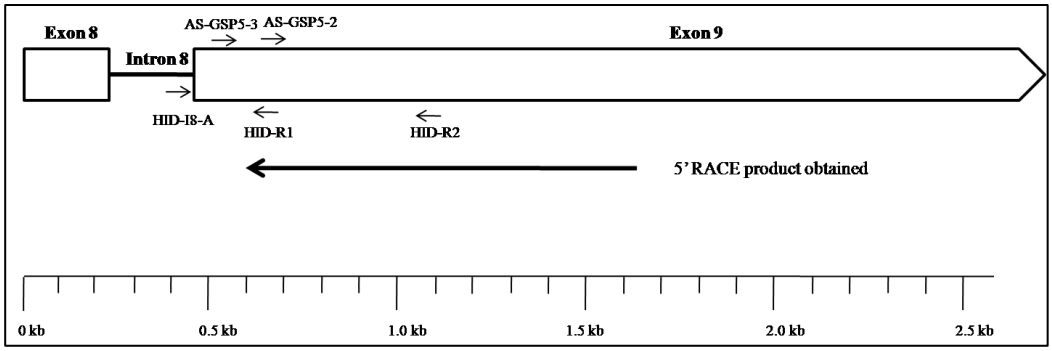

Figure 3-11. Structure of the human *CECR1* antisense transcript.

Diagram of the human *CECR1* antisense transcript detected by using 5' RACE was showed. Only exons 8 and 9 of the *CECR1* gene were showed. Primers used in 5' RACE and RT-PCR were indicated in the figure. The antisense transcript obtained by 5' RACE was represented as an arrow from 5' to 3'. Exons 8, 9 and intron 8 are in scale.

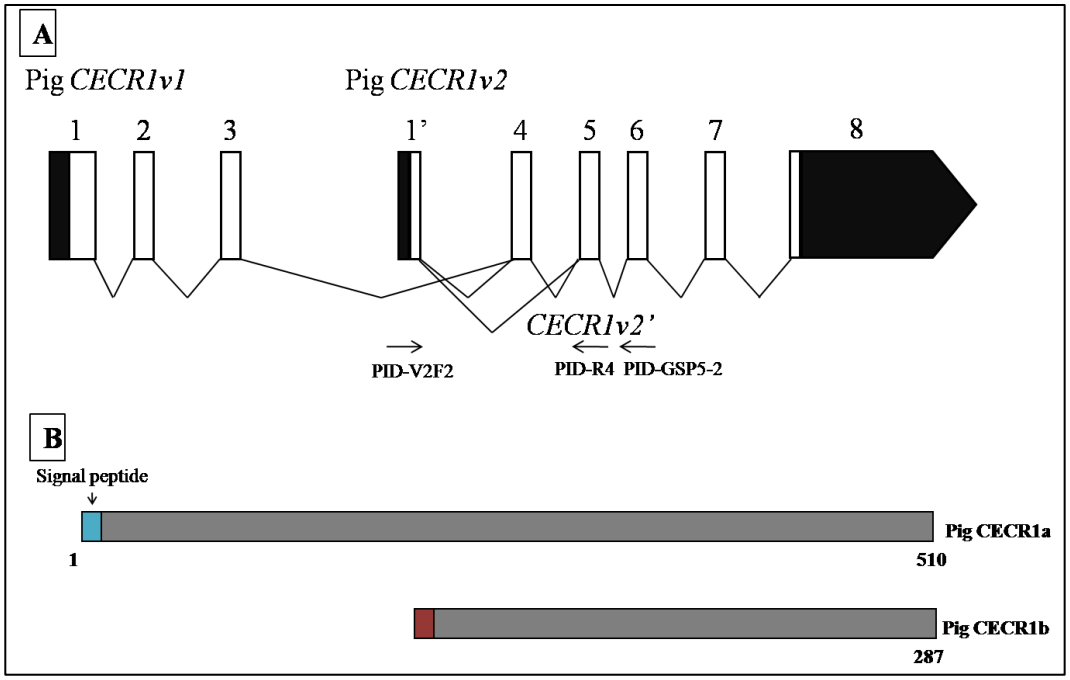

Figure 3-12. Genetic structure and predicted protein sequences of pig CECR1a and CECR1b.

A) Pig *CECR1v1* contains 8 exons comprising 2219 bp. Pig *CECR1v2* starts in intron 3 of *CECR1v1*. Its predicted cDNA encompasses 1531 bp. The primers used to conduct 5' RACE and RT-PCR are shown in the figure. B) Predicted protein sequences of pig CECR1a and CECR1b. The green box indicates the location of the signal peptide. The red box shows the 25 unique amino acids encoded by exon 1' in pig CECR1b protein.

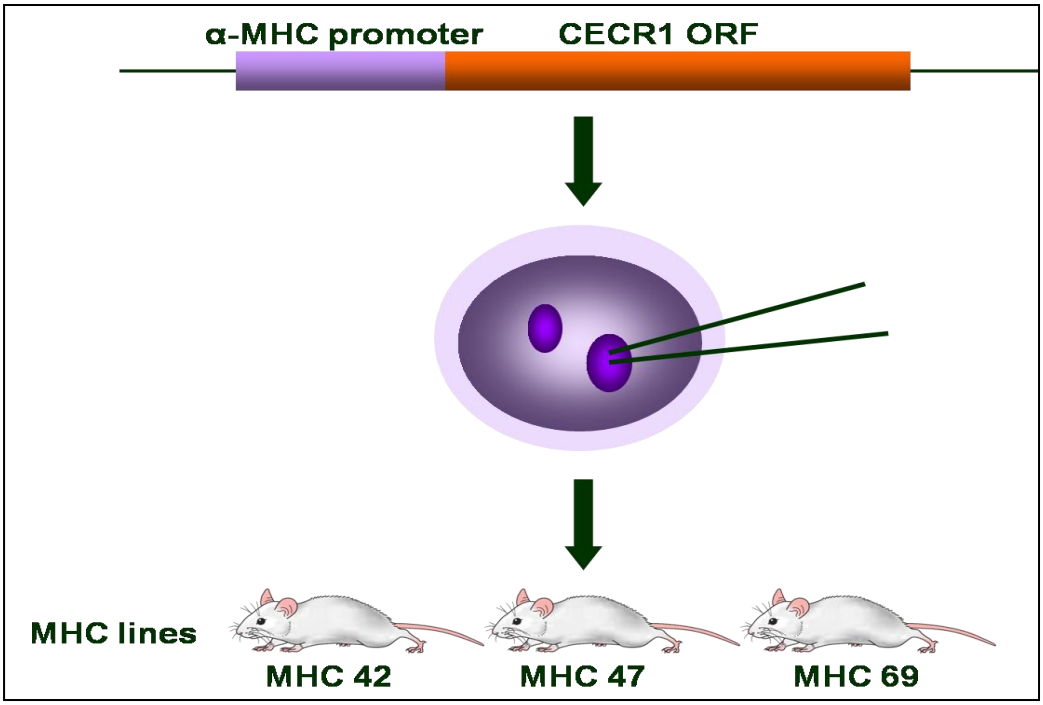

Figure 3-13. Diagrammatic representation of the α-MHC promoter regulated *CECR1* expression mouse model.

The FVB/N-Tg(MHC-hCECR1) lines (the MHC lines) overexpressing human *CECR1v1* were generated by pronuclear injection of a DNA fragment of human *CECR1v1* ORF controlled by the heart specific α-myosine heavy chain (α-MHC) promoter.

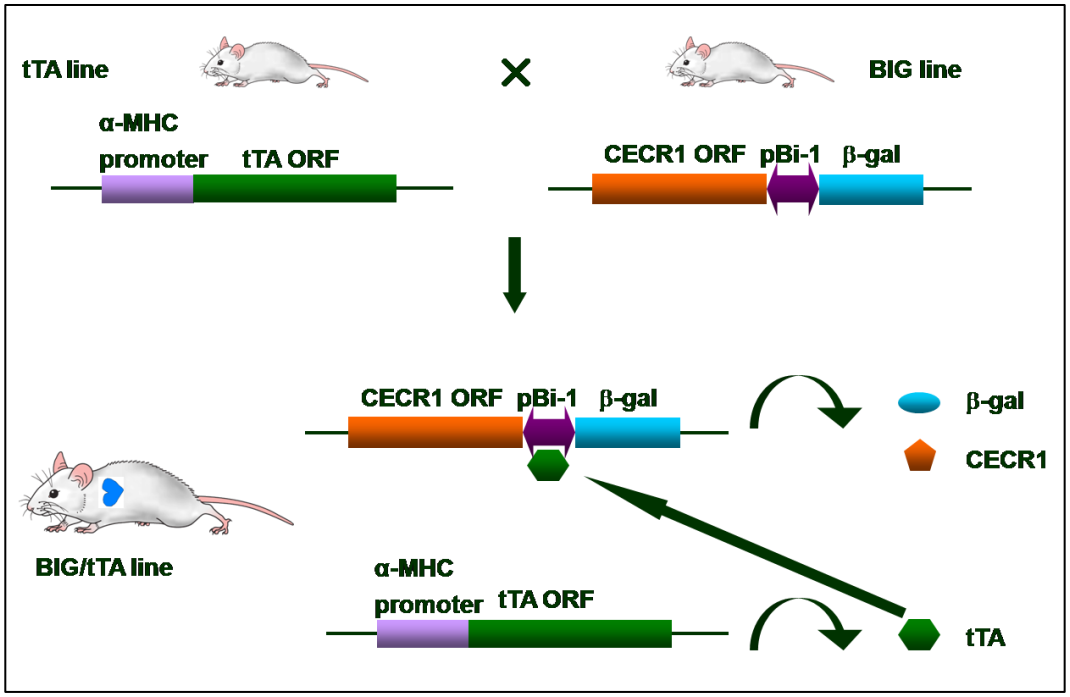

Figure 3-14. Diagrammatic representation of the "tet off" binary tetracycline-regulated *CECR1* expression mouse model.

The FVB/N-Tg(tTA-hCECR1/βgal) line (the BIG line) was generated by pronuclear injection of a DNA fragment containing the human *CECR1v1* gene and β-gal gene controlled by a tTA-responsive bidirectional promoter pBi-1. CECR1a was not expressed in the BIG line without the tetracycline-controlled transactivator (tTA), thus the mouse should be phenotypic normal. The FVB/N-Tg(MHCAtTA) line (the tTA line) contained an insert of *tTA* gene controlled by a α-MHC promoter. When the BIG line and the tTA line were mated, CECR1a should be expressed specifically in the heart of the BIG/tTA mouse.

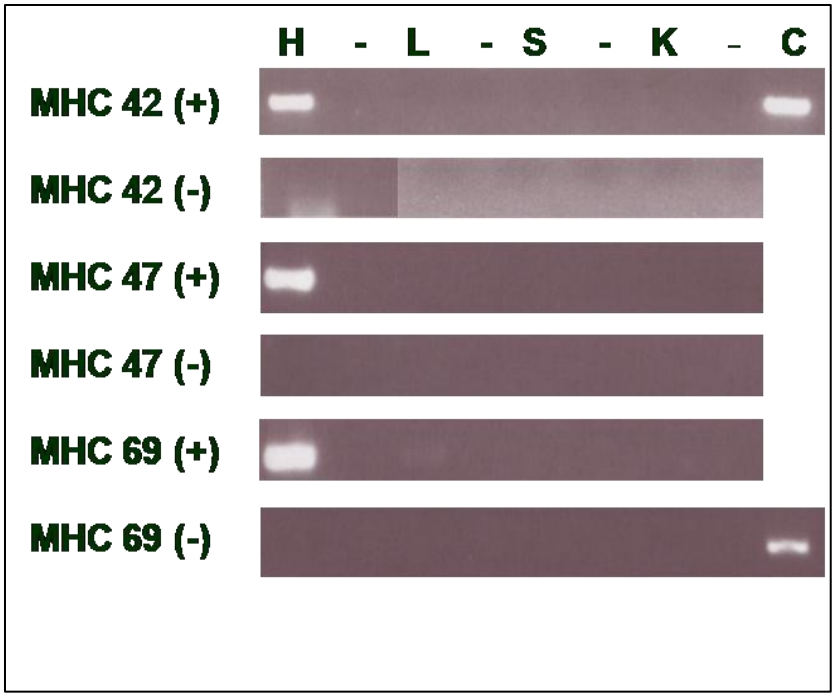

Figure 3-15. *CECR1* expression in FVB/N-Tg(MHC-hCECR1) mice.

RT-PCR analysis of human *CECR1* expression was conducted in MHC lines. 0.5-1 μg of total RNA from several tissues of 3-week old mice were used for the analysis. MHC (+), MHC-hCECR1 transgenic mice; MHC (-), wild type littermates. H, heart; L, lung; S, spleen; K, kidney; C, pMHC-hCECR1 plasmid control. "-", thermoscript-negative controls. *CECR1* transcripts were only observed in hearts of the MHC-hCECR1 transgenic pups.

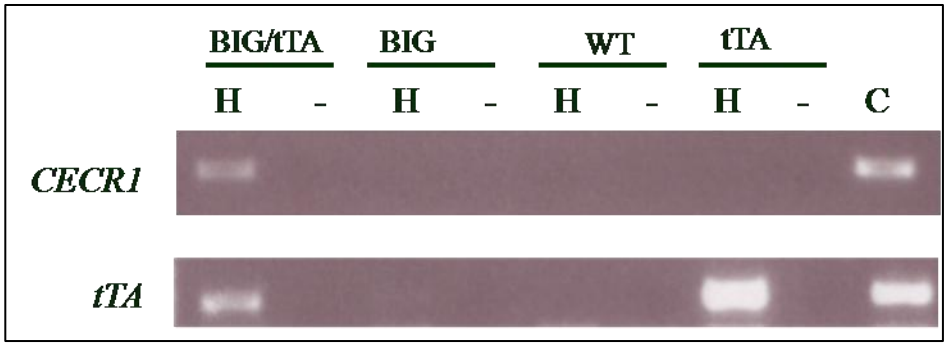

Figure 3-16. *CECR1* expression in BIG/tTA double transgenic mice.

RT-PCR analysis was conducted in the littermates generated from the mating of tTA and BIG mice. 1 μg of total RNA from several tissues of 3-week old mice were used for the analysis. H, heart; C, pBIG-CECR1 plasmid control; "-", thermoscript-negative controls. *CECR1* expression was only seen in the heart of the BIG/tTA double transgenic mouse.

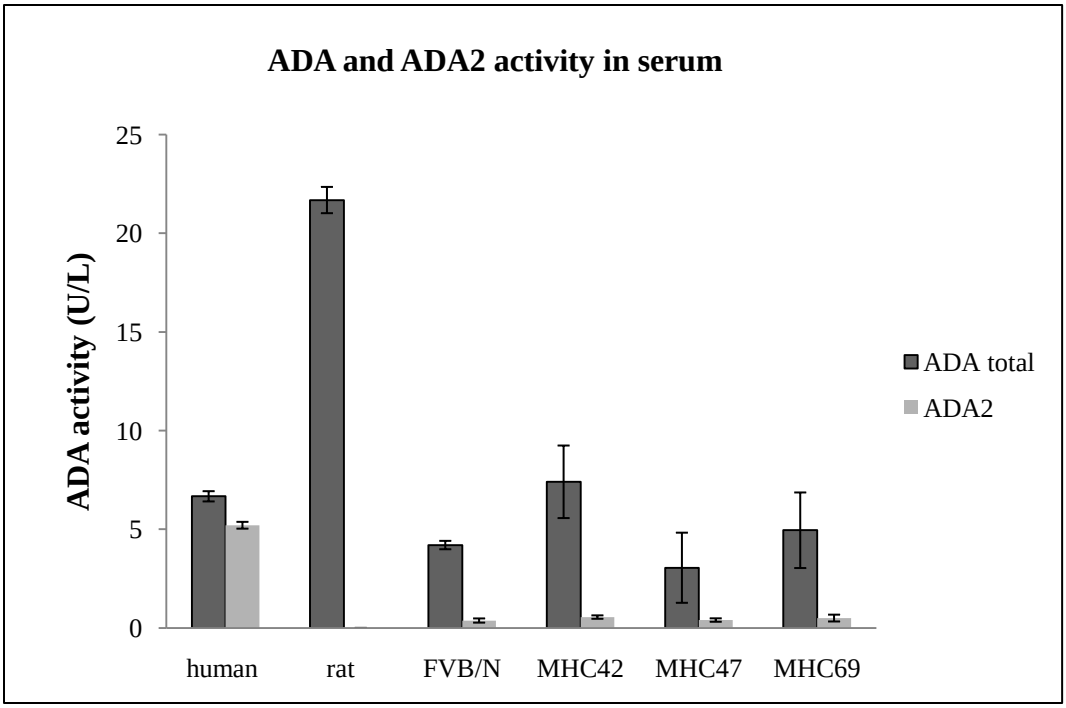

Figure 3-17. ADA2 activity in serum of humans, mice and rats.

Total ADA activity was tested using the Adenosine Deaminase Assay kit. ADA2 activity was tested using the same procedure but adding 0.1 mM of EHNA, which was the inhibitor of ADA1. ADA2 activity contributed to the majority (80%) of the total ADA activity in human serum. Normal mouse and rat, and MHC-hCECR1 transgenic mouse serum mostly exhibited ADA1 activity. The rat serum showed a much high ADA activity, which may suggest inflammation in the individual rat tested.

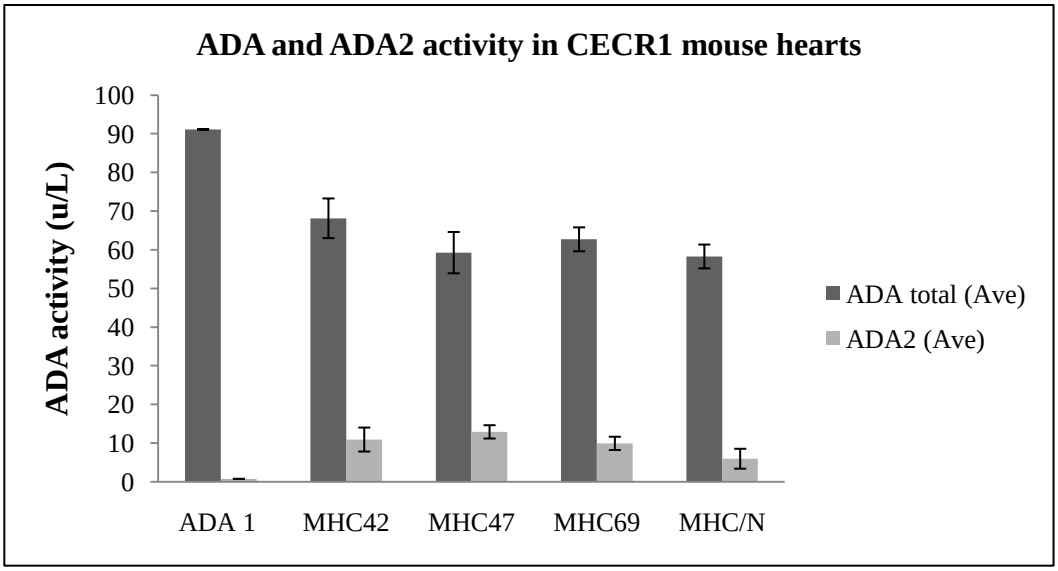

Figure 3-18. ADA2 activity compared to total ADA activity in mouse heart extracts.

Total ADA activity of mouse heart cytoplasmic proteins was tested by detecting the consumption of adenosine by ADA. ADA2 activity was determined using the same methods with addition of 10 μM EHNA. Each bar represents the ADA activity of cytoplasmic protein of 5 combined mouse hearts. MHC47 line had a higher level of ADA2 activity comparing to normal littermates MHC/N with a p-value = 0.02, using single factor Anova test. MHC42 and MHC69 lines did not show a higher ADA2 activity, indicated by p-value = 0.1.

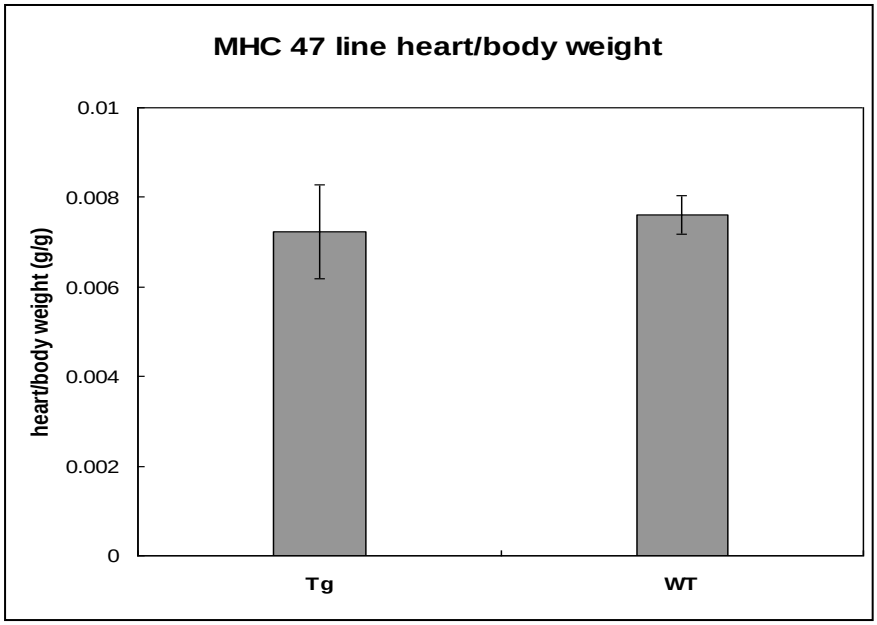

Figure 3-19. Comparison of total heart weight of 9-week old MHC47 male mice.

Mouse hearts and bodies were weighted in the MHC47 line. Each bar represented the average body/heart weight of 5-8 individuals. No significant difference in heart weight was observed based on single factor Anova test ($p = 0.775$). Tg, transgenic mice; WT, wild type mice.

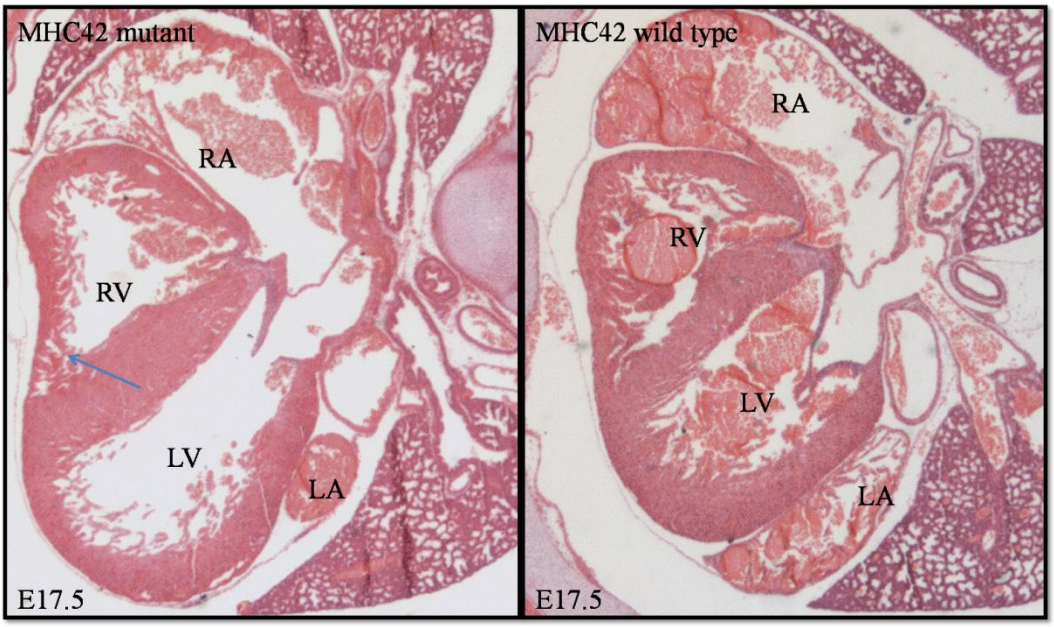

Figure 3-20. Histological section and H&E staining of E17.5 embryonic heart in MHC42 line.

Mouse embryos were embedded in paraffin and sectioned at 7 microns. Serial sections were mounted and stained with Harris's hematoxylin-eosin. A thinner right ventricular wall was observed in MHC-hCECR1 mice indicated by the arrow. Images were taken with a 10× objective and 1.6× aux. lens. LV, left ventricle; RV, right ventricle; LA, left atrium; RA, right atrium.

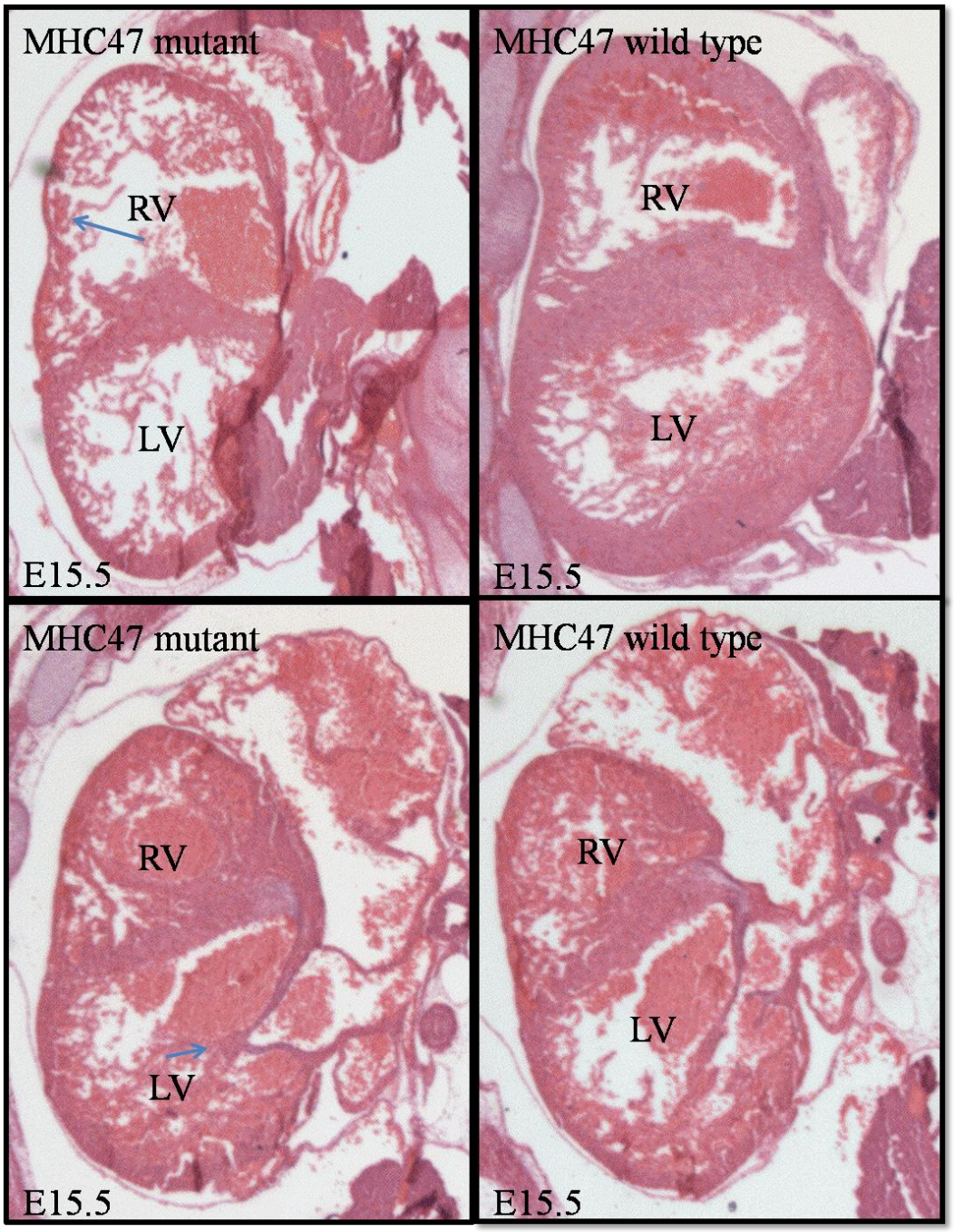

Figure 3-21. H&E staining of E15.5 embryonic heart in MHC47 line.

A thinner right ventricular wall and left atrioventricular valve disorganization were observed as indicated by the arrows. Images were taken with a 10× objective and 1.6× aux. lens. LV, left ventricle; RV, right ventricle.

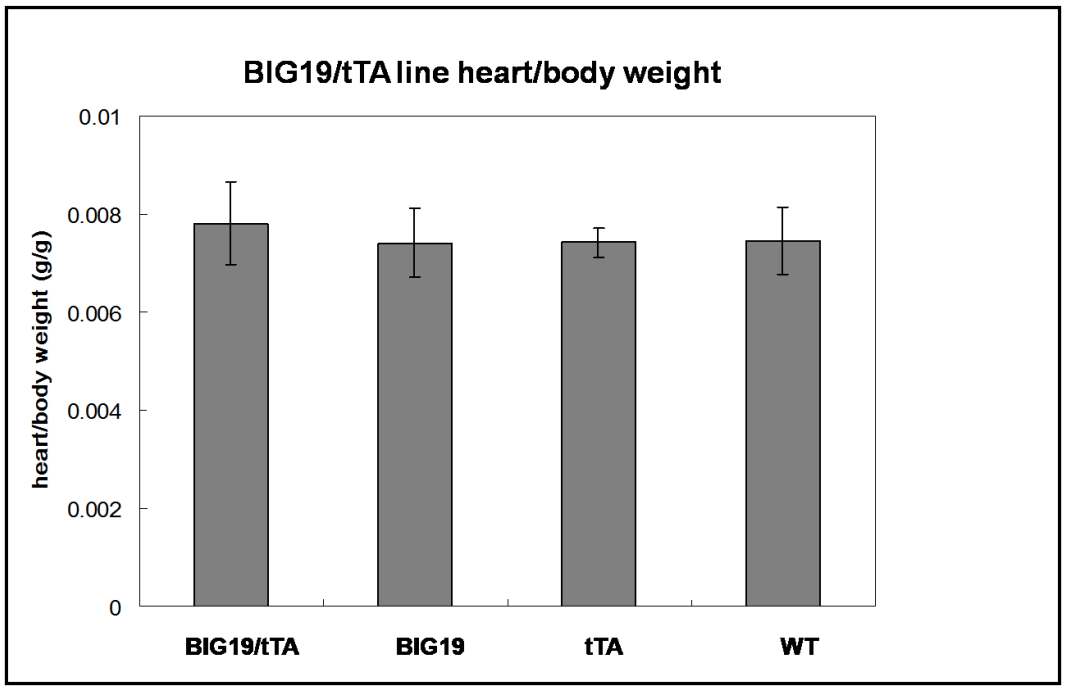

Figure 3-22. Comparison of total heart weight of 6-week old BIG19/tTA male mice.

Mouse hearts and bodies were weighted in BIG19/tTA's 4 types of pups. Each bar represents the average body/heart weight of 5-8 individuals. No significant difference in heart weight was observed according to Anova test ($p = 0.881$). BIG/tTA, BIG/tTA double transgenic genotype mice; BIG, BIG genotype mice; tTA, tTA genotype mice; WT, wild type mice.

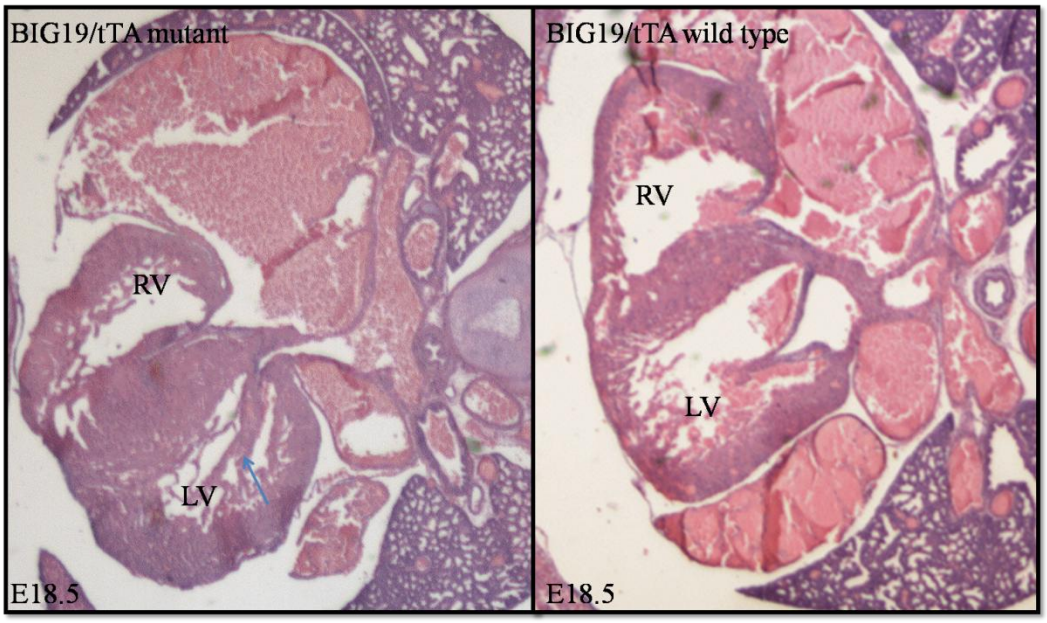

Figure 3-23. Histological section and H&E staining of E18.5 embryonic hearts in BIG19/tTA lines.

Mouse embryos were embedded in paraffin and sectioned at 7 microns. Serial sections were mounted and stained with Harris's hematoxylin-eosin. Incomplete left atrioventricular valve was observed as indicated with arrow. Images were taken with a 10× objective and 1.6× aux. lens. LV, left ventricle; RV, right ventricle.

Table 3-1. *CECR1* transcripts in pig tissues confirmed by RT-PCR.

Embryonic	***CECR1v1***	***CECR1v2***	***CECR1v2'***	**Newborn**	***CECR1v1***	***CECR1v2***	***CECR1v 2'***
heart	+	+	-	heart	+	+	+
kidney	+	+	-	kidney	+	+	+
liver	+	+	-	liver	+	+	-
brain	+	+	-	brain	+	+	-
muscle	+	+	-	muscle	+	+	+
				lung	+	+	+
				spleen	+	+	-
				placental	+	+	-

"+" indicated expression was observed in the tissue using RT-PCR. "-" indicated the expression was not observed in the tissue. Both pig *CECR1v1* and *CECR1v2* are expressed in all embryonic and adult tissues tested, while *CECR1v2'* is only expressed in a few tissues.

Table 3-2. *CECR1* copy number in MHC and BIG transgenic mice.

Transgenic line	**Copy number**
MHC42	>5
MHC47	>=2
MHC69	1
BIG1	>=2
BIG19	1

Table 3-3. Ratio of wild type and transgenic weaned mice in MHC, tTA and BIG lines.

Transgenic line	Tg	WT	p-value	Mendelian ratio?
tTA	78	76	0.87	yes
BIG1	125	154	0.083	yes
BIG19	75	96	0.108	yes
MHC42	83	104	0.125	yes
MHC47	91	129	0.010	yes
MHC69	46	90	0.00016	no

All pups were produced by crossing a heterozygous tTA, MHC, or BIG mouse with a normal FVB/N mouse. Numbers in the columns are pups weaned at 3 weeks. Mendelian ratio was observed in all of the transgenic lines, except the MHC69 line. P-value is indicated as *t* test.

Table 3-4. Ratio of four genotypes in weaned mice in BIG/tTA system.

Transgenic line	BIG/tTA	BIG	tTA	WT	p-value	Mendelian ratio?
BIG1/tTA	13	18	13	23	0.250	yes
BIG19/tTA	36	43	40	34	0.735	yes

Pups in BIG/tTA lines were produced by crossing a heterozygous tTA mouse with a heterozygous BIG mouse. Numbers in the columns are pups weaned at 3-week old. Mendelian ratio was observed in both of the transgenic lines. P-value is indicated as *t* test.

Table 3-5. Summary of abnormalities found in *CECR1* transgenic mice.

Transgenic line	Heart defects	Frequency
MHC42	Thinner right ventricular wall	2/5 tg; 0/4 n
MHC47	Thinner right ventricular wall, thinner intra-ventricular septum, enlargement of left and right atrioventricular valve	3/6 tg; 0/5 n 1/6 tg; 0/5 n 2/6 tg; 0/5 n
MHC69	Not detectable	0/5 tg; 0/3 n
BIG1/tTA	Possible atrial septum defect	1/6 tg; 0/3 n
BIG19/tTA	Possible atrial septum defect, abnormal left atrioventricular valve Indented right ventricle	1/8 tg; 0/5 n 1/8 tg; 0/5 n 2/8 tg; 0/5 n

Chapter 4 . Discussion

4.1 *cecr1* shows weak widespread expression in zebrafish

Mammals, such as mice or rats, are the most common models to address genotype-phenotype associations in human disease. However, *CECR1* is not present in the mouse or rat genome, thus making the use of a mouse model less relevant. Zebrafish was first considered as a model organism to study the role of *CECR1* in CES in this study, because *cecr1* is present in zebrafish and its embryos are easy to manipulate. Two *CECR1* homologues, *cecr1a* and *cecr1b*, are found in zebrafish. *cecr1a* was identified by the screening of a 19-25 hpf zebrafish lambda-ZAP cDNA library which was conducted by Dr. Stephanie Maier. The *cecr1a* gene resides at chromosome 25. Another *CECR1* homologue in zebrafish, *cecr1b*, was first predicted by Dr. Maier through the GENSCAN program and then confirmed by RT-PCR. *cecr1b* is located on chromosome 4 in zebrafish. Both *cecr1a* and *cecr1b* are expressed throughout the development of zebrafish embryos and at the adult stage, as examined by northern blot analysis (*cecr1a*, see Figure 3-10 in Dr. Maier's thesis) or RT-PCR (*cecr1b*, see my Figure 3-1). My *in situ* hybridization results showed that both *cecr1a* and *cecr1b* were faintly expressed widespread throughout development. In 14 hpf embryos, which are around the 8-somite stage when the optic primordium is clearly visible, faint purple staining was observed throughout the body (Figure 3-5). Faint expression was observed in all developing tissues, but was mainly concentrated in the midbrain and cerebellum area in 24 hpf and 48 hpf stage with increased expression level in ventral neural tube in 24 hpf embryos and in roof plate

midbrain in 48 hpf embryos using ZID2 probe (Figure 3-6 to Figure 3-8). It is not surprising that the same observation was obtained by other investigators independently (Rosemberg et al., 2007; Thisse, 2004).

In human and pig embryo *in situ* hybridization (Maier, 2005), *CECR1* was found to be expressed in a general faint pattern throughout early development, but with stronger, more specific staining in some of the tissues affected in CES patients, such as fetal heart and kidney tubules. Expression in other tissues such as gut epithelium and liver was also observed. In comparison to human and pig *CECR1*, the two zebrafish homologues are only expressed generally in all tissues. Since zebrafish is distant from mammals in evolution, it is possible that the function of Cecr1 in zebrafish may not be identical to the function of CECR1 in mammals, thus the study of *cecr1* in zebrafish may not give valuable information on the role of the *CECR1* duplication in CES in humans.

4.2 Overexpression and knockdown of zebrafish *cecr1* does not lead to significant abnormality in zebrafish

The overexpression of *cecr1a* was conducted to find out if it could contribute to any CES-like features in zebrafish. Knockdown of *cecr1a* was also carried out, since the study of the absence of a gene will give a clue of the function of that gene.

In vitro synthesized *cecr1a* mRNA or *myc* tagged *cecr1a* were injected separately into the zebrafish embryos between 1 to-8 cell stages when the cell membrane was not closed and mRNA could still travel through the cells. No obvious abnormal phenotype was observed up to 72 hpf stage when most of the

tissues are completed formed. The *cecr1a* mRNA was prepared from pBluescript cloning vector inserted with *cecr1a* cDNA containing polyadenlyation site. Since pBluescript is not an expression vector, which does not contain a strong promoter and strong termination codon, the translation of the *in vitro* synthesized mRNA may not be successful in zebrafish embryos. In the meantime, *myc-cecr1a* mRNA was prepared from pGEMT-Easy cloning vector containing the *cecr1a* ORF and a 3' end *myc* tag and injected to zebrafish embryos. The presence of the myc-Cecr1a protein was identified by antibody identification of the myc tag using immunofluorescence at 3 hpf (Figure 3-9) and western blot analysis at 9 hpf (Figure 3-10). The phenotype of the embryos was not recorded due to a small number of injected embryos. However, these results indirectly suggest that Cecr1a protein may be translated in the *cecr1a* mRNA injected embryos. To circumvent the translational failure *of in vitro* synthesized mRNA, the *cecr1a* ORF should be subcloned to an expression vector specific for expression in zebrafish, such as pCS2+.

It is most likely that the overexpression of Cecr1a did not affect the development of zebrafish. The *cecr1a* gene may not be dosage sensitive. *cecr1a* was knocked down by using morpholino oligonucleotide which will block the translation of *cecr1a*. However, no obvious phenotype was observed in the embryos.

These results are not surprising, since there are two CECR1 homologues present in the zebrafish genome. Both of the homologues have the 8 conserved residues important for the catalytic activity of ADA, thus both may be functional

and redundant. The presence or absence of one of the homologues may not produce a sufficient effect on the normal development of zebrafish. However, the study of *cecr1* function in zebrafish was not continued in order to concentrate on the mouse studies.

4.3 CECR1 antibodies only detect the purified control proteins

Antibodies to CECR1 could be very useful in this study. These antibodies could be used to detect whether the protein is present in the organism engineered to overexpress CECR1. CECR1 is predicted to be secreted and function as a growth factor by controlling the level of extracellular adenosine. An antibody could be used to confirm the subcellular localization of CECR1 by immunofluorescence or immunohistochemistry. It could also be used to detect the interaction of CECR1 with its receptors or other proteins through immunoprecipitation.

Five human CECR1 antibodies have previously been produced by Dr. Maier. One of them was generated against the HIDExp1 recombinant protein and four of them were raised against peptides CECR1-Pep1 and CECR1-Pep2. Although each antibody could detect their respective protein purified from bacteria or conjugated peptide, none of them successfully detected the CECR1 protein in human heart and kidney protein extracts.

Two antibodies against two new peptides NZW-HMA-1A and NZW-HMA-1B were generated and characterized. Both of the two antibodies could detect a 30 kDa band (the predicted size of the HIDExp1 recombinant protein with the N-terminal 30 kDa of the CECR1 protein) in the HIDEXP1 control

protein. Both antibodies also detected an 85 kDa band (the predicted size of GST-CECR1 recombinant protein) and a 60 kDa band in the GST-CECR1 control protein purified from bacteria at equal intensity. The 85 kDa protein should be the GST-CECR1 recombinant protein and the 60 kDa protein might be a degraded GST-CECR1 protein without the GST tag. Mass spectrometry suggested that the 85 kDa band was indeed the GST-CECR1 fusion protein. However, the 60 kDa protein turned out to be a 60 kDa chaperonin (protein Cpn60) in E.*coli*. Thus these two antibodies were not specific to CECR1.

4.4 Human and pig have two *CECR1* variants

CECR1v2 was first discovered as EST 2190534 by Dr. Maier through a search of human EST database. Northern blot analysis using a probe specific for *CECR1v2* suggested that *CECR1v2* was expressed specifically in adult heart and kidney, fetal lung, kidney and heart in humans (Figure 1-4). Heart and kidney are two of the major tissues affected in CES patients. This expression pattern suggests that *CECR1v2* may be involved in the production of CES phenotypes.

The analysis of the "full sequence" *CECR1v1* (Accession # AK074702) shows that exon 1' of *CECR1v2* starts in the intron 3 of *CECR1v1* and is followed by the exon 4 to exon 9 region of *CECR1v1*, including the 3' UTR and poly A signal. The specific exon 1' of *CECR1v2* encodes a 10 amino acid sequence. Since the predicted CECR1b protein does not contain a signal peptide, it may not be secreted out of cell membrane, thus may not have the function of depleted extracellular adenosine. 5' RACE using human fetal kidney RNA identified an additional 47 bp sequence 5' upstream of the AK074702 EST, which included an

in frame stop codon, thus I confirmed that *CECR1v1* encodes a truncated CECR1 protein CECR1b, with a unique 10 amino acid sequence at the N-terminus.

The first two ADA catalytic residues (His15 and His17) are not included in the CECR1b protein, suggesting that the CECR1b may not have the same ADA function and growth factor function as CECR1a is predicted to have. It is possible that CECR1b may regulate the activity of CECR1a by interacting with CECR1a in a dominant negative manner. Alternative splicing is a well known form of regulation of protein expression. One consequence of alternative splicing is to generate an inactive isoform, which can then negatively regulate the active isoform either at a transcriptional level or at a protein level by competing with the functional isoform or through the formation of a heterodimer. For example, the human glucocorticoid receptor (GR) β isoform lacking the C-terminal ligand-binding domain inhibits the active GR α isoform probably by forming an inactive heterodimer (Oakley et al., 1999). Human SNF2L+13 isoform inhibits the SNF2L function by competing in the formation of the chromatin-remodeling complex (Barak et al., 2004).

CECR1a functions as a homodimer in human plasma (Zavialov & Engstrom, 2005). In tissues where both isoforms are present, CECR1b may interact with CECR1a and deplete the functional CECR1a homodimer, probably by inhibition of the transfer of functional CECR1a extracellularly, thus inhibiting the function of CECR1a as a growth factor through its ADA activity. It is possible that functional CECR1a may be not required or required at a lower level in the developing tissues with both variants, such as heart and kidney. Overexpression of

the region with *CECR1* may alter the overall ratio of *CECR1v1* and *CECR1v2* and thus affect tissue development.

The *CECR1v2* specific exon 1' was also found in chimps and baboons by BLAST searches of genomic sequences. The exon 1' isn't found in mice or rats since the *CECR1* gene is absent in these two organism. The exon 1' was found in pigs by 5'RACE using pig adult kidney RNA (Figure 3-12). *CECR1v2* was not detected in chickens using chicken E12 kidney RNA, which was not surprising based on a BLAST search of *Cecr1v2* in chicken genome. *CECR1v2* was not found by BLAST search in either zebrafish or xenopus genomes. It is quite possible that *CECR1v2* is specifically present in mammals with the exception of rodents. Considering that *CECR1v2* may play an important role in the regulation of *CECR1v1* based on its expression pattern, it is quite possible that the role of *CECR1* in CES can only be shown and examined in mammalian system. Thus mouse model was used to study the role of *CECR1* in the production of CES features.

RT-PCR with RNA derived from various tissues in pigs was conducted to confirm the presence of *CECR1v2* and to examine the expression pattern of *CECR1v2*. Both *CECR1v1* and *CECR1v2* were detected in all the tissues examined, including fetal heart, kidney, liver, brain and muscle, newborn heart, kidney, liver, brain, muscle, lung, spleen and placental (Table 3-1). Furthermore, a *CECR1v2'* transcript was discovered in newborn heart, kidney, muscle and lung. This *CECR1v2'* shares the same sequence of *CECR1v2*, except for the absence of

exon 4, which creates a transcript not in frame with *CECR1v1*. Thus *CECR1v2'* might not be translated into protein.

Northern blot analysis of *CECR1v2* was previously conducted in human but not in pig tissues. RT-PCR is a much more sensitive technique to detect transcripts than northern blot analysis. Based on the data revealed by RT-PCR in pigs, it is possible that *CECR1v2* is expressed in all human tissues (other than in adult heart and kidney, and fetal lung, kidney and heart) at a lower level. Further information on the expression of the two variants in pig could be obtained by real-time PCR. However, the unsuccessful attempt of designing primer pairs that could distinguish pig *CECR1v1* and *CECR1v2* made the task hard to accomplish.

4.5 Overexpession of human *CECR1* leads to thinner ventricular wall in embryonic mouse hearts

An overexpression mouse model for CECR1a was generated in this project. Several previous attempts met with varied success. Previously performed by Dr. Maier, transgenic mice were first generated with genomic *CECR1* sequence using the human BAC 609c6. Only 1 founder out of 230 injected embryos survived at injection concentrations ranging from 0.2 μg/ml to 2.5 μg/ml. Aborted fetuses or implantation scars were founded in uteri of mice with pronuclear injected eggs. There might have been a toxic effect of genomic *CECR1* that caused the loss of pregnancies. Three more founders were produced in one litter of eight when injected at a lower concentration of 0.1 μg/ml. Although expression of the human *CECR1* had been verified by northern blotting, all of the four founders gave birth to phenotypically normal, health offspring in most cases.

The expression of CECR1 protein could not be conducted at that time, since no CECR1 antibodies were successfully generated.

Another former graduate student Dr. Ali Riazi developed transgenic mice overexpressing human *CECR1v1* by injection of the human *CECR1v1* cDNA controlled by the heart specific α-MHC promoter or the ubiquitously β-actin promoter in C57B1/6 strain. The pups showed some phenotypes similar to CES (Riazi et al., 2005), such as hypoplastic kidney in all β-actin lines, atria and ventricle enlargement, as well as vena cava and pulmonary vein dilation and atrial septal defects in the dead pups in one of the α-MHC lines. However, the lines were not maintained and thus further analysis was not performed. These preliminary results suggest an important role of *CECR1* in CES and the possibility of using mouse as a model to study this gene.

In this project, two models have been produced and the phenotypes were characterized. The first model was the FVB/N-Tg(MHC-hCECR1) transgenic line using Dr. Riazi's construct, since heart defects were of most interest at the time. Expression analysis by RT-PCR showed that *CECR1v1* is specifically expressed in the hearts of the three MHC42, MHC47 and MHC69 lines (Figure 3-15). Of the three MHC lines, analysis was focused on MHC42 and MHC47. These two lines harbored one insertion with 2-5 copies of *CECR1v1* and were able to produce transgenic offspring at a 50% Mendelian ratio (Table 3-2 and Table 3-3). Only one copy of *CECR1v1* was detected in the MHC69 line. Furthermore, the transgenic pups were produced at a ratio less than the expected 50% Mendelian ratio, although the number of the pups produced and the litter size of this line was

normal compared to the other two MHC lines. The transmission of the transgene to its offspring was not stable for some unknown reason. In addition, none of the fetuses examined showed any abnormalities.

The RT-PCR results can only suggest that the *CECR1v1* transcripts were present in the heart. Although CECR1 antibodies were not available to detect the protein levels of CECR1a in these transgenic mice, the presence of CECR1a was examined indirectly by its CECR1/ADA2 activity. More ADA2 activity compared to the total ADA activity in mouse heart extract was observed in the transgenic pups in the MHC47 lines, using a modified procedure from Sigma for adenosine deaminase enzymatic assay. CECR1/ADA2 activity was also examined in mouse sera as CECR1a was predicted to be secreted and the functional CECR1/ADA2 has only been detected in human serum (Ungerer et al., 1992). However, sera from both the control normal FVB/N mice and the three transgenic lines showed no ADA2 activity within the detection limit of the Diazyme ADA kit (Figure 3-17). These results are not surprising, because the CECR1a secreted into mouse plasma may be too diluted to be detected.

Enlarged hearts were not observed in any of the three MHC lines in embryonic hearts examined using histological techniques (Figure 3-20 and 3-21) or adult hearts by comparing heart weight (Figure 3-19). This observation is in contrast to the results obtained by Dr. Riazi. This might be due to the fact that the FVB/N mouse strain was used in this project, while the C57B1/6 strain was used in Dr. Riazi's research. Different genetic backgrounds might lead to the different phenotypes observed.

A close examination of the embryonic hearts of MHC42 and MHC47 lines showed heart defects including thinner ventricular walls, disrupted atrioventricular valves and possible atrial septal defects seen by histological staining with H&E at E15.5 or E17.5, when both the heart and the vascular system have achieved their definitive prenatal configuration. The most common defect was thinner ventricular wall, which was found in 2 of the 5 MHC42 and 3 of the 6 MHC47 embryos examined (Figure 3-20 and 3-21). 3D imaging of one of the MHC47 embryonic hearts was also carried out, which made the phenotypes more obvious.

Adenosine has been suggested to modulate cell proliferation, cell death and migration of many cell types such as epithelial, endothelial, smooth muscle cells, and immune and neural lineages cells (Jacobson et al., 1999). Adenosine may have different effects on the cells depending on cell type, the adenosine concentration and type of adenosine receptor on the cell. A low level of adenosine is required for the growth of cardiac smooth muscle cells during normal heart development. The overexpressed CECR1a may deplete extracellular adenosine and cause a decrease in the growth of cardiac smooth muscle cells, and thus lead to the observed thinner ventricular wall.

The second model is the “tet off” binary transgenic system with the FVB/N-Tg (tTA-CECR1/βgal) line (BIG) and FVB/N-Tg (MHCAtTA) line (the tTA line). The transgenic lines were generated to circumvent the possible death of the embryos due to severe phenotypes. However, overexpression of CECR1a did not result in a fatal phenotype in fetuses, based on the observed Mendelian ratio of 4

genotypes of the pups. Thus, the controlled expression of CECR1a at a certain developmental stage of mouse embryos by tetracycline was not conducted. BIG/tTA transgenic embryos were analyzed by histological staining. Abnormal left atrioventricular valve and atrial septum defects were observed at a low penetrance in only 1 of the 8 BIG/tTA embryos, which lead to the conclusion that the phenotype may be an unrelated sporadic abnormality.

4.6 Future directions

4.6.1 Role of CECR1 in mouse heart development

Considering the ADA2 activity of CECR1, it is possible that the abnormal phenotypes seen in the MHC lines are caused by the decreased concentration of extracellular adenosine in the mouse hearts. Adenosine is tightly regulated. The biological effect of adenosine is mediated by the four adenosine receptors (Fredholm et al., 2000). Through the interaction with its specific receptor, adenosine can inhibit the growth of one cell line, such as cultured vascular smooth muscle cells via A_{2b}AR, but stimulate the proliferation of another type of cell line, such as cultured coronary artery smooth muscle cells via A_1AR, and cultured endothelial cells via A_2AR. It was also found that adenosine stimulates endothelial progenitor cells migrating to the cardiac endothelium through both A_1AR and A_{2b}AR (Dubey et al., 1996). CECR1a overexpression should decrease the adenosine concentration in the heart. Low level of adenosine may lead to thinner ventricular wall in the transgenic mouse hearts resulting from growth inhibition of the mouse embryonic ventricular muscle cells through the interaction with the

adenosine receptor (possibly A_{2b}AR). Low level of adenosine might also inhibit migration of endothelial progenitor cells, possibly through A_1AR, thus leading to disorganized AV valve. To test this hypothesis, first, the type of adenosine receptors in embryonic muscle and endothelial cells would need to be identified using *in situ* hybridization during early embryogenesis. Primary cells from transgenic and normal mouse muscle and endothelial cells could be cultured. The growth rate of the cells from the transgenic and normal mice could then be compared. Cells from the CECR1a mice would be expected to have a lower growth rate. Agonist of selective adenosine receptors could be used, which would be expected to rescue the inhibited growth of cultured cells from the CECR1a mice.

4.6.2 Role of hypoxia in mouse development

The adenosine concentration increases dramatically during hypoxia to protect against damage. A_1AR is expressed in embryonic mouse heart (Rivkees, 1995). A_1AR knockout mice embryos are normal in normoxia, but show great growth retardation under hypoxic condition (Wendler et al., 2007). When A_1AR was present, interaction between adenosine and A_1ARs could partially protect the severe effect of hypoxia during early mouse development, although less severe phenotypes, such as smaller heart size and thinner ventricular wall were still present. It is possible that the MHC and BIG/tTA embryos are more susceptible to partial hypoxia required in normal development because of the lack of adenosine to interact with the A_1AR. If this is true, exposing CECR1 overexpressing embryos to hypoxia would lead to more severe phenotypes than seen in their

normal littermates. To test this hypothesis, pregnant mice could be exposed to 10% O_2 during E7.5 to E10.5, the critical stages for heart development. Embryos could be collected at the end of the hypoxia treatment for histological analysis. In a preliminary experiment, I exposed E7.5 embryos of MHC42 and MHC69 lines to hypoxia for 3 days. Smaller heart size and thinner ventricle walls were not observed in MHC embryos compared to normal littermates under hypoxia, however normoxic controls were not done. Comparison between wild type E10.5 embryos under normoxic and hypoxic condition would better address if the hypoxic treated embryos have a smaller heart size. However, less organized trabeculae in ventricles and thinner endocardial cushions were observed in MHC42 transgenic embryos (2 out of 3 transgenic embryos), but not in the wild type littermates (5 embryos) (see Figure 4-1). The same heart components, the ventricular walls and the AV valves, are affected in both CECR1 overexpressed and hypoxia treated embryos, perhaps suggesting that the abnormal phenotypes are linked to the altered extracellular adenosine concentration caused by altered CECR1 expression. More embryos from the MHC lines and BIG/tTA lines treated by hypoxia could be collected and analyzed histologically. In each MHC lines, 2 litters of E10.5 embryos under normoxia have been collected, sectioned and mounted on slides.

Hypoxia-inducible factor 1α (HIF1α) plays an important role in mediating responses to hypoxia and is regulated by A_3AR in a cell-based system (Merighi et al., 2006). It is quite possible that HIF1α is also regulated by other adenosine receptors in mouse embryonic heart. HIF1α protein is less stable in A_1AR

knockout embryos under hypoxia compared to heterozygous embryos (Wendler et al., 2007). HIF1α protein may be less stable as well in the CECR1 overexpressing embryos because of their reduced adenosine receptor activity. HIF1α protein levels could be examined by western blot analysis in mutant and normal whole embryos at E14.5. HIF1α regulates expression of some genes by binding to hypoxia-response elements in the promoter region of these genes (Liu & Simon, 2004). Transcription levels of these genes could be examined by real-time PCR in CECR1 overexpression embryonic hearts and normal hearts. If there was altered level of expression in these genes, it would give hints as to the signal pathways that might be initiated by CECR1 overexpression.

4.7 Significance of this work

Overexpression of human CECR1 in the mouse produces phenotypes such as thinner right ventricular walls, abnormal left and right AV valves, and possible atrial septal defects, but with only moderate penetrance. The first two phenotypes are not the typical CES heart defects observed in human. Since the mouse does not have a *Cecr1* gene, the expression of human CECR1 may not completely mimic the phenotypes observed in patients. However, the observed phenotypes may lead to an understanding of the function of human CECR1.

The study of the expression and function of CECR1 will shed light on the role of *CECR1* in the production of CES phenotypes. The mechanism of the formation of the heart defects in the transgenic mouse model will give useful knowledge about normal heart development and provide information about the prevention of heart defects resulting from similar causations.

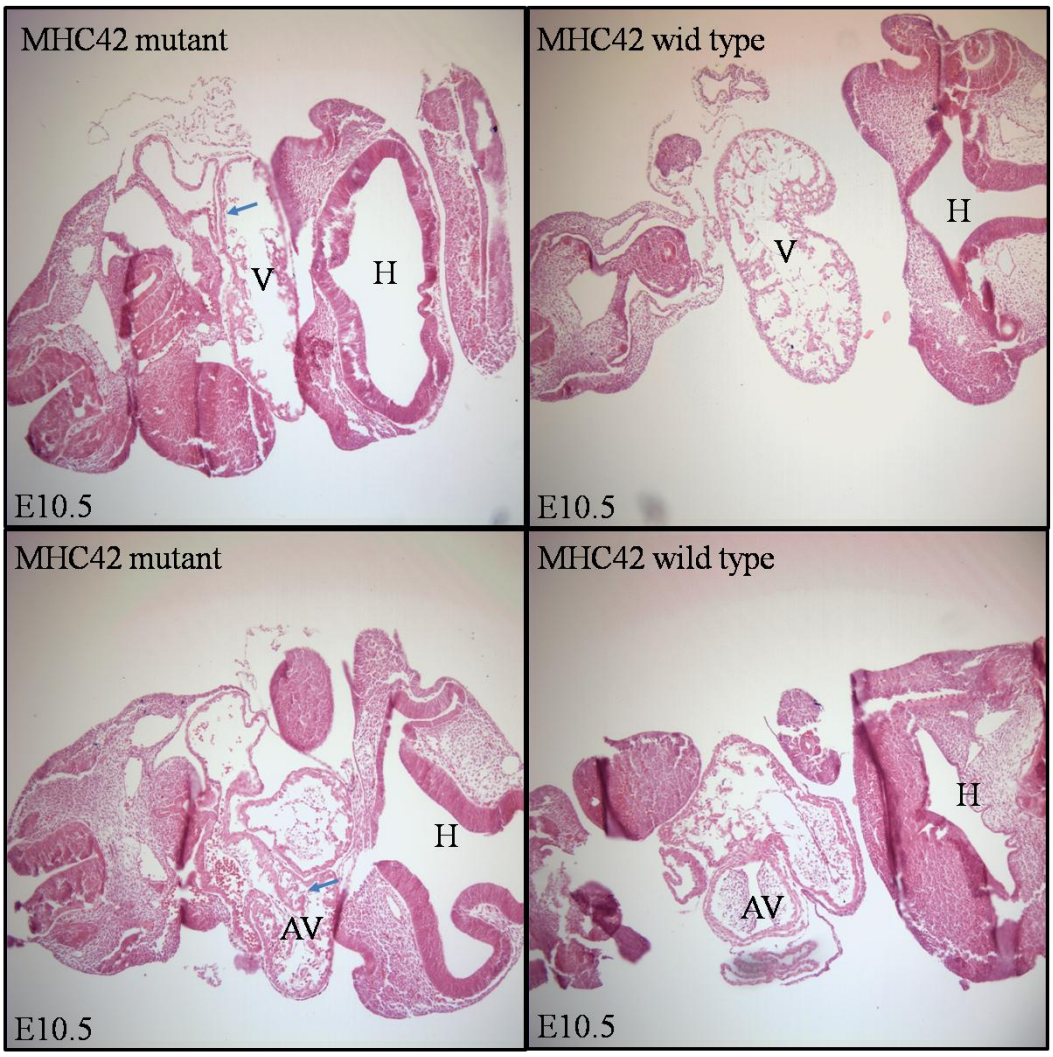

Figure 4-1. Histological section and H&E staining of E10.5 embryonic heart in MHC42 line under hypoxic condition (preliminary results).

Dams were exposed to hypoxia from E7.5 to E10.5. In MHC42 mutant mouse embryos, less trabeculae were observed in ventricular canal in the top image indicated by the arrow; misshapen endocardial cushion was observed in the bottom image indicated by the arrow. Images were taken with a 10× objective and 1.6× aux. lens. AV: atrioventricular canal cushion; H: head; V, ventricular canal.

References

AKALAL, D. B., BOTTENSTEIN, J. E., LEE, S. H., HAN, J. H., CHANG, D. J., KAANG, B. K. & NAGLE, G. T. (2003). Aplysia mollusk-derived growth factor is a mitogen with adenosine deaminase activity and is expressed in the developing central nervous system. *Brain Res Mol Brain Res* 117, 228-36.

AKALAL, D. B., SCHEIN, C. H. & NAGLE, G. T. (2004). Mollusk-derived growth factor and the new subfamily of adenosine deaminase-related growth factors. *Curr Pharm Des* 10, 3893-900.

AMES, T. M. (2006). Characterization of *Cecr2* expression and the *Cecr2*^{Gt45Bic} mutation on different mouse genetic backgrounds, University of Alberta.

ANDRAS NAGY, M. G., KRISTINA VINTERSTEN, RICHARD BEHRINGER. (2003). *Manipulating the Mouse Embryo: A Laboratory Manual*, 3rd edition. Cold Spring Harbor Laboratory Press.

ANTONARAKIS, S. E., LYLE, R., DERMITZAKIS, E. T., REYMOND, A. & DEUTSCH, S. (2004). Chromosome 21 and down syndrome: from genomics to pathophysiology. *Nat Rev Genet* 5, 725-38.

AZMANOV, D. N., MILACHICH, T. V., ZAHARIEVA, B. M., MICHAILOVA, G. I., DIMITROVA, V. G., KARAGIOZOVA, Z. H., MAZNEJKOVA, V. T., CHERNEV, T. A. & TONCHEVA, D. I. (2007). Profile of chromosomal aberrations in different gestational age spontaneous abortions detected by comparative genomic hybridization. *Eur J Obstet Gynecol Reprod Biol* 131, 127-31.

BAILEY, J. A., YAVOR, A. M., MASSA, H. F., TRASK, B. J. & EICHLER, E. E. (2001). Segmental duplications: organization and impact within the current human genome project assembly. *Genome Res* 11, 1005-17.

BANTING, G. S. (2003). Characterization of the cat eye syndrome candidate gene *CECR2*, University of Alberta.

BANTING, G. S., BARAK, O., AMES, T. M., BURNHAM, A. C., KARDEL, M. D., COOCH, N. S., DAVIDSON, C. E., GODBOUT, R., MCDERMID, H. E. & SHIEKHATTAR, R. (2005). CECR2, a protein involved in neurulation, forms a novel chromatin remodeling complex with SNF2L. *Hum Mol Genet* 14, 513-24.

BARAK, O., LAZZARO, M. A., COOCH, N. S., PICKETTS, D. J. & SHIEKHATTAR, R. (2004). A tissue-specific, naturally occurring human SNF2L variant inactivates chromatin remodeling. *J Biol Chem* 279, 45130-8.

BARLOW, G. M., CHEN, X. N., SHI, Z. Y., LYONS, G. E., KURNIT, D. M., CELLE, L., SPINNER, N. B., ZACKAI, E., PETTENATI, M. J., VAN RIPER, A. J., VEKEMANS, M. J., MJAATVEDT, C. H. & KORENBERG, J. R. (2001). Down syndrome congenital heart disease: a narrowed region and a candidate gene. *Genet Med* 3, 91-101.

BASSETT, A. S., CHOW, E. W., HUSTED, J., WEKSBERG, R., CALUSERIU, O., WEBB, G. D. & GATZOULIS, M. A. (2005). Clinical features of 78 adults with 22q11 Deletion Syndrome. *Am J Med Genet A* 138, 307-13.

BERENDS, M. J., TAN-SINDHUNATA, G., LEEGTE, B. & VAN ESSEN, A. J. (2001). Phenotypic variability of Cat-Eye syndrome. *Genet Couns* 12, 23-34.

BOROWIEC, A., LECHWARD, K., TKACZ-STACHOWSKA, K. & SKLADANOWSKI, A. C. (2006). Adenosine as a metabolic regulator of tissue function: production of adenosine by cytoplasmic 5'-nucleotidases. *Acta Biochim Pol* 53, 269-78.

CARVER, E. A. & STUBBS, L. (1997). Zooming in on the human-mouse comparative map: genome conservation re-examined on a high-resolution scale. *Genome Res* 7, 1123-37.

CHARLAB, R., VALENZUELA, J. G., ANDERSEN, J. & RIBEIRO, J. M. (2001). The invertebrate growth factor/CECR1 subfamily of adenosine deaminase proteins. *Gene* 267, 13-22.

DAVISSON, M. T., SCHMIDT, C., REEVES, R. H., IRVING, N. G., AKESON, E. C., HARRIS, B. S. & BRONSON, R. T. (1993). Segmental trisomy as a mouse model for Down syndrome. *Prog Clin Biol Res* 384, 117-33.

DENAVIT, T. M., MALAN, V., GRILLON, C., SANLAVILLE, D., ARDALAN, A., JACQUEMONT, M. L., BURGLEN, L., TAILLEMITE, J. L. & PORTNOI, M. F. (2004). A new case of a severe clinical phenotype of the cat-eye syndrome. *Genet Couns* 15, 443-8.

DUBEY, R. K., GILLESPIE, D. G., OSAKA, K., SUZUKI, F. & JACKSON, E. K. (1996). Adenosine inhibits growth of rat aortic smooth muscle cells. Possible role of A2b receptor. *Hypertension* 27, 786-93.

DUNHAM, I., SHIMIZU, N., ROE, B. A., CHISSOE, S., HUNT, A. R., COLLINS, J. E., BRUSKIEWICH, R., BEARE, D. M., CLAMP, M., SMINK, L. J., AINSCOUGH, R., ALMEIDA, J. P., BABBAGE, A., BAGGULEY, C., BAILEY, J., BARLOW, K., BATES, K. N., BEASLEY, O., BIRD, C. P., BLAKEY, S., BRIDGEMAN, A. M., BUCK, D., BURGESS, J., BURRILL, W. D., O'BRIEN, K. P. & ET AL. (1999). The DNA sequence of human chromosome 22. *Nature* 402, 489-95.

EDELMANN, L., PANDITA, R. K., SPITERI, E., FUNKE, B., GOLDBERG, R., PALANISAMY, N., CHAGANTI, R. S., MAGENIS, E., SHPRINTZEN, R. J. & MORROW, B. E. (1999). A common molecular basis for rearrangement disorders on chromosome 22q11. *Hum Mol Genet* 8, 1157-67.

ENSENAUER, R. E., ADEYINKA, A., FLYNN, H. C., MICHELS, V. V., LINDOR, N. M., DAWSON, D. B., THORLAND, E. C., LORENTZ, C. P., GOLDSTEIN, J. L., MCDONALD, M. T., SMITH, W. E., SIMON-FAYARD, E., ALEXANDER, A. A., KULHARYA, A. S., KETTERLING, R. P., CLARK, R. D. & JALAL, S. M. (2003). Microduplication 22q11.2, an emerging syndrome: clinical, cytogenetic, and molecular analysis of thirteen patients. *Am J Hum Genet* 73, 1027-40.

EPSTEIN, C. J., AVRAHAM, K. B., LOVETT, M., SMITH, S., ELROY-STEIN, O., ROTMAN, G., BRY, C. & GRONER, Y. (1987). Transgenic mice with increased Cu/Zn-superoxide dismutase activity: animal model of dosage effects in Down syndrome. *Proc Natl Acad Sci U S A* 84, 8044-8.

FOOTZ, T. K., BRINKMAN-MILLS, P., BANTING, G. S., MAIER, S. A., RIAZI, M. A., BRIDGLAND, L., HU, S., BIRREN, B., MINOSHIMA, S., SHIMIZU, N., PAN, H., NGUYEN, T., FANG, F., FU, Y., RAY, L., WU, H., SHAULL, S., PHAN, S., YAO, Z., CHEN, F., HUAN, A., HU, P., WANG, Q., LOH, P., QI, S., ROE, B. A. & MCDERMID, H. E. (2001). Analysis of the cat eye syndrome critical

region in humans and the region of conserved synteny in mice: a search for candidate genes at or near the human chromosome 22 pericentromere. *Genome Res* 11, 1053-70.

FRACCARO, M., LINDSTEN, J., FORD, C. E. & ISELIUS, L. (1980). The 11q;22q translocation: a European collaborative analysis of 43 cases. *Hum Genet* 56, 21-51.

FRANCO, R., CASADO, V., CIRUELA, F., SAURA, C., MALLOL, J., CANELA, E. I. & LLUIS, C. (1997). Cell surface adenosine deaminase: much more than an ectoenzyme. *Prog Neurobiol* 52, 283-94.

FREDHOLM, B. B., ABBRACCHIO, M. P., BURNSTOCK, G., DALY, J. W., HARDEN, T. K., JACOBSON, K. A., LEFF, P. & WILLIAMS, M. (1994). Nomenclature and classification of purinoceptors. *Pharmacol Rev* 46, 143-56.

FREDHOLM, B. B., ARSLAN, G., HALLDNER, L., KULL, B., SCHULTE, G. & WASSERMAN, W. (2000). Structure and function of adenosine receptors and their genes. *Naunyn Schmiedebergs Arch Pharmacol* 362, 364-74.

FUNKE, B., EDELMANN, L., MCCAIN, N., PANDITA, R. K., FERREIRA, J., MERSCHER, S., ZOHOURI, M., CANNIZZARO, L., SHANSKE, A. & MORROW, B. E. (1999). Der(22) syndrome and velo-cardio-facial syndrome/DiGeorge syndrome share a 1.5-Mb region of overlap on chromosome 22q11. *Am J Hum Genet* 64, 747-58.

GHATPANDE, S. K., BILLINGTON, C. J., JR., RIVKEES, S. A. & WENDLER, C. C. (2008). Hypoxia induces cardiac malformations via A1 adenosine receptor activation in chicken embryos. *Birth Defects Res A Clin Mol Teratol* 82, 121-30.

GIUSSANI, D. A. (2006). Hypoxia Fetal Growth and Developmental origins of Health and Disease. In *Early Life Origins of Health and Disease* (ed. E. M. W. a. J. A. Owens). Birkhauser.

GOUAS, L., GOUMY, C., VERONESE, L., TCHIRKOV, A. & VAGO, P. (2008). Gene dosage methods as diagnostic tools for the identification of chromosome abnormalities. *Pathol Biol (Paris)* 56, 345-53.

GULICK, J., SUBRAMANIAM, A., NEUMANN, J. & ROBBINS, J. (1991). Isolation and characterization of the mouse cardiac myosin heavy chain genes. *J Biol Chem* 266, 9180-5.

HATTORI, M., FUJIYAMA, A., TAYLOR, T. D., WATANABE, H., YADA, T., PARK, H. S., TOYODA, A., ISHII, K., TOTOKI, Y., CHOI, D. K., GRONER, Y., SOEDA, E., OHKI, M., TAKAGI, T., SAKAKI, Y., TAUDIEN, S., BLECHSCHMIDT, K., POLLEY, A., MENZEL, U., DELABAR, J., KUMPF, K., LEHMANN, R., PATTERSON, D., REICHWALD, K., RUMP, A., SCHILLHABEL, M., SCHUDY, A., ZIMMERMANN, W., ROSENTHAL, A., KUDOH, J., SCHIBUYA, K., KAWASAKI, K., ASAKAWA, S., SHINTANI, A., SASAKI, T., NAGAMINE, K., MITSUYAMA, S., ANTONARAKIS, S. E., MINOSHIMA, S., SHIMIZU, N., NORDSIEK, G., HORNISCHER, K., BRANT, P., SCHARFE, M., SCHON, O., DESARIO, A., REICHELT, J., KAUER, G., BLOCKER, H., RAMSER, J., BECK, A., KLAGES, S., HENNIG, S., RIESSELMANN, L., DAGAND, E., HAAF, T., WEHRMEYER, S., BORZYM, K., GARDINER, K., NIZETIC, D., FRANCIS, F.,

LEHRACH, H., REINHARDT, R. & YASPO, M. L. (2000). The DNA sequence of human chromosome 21. *Nature* 405, 311-9.

HEADRICK, J. P. & PEART, J. (2005). A3 adenosine receptor-mediated protection of the ischemic heart. *Vascul Pharmacol* 42, 271-9.

HIRSCHHORN, R. & RATECH, H. (1980). Isozymes of adenosine deaminase. *Isozymes Curr Top Biol Med Res* 4, 131-57.

HOMMA, K., MATSUSHITA, T. & NATORI, S. (1996). Purification, characterization, and cDNA cloning of a novel growth factor from the conditioned medium of NIH-Sape-4, an embryonic cell line of Sarcophaga peregrina (flesh fly). *J Biol Chem* 271, 13770-5.

HOMMA, K. J., TANAKA, Y., MATSUSHITA, T., YOKOYAMA, K., MATSUI, H. & NATORI, S. (2001). Adenosine deaminase activity of insect-derived growth factor is essential for its growth factor activity. *J Biol Chem* 276, 43761-6.

HUXLEY, C., PASSAGE, E., MANSON, A., PUTZU, G., FIGARELLA-BRANGER, D., PELLISSIER, J. F. & FONTES, M. (1996). Construction of a mouse model of Charcot-Marie-Tooth disease type 1A by pronuclear injection of human YAC DNA. *Hum Mol Genet* 5, 563-9.

IIJIMA, R., KUNIEDA, T., YAMAGUCHI, S., KAMIGAKI, H., FUJII-TAIRA, I., SEKIMIZU, K., KUBO, T., NATORI, S. & HOMMA, K. J. (2008). The extracellular adenosine deaminase growth factor, ADGF/CECR1, plays a role in Xenopus embryogenesis via the adenosine/P1 receptor. *J Biol Chem* 283, 2255-64.

IJZERMAN A, V. R. A. (July 1997). In *Purinergic Approaches in Experimental Therapeutics* (ed. M. F. J. Kenneth A. Jacobson), pp. 129-148. Wilcy-Liss, New York.

INOUE, K., DEWAR, K., KATSANIS, N., REITER, L. T., LANDER, E. S., DEVON, K. L., WYMAN, D. W., LUPSKI, J. R. & BIRREN, B. (2001). The 1.4-Mb CMT1A duplication/HNPP deletion genomic region reveals unique genome architectural features and provides insights into the recent evolution of new genes. *Genome Res* 11, 1018-33.

IWAKI-EGAWA, S., NAMIKI, C. & WATANABE, Y. (2004). Adenosine deaminase 2 from chicken liver: purification, characterization, and N-terminal amino acid sequence. *Comp Biochem Physiol B Biochem Mol Biol* 137, 247-54.

IWAKI-EGAWA, S., YAMAMOTO, T. & WATANABE, Y. (2006). Human plasma adenosine deaminase 2 is secreted by activated monocytes. *Biol Chem* 387, 319-21.

JACOBSON, K. A., HOFFMANN, C., CATTABENI, F. & ABBRACCHIO, M. P. (1999). Adenosine-induced cell death: evidence for receptor-mediated signalling. *Apoptosis* 4, 197-211.

JEROME, L. A. & PAPAIOANNOU, V. E. (2001). DiGeorge syndrome phenotype in mice mutant for the T-box gene, Tbx1. *Nat Genet* 27, 286-91.

JOHNSON, A., MINOSHIMA, S., ASAKAWA, S., SHIMIZU, N., SHIZUYA, H., ROE, B. A. & MCDERMID, H. E. (1999). A 1.5-Mb contig within the cat eye syndrome critical region at human chromosome 22q11.2. *Genomics* 57, 306-9.

KIDD, J. M., COOPER, G. M., DONAHUE, W. F., HAYDEN, H. S., SAMPAS, N., GRAVES, T., HANSEN, N., TEAGUE, B., ALKAN, C., ANTONACCI, F., HAUGEN, E., ZERR, T., YAMADA, N. A., TSANG, P., NEWMAN, T. L., TUZUN, E., CHENG, Z., EBLING, H. M., TUSNEEM, N., DAVID, R., GILLETT, W., PHELPS, K. A., WEAVER, M., SARANGA, D., BRAND, A., TAO, W., GUSTAFSON, E., MCKERNAN, K., CHEN, L., MALIG, M., SMITH, J. D., KORN, J. M., MCCARROLL, S. A., ALTSHULER, D. A., PEIFFER, D. A., DORSCHNER, M., STAMATOYANNOPOULOS, J., SCHWARTZ, D., NICKERSON, D. A., MULLIKIN, J. C., WILSON, R. K., BRUHN, L., OLSON, M. V., KAUL, R., SMITH, D. R. & EICHLER, E. E. (2008). Mapping and sequencing of structural variation from eight human genomes. *Nature* 453, 56-64.

KNOLL, J. H., ASAMOAH, A., PLETCHER, B. A. & WAGSTAFF, J. (1995). Interstitial duplication of proximal 22q: phenotypic overlap with cat eye syndrome. *Am J Med Genet* 55, 221-4.

LEE, J. A., MADRID, R. E., SPERLE, K., RITTERSON, C. M., HOBSON, G. M., GARBERN, J., LUPSKI, J. R. & INOUE, K. (2006). Spastic paraplegia type 2 associated with axonal neuropathy and apparent PLP1 position effect. *Ann Neurol* 59, 398-403.

LEJEUNE, J., TURPIN, R. & GAUTIER, M. (1959). [Mongolism; a chromosomal disease (trisomy).]. *Bull Acad Natl Med* 143, 256-65.

LINDSAY, E. A., SHAFFER, L. G., CARROZZO, R., GREENBERG, F. & BALDINI, A. (1995). De novo tandem duplication of chromosome segment 22q11-q12: clinical, cytogenetic, and molecular characterization. *Am J Med Genet* 56, 296-9.

LIU, L. & SIMON, M. C. (2004). Regulation of transcription and translation by hypoxia. *Cancer Biol Ther* 3, 492-7.

LONNROTH, P., JANSSON, P. A., FREDHOLM, B. B. & SMITH, U. (1989). Microdialysis of intercellular adenosine concentration in subcutaneous tissue in humans. *Am J Physiol* 256, E250-5.

LUKASHEV, D., OHTA, A., APASOV, S., CHEN, J. F. & SITKOVSKY, M. (2004). Cutting edge: Physiologic attenuation of proinflammatory transcription by the Gs protein-coupled A2A adenosine receptor in vivo. *J Immunol* 173, 21-4.

LUPSKI, J. R. (1998). Genomic disorders: structural features of the genome can lead to DNA rearrangements and human disease traits. *Trends Genet* 14, 417-22.

LUPSKI, J. R. (2009). Genomic disorders ten years on. *Genome Med* 1, 42.

LYLE, R., BENA, F., GAGOS, S., GEHRIG, C., LOPEZ, G., SCHINZEL, A., LESPINASSE, J., BOTTANI, A., DAHOUN, S., TAINE, L., DOCO-FENZY, M., CORNILLET-LEFEBVRE, P., PELET, A., LYONNET, S., TOUTAIN, A., COLLEAUX, L., HORST, J., KENNERKNECHT, I., WAKAMATSU, N., DESCARTES, M., FRANKLIN, J. C., FLORENTIN-ARAR, L., KITSIOU, S., AIT YAHYA-GRAISON, E., COSTANTINE, M., SINET, P. M., DELABAR, J. M. & ANTONARAKIS, S. E. (2009). Genotype-phenotype correlations in Down syndrome identified by array CGH in 30 cases of partial trisomy and partial monosomy chromosome 21. *Eur J Hum Genet* 17, 454-66.

MAIER, S. A. (2005). Use of model organisms and phyloenetic analysis to characterize the role of *CECR1* in cat eye syndrome. PhD thesis, University of Alberta.

MAIER, S. A., GALELLIS, J. R. & MCDERMID, H. E. (2005). Phylogenetic analysis reveals a novel protein family closely related to adenosine deaminase. *J Mol Evol* 61, 776-94.

MAIER, S. A., PODEMSKI, L., GRAHAM, S. W., MCDERMID, H. E. & LOCKE, J. (2001). Characterization of the adenosine deaminase-related growth factor (ADGF) gene family in Drosophila. *Gene* 280, 27-36.

MCDERMID, H. E., DUNCAN, A. M., BRASCH, K. R., HOLDEN, J. J., MAGENIS, E., SHEEHY, R., BURN, J., KARDON, N., NOEL, B., SCHINZEL, A. & ET AL. (1986). Characterization of the supernumerary chromosome in cat eye syndrome. *Science* 232, 646-8.

MCDERMID, H. E., MCTAGGART, K. E., RIAZI, M. A., HUDSON, T. J., BUDARF, M. L., EMANUEL, B. S. & BELL, C. J. (1996). Long-range mapping and construction of a YAC contig within the cat eye syndrome critical region. *Genome Res* 6, 1149-59.

MCDERMID, H. E. & MORROW, B. E. (2002). Genomic disorders on 22q11. *Am J Hum Genet* 70, 1077-88.

MCTAGGART, K. E., BUDARF, M. L., DRISCOLL, D. A., EMANUEL, B. S., FERREIRA, P. & MCDERMID, H. E. (1998). Cat eye syndrome chromosome breakpoint clustering: identification of two intervals also associated with 22q11 deletion syndrome breakpoints. *Cytogenet Cell Genet* 81, 222-8.

MEARS, A. J., DUNCAN, A. M., BUDARF, M. L., EMANUEL, B. S., SELLINGER, B., SIEGEL-BARTELT, J., GREENBERG, C. R. & MCDERMID, H. E. (1994). Molecular characterization of the marker chromosome associated with cat eye syndrome. *Am J Hum Genet* 55, 134-42.

MEARS, A. J., EL-SHANTI, H., MURRAY, J. C., MCDERMID, H. E. & PATIL, S. R. (1995). Minute supernumerary ring chromosome 22 associated with cat eye syndrome: further delineation of the critical region. *Am J Hum Genet* 57, 667-73.

MEINS, M., BURFEIND, P., MOTSCH, S., TRAPPE, R., BARTMUS, D., LANGER, S., SPEICHER, M. R., MUHLENDYCK, H., BARTELS, I. & ZOLL, B. (2003). Partial trisomy of chromosome 22 resulting from an interstitial duplication of 22q11.2 in a child with typical cat eye syndrome. *J Med Genet* 40, e62.

MERIGHI, S., BENINI, A., MIRANDOLA, P., GESSI, S., VARANI, K., LEUNG, E., MACLENNAN, S. & BOREA, P. A. (2006). Adenosine modulates vascular endothelial growth factor expression via hypoxia-inducible factor-1 in human glioblastoma cells. *Biochem Pharmacol* 72, 19-31.

MOSER, G. H., SCHRADER, J. & DEUSSEN, A. (1989). Turnover of adenosine in plasma of human and dog blood. *Am J Physiol* 256, C799-806.

MOSQUEDA-GARCIA, R. (1992). Adenosine as a therapeutic agent. *Clin Invest Med* 15, 445-55.

MOUSSEAU, I. (2005). CECR6: Evidence of two overlaping reading frames in the cat eye syndrome critical region. MSc thesis, University of Alberta.

NASEVICIUS, A. & EKKER, S. C. (2000). Effective targeted gene 'knockdown' in zebrafish. *Nat Genet* 26, 216-20.

NIEDZWICKI, J. G., LIOU, C., ABERNETHY, D. R., LIMA, J. E., HOYT, A., LIEBERMAN, M. & BETHLENFALVAY, N. C. (1995). Adenosine deaminase isoenzymes of the opossum Didelphis virginiana: initial chromatographic and kinetic studies. *Comp Biochem Physiol B Biochem Mol Biol* 111, 291-8.

NIKOLAIENKO, O., NGUYEN, C., CRINC, L. S., CIOS, K. J. & GARDINER, K. (2005). Human chromosome 21/Down syndrome gene function and pathway database. *Gene* 364, 90-8.

O'DOHERTY, A., RUF, S., MULLIGAN, C., HILDRETH, V., ERRINGTON, M. L., COOKE, S., SESAY, A., MODINO, S., VANES, L., HERNANDEZ, D., LINEHAN, J. M., SHARPE, P. T., BRANDNER, S., BLISS, T. V., HENDERSON, D. J., NIZETIC, D., TYBULEWICZ, V. L. & FISHER, E. M. (2005). An aneuploid mouse strain carrying human chromosome 21 with Down syndrome phenotypes. *Science* 309, 2033-7.

OAKLEY, R. H., JEWELL, C. M., YUDT, M. R., BOFETIADO, D. M. & CIDLOWSKI, J. A. (1999). The dominant negative activity of the human glucocorticoid receptor beta isoform. Specificity and mechanisms of action. *J Biol Chem* 274, 27857-66.

PENTAO, L., WISE, C. A., CHINAULT, A. C., PATEL, P. I. & LUPSKI, J. R. (1992). Charcot-Marie-Tooth type 1A duplication appears to arise from recombination at repeat sequences flanking the 1.5 Mb monomer unit. *Nat Genet* 2, 292-300.

PLETCHER, M. T., WILTSHIRE, T., CABIN, D. E., VILLANUEVA, M. & REEVES, R. H. (2001). Use of comparative physical and sequence mapping to annotate mouse chromosome 16 and human chromosome 21. *Genomics* 74, 45-54.

PORTER, G. A., JR. & RIVKEES, S. A. (2001). Ontogeny of humoral heart rate regulation in the embryonic mouse. *Am J Physiol Regul Integr Comp Physiol* 281, R401-7.

PORTNOI, M. F. (2009). Microduplication 22q11.2: a new chromosomal syndrome. *Eur J Med Genet* 52, 88-93.

REISS, J. A., WELEBER, R. G., BROWN, M. G., BANGS, C. D., LOVRIEN, E. W. & MAGENIS, R. E. (1985). Tandem duplication of proximal 22q: a cause of cat-eye syndrome. *Am J Med Genet* 20, 165-71.

RIAZI, A. M., VAN ARSDELL, G. & BUCHWALD, M. (2005). Transgenic expression of CECR1 adenosine deaminase in mice results in abnormal development of heart and kidney. *Transgenic Res* 14, 333-6.

RIAZI, M. A., BRINKMAN-MILLS, P., NGUYEN, T., PAN, H., PHAN, S., YING, F., ROE, B. A., TOCHIGI, J., SHIMIZU, Y., MINOSHIMA, S., SHIMIZU, N., BUCHWALD, M. & MCDERMID, H. E. (2000). The human homolog of insect-derived growth factor, CECR1, is a candidate gene for features of cat eye syndrome. *Genomics* 64, 277-85.

RINN, J. L., EUSKIRCHEN, G., BERTONE, P., MARTONE, R., LUSCOMBE, N. M., HARTMAN, S., HARRISON, P. M., NELSON, F. K., MILLER, P., GERSTEIN,

M., WEISSMAN, S. & SNYDER, M. (2003). The transcriptional activity of human Chromosome 22. *Genes Dev* 17, 529-40.

RIVKEES, S. A. (1995). The ontogeny of cardiac and neural A1 adenosine receptor expression in rats. *Brain Res Dev Brain Res* 89, 202-13.

ROSEMBERG, D. B., RICO, E. P., GUIDOTI, M. R., DIAS, R. D., SOUZA, D. O., BONAN, C. D. & BOGO, M. R. (2007). Adenosine deaminase-related genes: molecular identification, tissue expression pattern and truncated alternative splice isoform in adult zebrafish (Danio rerio). *Life Sci* 81, 1526-34.

ROSIAS, P. R., SIJSTERMANS, J. M., THEUNISSEN, P. M., PULLES-HEINTZBERGER, C. F., DE DIE-SMULDERS, C. E., ENGELEN, J. J. & VAN DER MEER, S. B. (2001). Phenotypic variability of the cat eye syndrome. Case report and review of the literature. *Genet Couns* 12, 273-82.

SAGO, H., CARLSON, E. J., SMITH, D. J., KILBRIDGE, J., RUBIN, E. M., MOBLEY, W. C., EPSTEIN, C. J. & HUANG, T. T. (1998). Ts1Cje, a partial trisomy 16 mouse model for Down syndrome, exhibits learning and behavioral abnormalities. *Proc Natl Acad Sci U S A* 95, 6256-61.

SAGO, H., CARLSON, E. J., SMITH, D. J., RUBIN, E. M., CRNIC, L. S., HUANG, T. T. & EPSTEIN, C. J. (2000). Genetic dissection of region associated with behavioral abnormalities in mouse models for Down syndrome. *Pediatr Res* 48, 606-13.

SAMBROOK, J. A. R., D. (2001). *Molecular Cloning: A Laboratory Manual*, Third edition. Cold Spring Harbor Laboratory Press, Cold Spring Harbor.

SCHACHENMANN, G., SCHMID, W., FRACCARO, M., MANNINI, A., TIEPOLO, L., PERONA, G. P. & SARTORI, E. (1965). Chromosomes in Coloboma and Anal Atresia. *Lancet* 2, 290.

SCHINZEL, A., SCHMID, W., FRACCARO, M., TIEPOLO, L., ZUFFARDI, O., OPITZ, J. M., LINDSTEN, J., ZETTERQVIST, P., ENELL, H., BACCICHETTI, C., TENCONI, R. & PAGON, R. A. (1981). The "cat eye syndrome": dicentric small marker chromosome probably derived from a no.22 (tetrasomy 22pter to q11) associated with a characteristic phenotype. Report of 11 patients and delineation of the clinical picture. *Hum Genet* 57, 148-58.

SEBAT, J., LAKSHMI, B., TROGE, J., ALEXANDER, J., YOUNG, J., LUNDIN, P., MANER, S., MASSA, H., WALKER, M., CHI, M., NAVIN, N., LUCITO, R., HEALY, J., HICKS, J., YE, K., REINER, A., GILLIAM, T. C., TRASK, B., PATTERSON, N., ZETTERBERG, A. & WIGLER, M. (2004). Large-scale copy number polymorphism in the human genome. *Science* 305, 525-8.

SHAW, C. J. & LUPSKI, J. R. (2004). Implications of human genome architecture for rearrangement-based disorders: the genomic basis of disease. *Hum Mol Genet* 13 Spec No 1, R57-64.

SHPRINTZEN, R. J., GOLDBERG, R. B., YOUNG, D. & WOLFORD, L. (1981). The velo-cardio-facial syndrome: a clinical and genetic analysis. *Pediatrics* 67, 167-72.

STANKIEWICZ, P. & LUPSKI, J. R. Structural variation in the human genome and its role in disease. *Annu Rev Med* 61, 437-55.

STANKIEWICZ, P. & LUPSKI, J. R. (2010). Structural variation in the human genome and its role in disease. *Annu Rev Med* 61, 437-55.

SUGISHITA, Y., WATANABE, M. & FISHER, S. A. (2004). Role of myocardial hypoxia in the remodeling of the embryonic avian cardiac outflow tract. *Dev Biol* 267, 294-308.

SUSSAN, T. E., YANG, A., LI, F., OSTROWSKI, M. C. & REEVES, R. H. (2008). Trisomy represses Apc(Min)-mediated tumours in mouse models of Down's syndrome. *Nature* 451, 73-5.

TANAKA, Y., YAMAGUCHI, S., FUJII-TAIRA, I., IIJIMA, R., NATORI, S. & HOMMA, K. J. (2006). Involvement of insect-derived growth factor (IDGF) in the cell growth of an embryonic cell line of flesh fly. *Biochem Biophys Res Commun* 350, 334-8.

THIEL, M., CHOUKER, A., OHTA, A., JACKSON, E., CALDWELL, C., SMITH, P., LUKASHEV, D., BITTMANN, I. & SITKOVSKY, M. V. (2005). Oxygenation inhibits the physiological tissue-protecting mechanism and thereby exacerbates acute inflammatory lung injury. *PLoS Biol* 3, e174.

THISSE, B., THISSE, C. (2004). Fast Release Clones: A High Throughput Expression Analysis ZFIN.

UNGERER, J. P., OOSTHUIZEN, H. M., BISSBORT, S. H. & VERMAAK, W. J. (1992). Serum adenosine deaminase: isoenzymes and diagnostic application. *Clin Chem* 38, 1322-6.

URBAN, A. E., KORBEL, J. O., SELZER, R., RICHMOND, T., HACKER, A., POPESCU, G. V., CUBELLS, J. F., GREEN, R., EMANUEL, B. S., GERSTEIN, M. B., WEISSMAN, S. M. & SNYDER, M. (2006). High-resolution mapping of DNA copy alterations in human chromosome 22 using high-density tiling oligonucleotide arrays. *Proc Natl Acad Sci U S A* 103, 4534-9.

VALENTIJN, L. J., BAAS, F., WOLTERMAN, R. A., HOOGENDIJK, J. E., VAN DEN BOSCH, N. H., ZORN, I., GABREELS-FESTEN, A. W., DE VISSER, M. & BOLHUIS, P. A. (1992). Identical point mutations of PMP-22 in Trembler-J mouse and Charcot-Marie-Tooth disease type 1A. *Nat Genet* 2, 288-91.

VAN DER WEYDEN, M. B., BAILEY, L. & GARSON, O. M. (1978). Human adenosine deaminase and chromosome 20. *Experientia* 34, 531-2.

VAN DER WEYDEN, M. B. & KELLEY, W. N. (1976). Human adenosine deaminase. Distribution and properties. *J Biol Chem* 251, 5448-56.

WENDLER, C. C., AMATYA, S., MCCLASKEY, C., GHATPANDE, S., FREDHOLM, B. B. & RIVKEES, S. A. (2007). A1 adenosine receptors play an essential role in protecting the embryo against hypoxia. *Proc Natl Acad Sci U S A* 104, 9697-702.

WESTERFIELD, M. (1995). *The Zebrafish Book. A Guide for the Laboratory Use of Zebrafish (Danio rerio)*, 3rd edition. University of Oregon Press.

WOHLGEMUTH, S. L., CRAWFORD, B. D. & PILGRIM, D. B. (2007). The myosin co-chaperone UNC-45 is required for skeletal and cardiac muscle function in zebrafish. *Dev Biol* 303, 483-92.

YAGI, H., FURUTANI, Y., HAMADA, H., SASAKI, T., ASAKAWA, S., MINOSHIMA, S., ICHIDA, F., JOO, K., KIMURA, M., IMAMURA, S., KAMATANI, N., MOMMA,

K., TAKAO, A., NAKAZAWA, M., SHIMIZU, N. & MATSUOKA, R. (2003). Role of TBX1 in human del22q11.2 syndrome. *Lancet* 362, 1366-73.

YAO, Z., PAINTER, S. L., FANSLOW, W. C., ULRICH, D., MACDUFF, B. M., SPRIGGS, M. K. & ARMITAGE, R. J. (1995). Human IL-17: a novel cytokine derived from T cells. *J Immunol* 155, 5483-6.

YAO, Z., SPRIGGS, M. K., DERRY, J. M., STROCKBINE, L., PARK, L. S., VANDENBOS, T., ZAPPONE, J. D., PAINTER, S. L. & ARMITAGE, R. J. (1997). Molecular characterization of the human interleukin (IL)-17 receptor. *Cytokine* 9, 794-800.

YOBB, T. M., SOMERVILLE, M. J., WILLATT, L., FIRTH, H. V., HARRISON, K., MACKENZIE, J., GALLO, N., MORROW, B. E., SHAFFER, L. G., BABCOCK, M., CHERNOS, J., BERNIER, F., SPRYSAK, K., CHRISTIANSEN, J., HAASE, S., ELYAS, B., LILLEY, M., BAMFORTH, S. & MCDERMID, H. E. (2005). Microduplication and triplication of 22q11.2: a highly variable syndrome. *Am J Hum Genet* 76, 865-76.

ZACKAI, E. H. & EMANUEL, B. S. (1980). Site-specific reciprocal translocation, t(11;22) (q23;q11), in several unrelated families with 3:1 meiotic disjunction. *Am J Med Genet* 7, 507-21.

ZAVIALOV, A. V. & ENGSTROM, A. (2005). Human ADA2 belongs to a new family of growth factors with adenosine deaminase activity. *Biochem J* 391, 51-7.

ZHAO, Z. & RIVKEES, S. A. (2001). Inhibition of cell proliferation in the embryonic myocardium by A1 adenosine receptor activation. *Dev Dyn* 221, 194-200.

ZUROVEC, M., DOLEZAL, T., GAZI, M., PAVLOVA, E. & BRYANT, P. J. (2002). Adenosine deaminase-related growth factors stimulate cell proliferation in Drosophila by depleting extracellular adenosine. *Proc Natl Acad Sci U S A* 99, 4403-8.

Appendices

C. pGEM®-T Easy Vector Map and Sequence Reference Points

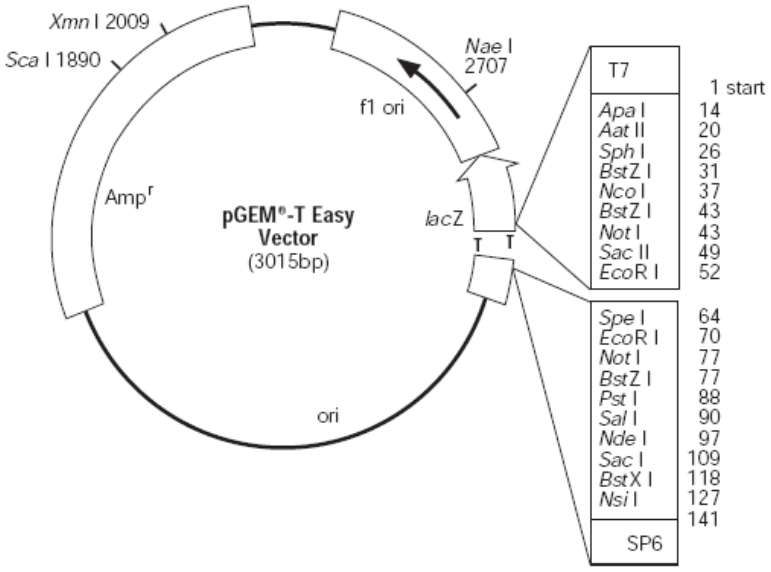

Figure 3. pGEM®-T Easy Vector circle map and sequence reference points.

pGEM®-T Easy Vector sequence reference points:

T7 RNA polymerase transcription initiation site	1
multiple cloning region	10–128
SP6 RNA polymerase promoter (–17 to +3)	139–158
SP6 RNA polymerase transcription initiation site	141
pUC/M13 Reverse Sequencing Primer binding site	176–197
*lac*Z start codon	180
lac operator	200–216
β-lactamase coding region	1337–2197
phage f1 region	2380–2835
lac operon sequences	2836–2996, 166–395
pUC/M13 Forward Sequencing Primer binding site	2949–2972
T7 RNA polymerase promoter (–17 to +3)	2999–3

Figure A 1. Vector map and multiple cloning site of pGEM-T Easy (Promega)

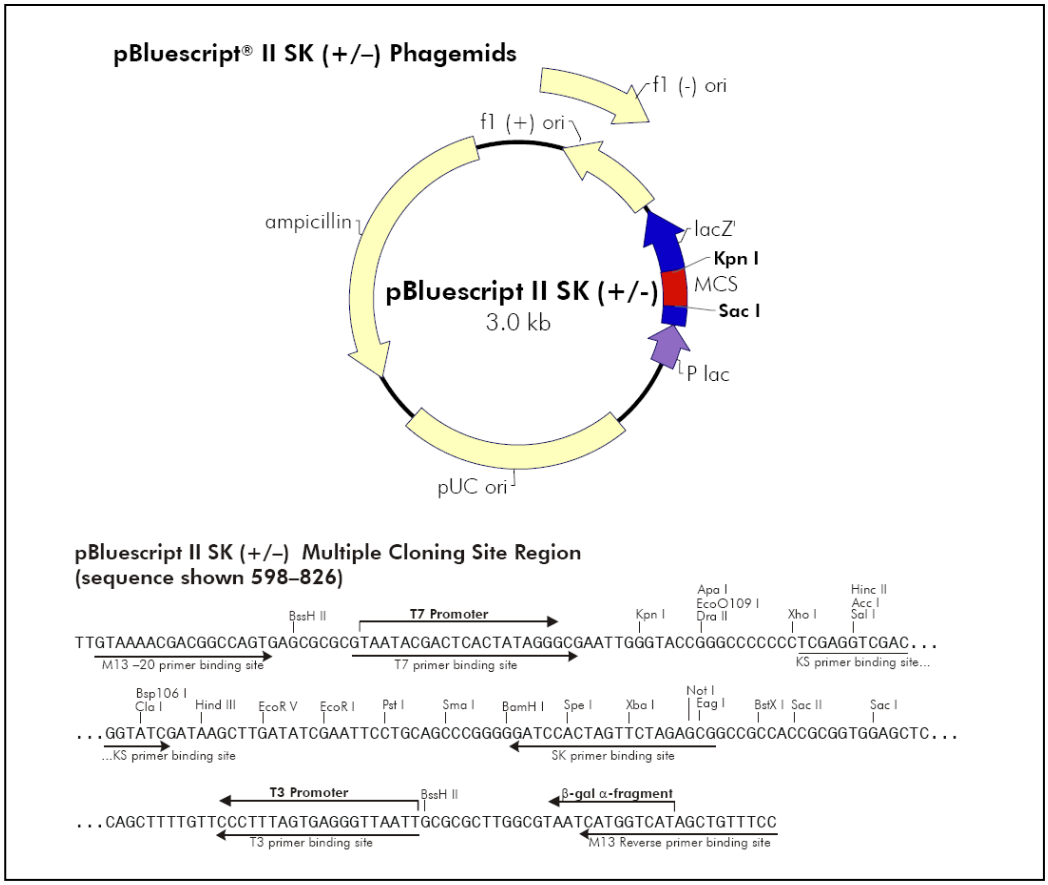

Figure A 2. Vector map and multiple cloning site of pBluescript II SK(+/-) (Stratagene)

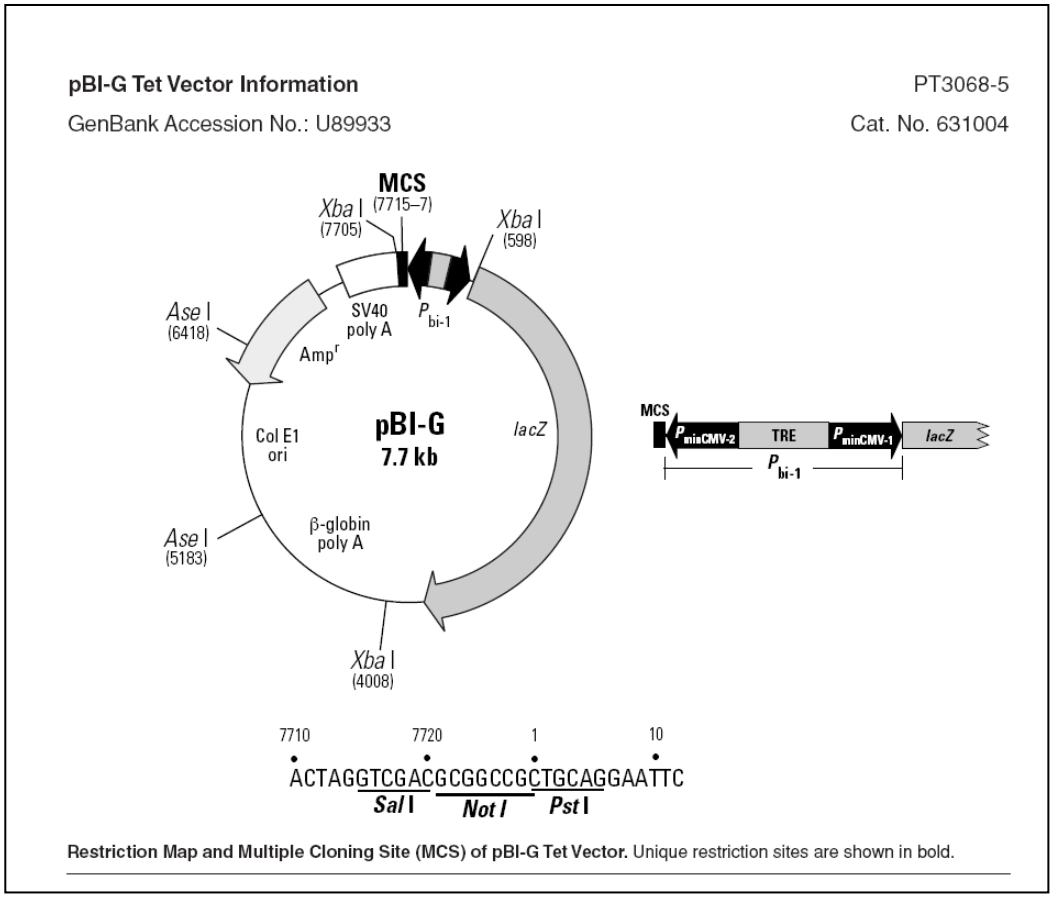

Figure A 3. Vector map and multiple cloning site of pBI-G (Clontech)